1-1-2018

Experimental Validation Of An Integrated Guidance And Control System For Marine Surface Vessels

Anthony Composto
Wayne State University,

EXPERIMENTAL VALIDATION OF AN INTEGRATED GUIDANCE AND CONTROL SYSTEM FOR MARINE SURFACE VESSELS

by

ANTHONY COMPOSTO

DISSERTATION

Submitted to the Graduate School

of Wayne State University,

Detroit, Michigan

in partial fulfillment of the requirements

for the degree of

DOCTOR OF PHILOSOPHY

2018

MAJOR: MECHANICAL ENGINEERING

Approved By:

_____

Advisor Date

_____

_____

_____

_____

ACKNOWLEDGMENTS

I would like to thank my family and friends for all their support and encouragement during this journey, there were many events that I missed due to the time requirements needed to complete this endeavor and through it all, you understood and never got upset with me. Without your support this would have been much more difficult.

I would like to thank my graduate committee members Dr. Leela Arava and Dr. Naeim Henein for their support and guidance. Your encouragement was greatly appreciated as it helped guide me through this journey.

Dr. Abhilash Pandya has been a staple in my education beginning with my undergraduate studies. Throughout the years you have been a boss, mentor and friend. I began working in his research lab which is where I realized that research was something I enjoyed and wanted to pursue as a career. Thank you for all your teachings and encouragement during my schooling career.

A special thank you to Dr. Nabil Chalhoub who has guided me from the beginning of my Ph.D. work until the end. We had many great conversations working out the best ways to approach and solve problems and I'm looking forward to continuing this relationship even after I have finished my formal education.

TABLE OF CONTENTS

TABLE OF FIGURES

NOMENCLATURE

d	cross track error
e_1	error in the surge displacement
e_2	error in the heading angle
k_i	switching term gain in the formulation of the controller
K_{o_i}	switching term gain in the formulation of the observer
s_i	i^{th} sliding surface for the sliding mode controller
s_{o_i}	i^{th} sliding surface for the sliding mode observer
u_i	i^{th} control signal
v_{c_s}, v_{c_h}	control signals for the surge displacement and the heading angle, respectively
VO	Velocity obstacle
$\hat{x}_{o_i}$	i^{th} state variable in the nominal model used in designing the observer
$\overline{X}$	distance along the desired path
(X, Y)	coordinates of the current location of the boat
(X_i, Y_i)	coordinates of the i^{th} waypoint
$\theta_{min}^{steering}$	minimum angular displacement of the ballscrew used in the steering mechanism
$\theta_{min}^{throttle}$	minimum angular displacement of the throttle handle
ψ	boat heading angle
ϕ_i	thickness of the boundary layer surrounding the i^{th} sliding surface
η_{o_i}	observer parameter
$(\,)_h$	a subscript "h" indicates a variable related to the heading angle
$(\,)_{MO}$	a subscript "MO" refers to a moving obstacle variable

$()_{PV}$	a subscript "PV" refers to a primary vessel variable
$()_o$	a subscript "o" refers to the SMC observer variable
$()_s$	a subscript "s" indicates a variable related to the surge motion
$(\dot{})$	a dot accent indicates differentiation with respect to time
$(\ddot{})$	a double dot accent indicates differentiation twice with respect to time
$(\underset{\sim}{})$	a tilde under a variable denotes a vector
$(\widetilde{})$	a tilde over a variable indicates that the variable represents an error signal
$(\widehat{})$	a hat over a variable refers to a nominal model variable

CHAPTER 1 BACKGROUND AND MOTIVATION

Problem Statement

Autonomous operation of marine surface vessels is vital for minimizing human errors during ship navigation. It also provides efficient operations of ships under significantly varying sea states and severe environmental conditions, which can be conducive to substantial external disturbances emanating from random sea waves, winds and sea currents.

The challenges of achieving autonomous operation of marine vessels are further complicated by the highly nonlinear dynamics of ships, which involve imprecise knowledge of or inaccurate modeling of wave excitations, nonlinear restoring forces, retardation forces, wind and current forces, viscous damping effects [1-13] along with structured uncertainties stemming from ice accretion on the ship hull, and/or ship-ice floes interactions [14-17]. The latter will significantly exacerbate the control problem of ships due to sharp, intermittent or persistent external disturbances generated by the ship-ice interactions.

Another difficulty in the control of ships stems from the fact that, in general, marine surface vessels are under-actuated. They usually have fewer actuators than degrees of freedom [18-20]. In open-sea operations, marine vessels usually rely on a propeller to provide the thrust required for controlling the surge speed and on a rudder to simultaneously steer the ship and compensate for its sway motion in order to keep the vessel on its desired track. Therefore, in general, a ship would have two actuators to control its surge speed, sway motion and heading angle. One approach for empowering under-actuated marine surface vessels to track their desired trajectories aims at pairing the controller with the ship navigation system. This will enable the steering mechanism to concurrently control the sway motion and the heading angle of the ship

[8, 19-30]. Such an approach does not need additional hardware to be mounted on the marine vessel and lays the foundation for autonomous operation of ships once the desired trajectory has been defined. This will considerably minimize human errors in both navigation and control that have historically led to catastrophic maritime accidents [31], which were induced by fatigue of the crew, unsuccessful maneuvering of the vessel, rough sea states and reduced visibility.

While the approach of integrating the navigation system with the ship controller has great potentials for the development of autonomous marine vessels, this topic remains a very active research field that has many significant challenges for researchers to overcome. Some of these challenges stem from the control of a nonlinear dynamical system with both structured and unstructured uncertainties, the robustness of the controlled system to significant and unpredictable environmental disturbances and the development of an efficient navigation system with obstacle avoidance capability.

The implementation of advanced controllers necessitates the availability of all state variables of the controlled system. In general, the number of state variables is greater than the number of sensors. Therefore, a nonlinear robust observer capable of providing accurate estimates of the state variables in the presence of both structured and unstructured uncertainties has to be developed for the current work.

As a consequence, a successful autonomous operation of a marine surface vessel would require a holistic approach encompassing a navigation system, robust nonlinear controllers and observers. Nassim and Chalhoub in [20] conducted a theoretical study proposing such a holistic approach. They proved the viability of such an approach through digital simulations. However, it should be emphasized that the theoretical development of advanced control algorithms and

nonlinear observers has greatly surpassed the experimental work in this field. Many potentials controllers and observers have been developed and never been validated experimentally in an uncontrolled real-world environment. The intent of the current study is to make a significant stride towards bridging the gap between the experimental validation and theoretical advancements in this field by aiming to accomplish the following tasks:

1. Experimentally validate the robust performance and tracking characteristic of a fully-integrated Line-of-Sight (LOS) guidance system with a sliding mode controller and observer.
2. Enhance the capabilities of the existing LOS guidance system by incorporating new features to avoid collision with both stationary and moving obstacles.
3. Integrate the enhanced LOS guidance system with the vessel's controller and observer and demonstrate through digital simulations the validity of the new approach in making the ship track its desired trajectory while occasionally deviating from the desired track to avoid collision with multiple moving obstacles.

The experimental work has been conducted on an under-actuated 16 ft tracker boat in a completely uncontrolled real-world setting of the open-water in Lake St. Clair, Michigan.

Contribution to the Research Field

This section provides an overview of the work's contribution to this field of research. Part of the contribution will be experimental validation of previously simulated work [provide references], while other parts involve new development in position control of the boat along with an obstacle avoidance scheme and its integration with the LOS Guidance system.

Experimental validation of an integrated guidance system, sliding mode controller and observer

As mentioned earlier, most of the literature regarding sliding mode control of marine vessels is simulation based which has served to demonstrate the robustness of these controllers to environmental disturbances and modeling inaccuracies [19, 20, 24, 29, 32-38]. So, while there exists much theoretical work with simulations involving the control and guidance of marine surface vessels [20, 29, 30, 32, 37], actual experimental studies are scarce as evidenced in the sample table provided by Fahimi and Van Kleeck in Ref. [39]. The overwhelming majority of the experimental work on autonomous marine surface vessels was not conducted in truly uncontrolled real-world environments.

This was the justification for this portion of the work. Although theoretical simulation is necessary, it is only the first step in proving the efficacy and robustness of this type of systems. For this effort, a fully-integrated guidance system with a sliding mode controller and observer has been successfully implemented on a 16' aluminum boat with a 60 hp outboard motor operating on Lake St. Clair, Michigan. All experiments were conducted under a variety of weather conditions involving significant variations in lake temperature, wind resistance, wave height, current magnitudes and directions.

Incorporate new features for avoiding both stationary and moving obstacles

For the application that is being studied, waypoint navigation is most common and therefore a LOS waypoint guidance system has been implemented on the test platform. However, this guidance system does not account for local obstacles that the vessel may encounter while operating. Therefore, there is a need for a robust obstacle avoidance system that can work alongside the LOS guidance scheme and follow the *International Regulations for Prevention of*

Collisions at Sea as commonly abbreviated by "COLREGS", which defines a strict set of rules for avoiding other vessels that are encountered. After reviewing the literature, it was determined that the most appropriate obstacle avoidance method for this application would be the "Velocity Obstacles (VO)" approach. This scheme was structured herein to override the LOS guidance system whenever the prospect of a collision between the vessel and an obstacle surpasses a preset threshold. The obstacle avoidance system will provide the controller with the desired heading angle that would allow the boat to safely navigate any encountered obstacle. Once the vessel clears all obstacles then the LOS guidance system will resume its command of the vessel.

Integration of the collision avoidance, COLREGS, LOS guidance systems, controllers and observers

The integration of the VO-based obstacle avoidance scheme with the LOS guidance system while accounting for the COLREGS regulations yields a powerful navigation system that is geared towards real-life applications. For a holistic approach to the autonomy problem of marine vessels, the enhanced guidance system is coupled in this phase of the work with the existing framework of sliding mode controllers and observers of the vessel. The performance and robustness of the fully integrated system will be assessed through digital simulations. The successful implementation of such a holistic approach represents a valuable contribution to the field of autonomous marine vessels.

Literature Survey

A brief summary of the literature pertaining to the application of controllers, observers and guidance systems in maritime application is provided in this Section.

Experimental Validation of Sliding Mode Controller for a Marine Surface Vessel

Ship Controllers

There are numerous challenges in the development of robust and accurate tracking controllers for marine surface vessels. These challenges stem from the fact that the dynamics of ships are highly nonlinear and not fully known [10, 13, 40-52], which makes their accurate modeling to be an insurmountably difficult task. Exemplary nonlinearities with significant modeling imprecision include retardation forces, nonlinear restoring forces, viscous damping, wind and sea-current resistive loads [5, 10, 13, 51, 53-57], external disturbances induced by ice floes and wave excitations [16, 17]. As a consequence, ship models would generally include considerable structured and unstructured uncertainties [18, 58]. The former are attributed to the fact that ship parameters are not exactly known, particularly, when the marine vessel is operated under severe weather conditions that may result in ice accretion on the ship hull [12, 14, 59-61]. While the latter are associated with omitted higher order dynamics of the ship. Most under-actuated ship controllers are designed based on a reduced-order model that only accounts for the surge, sway and yaw motions of the marine vessel. However, these controllers are implemented on full-order models that involve all six rigid body degrees of freedom of the ship. In such situations, the controlled system would exhibit significant unstructured uncertainties.

Conventional control techniques have been used in the design of ship auto-pilot for the Unites States Navy [62]. Since then Proportional-Integral-Derivative (PID) controllers have been widely used in the control of marine vessels due to their ease of implementation [9, 19, 32, 62-68]. In fact, over half of all controllers in the maritime industry are based on the PID technique [69]. Such controllers performed satisfactorily under calm or mild sea states. However, their

performances tend to significantly degrade under rough sea states or during intense ship maneuvers. This is because conventional controllers have limited capabilities in dealing with considerable disturbances, structured and unstructured uncertainties [9, 19, 62-71].

Some studies varied the gains of the PID controller with the vessel's speed in an attempt to improve the performance of the controller [63]. The success of this effort has been very limited. Other studies compared the performance of the PID controller to that of a robust sliding mode controller in digital simulations. As expected, the sliding mode controller yielded better tracking characteristics than that of the PID controller under varying operating conditions [37].

Furthermore, different model-based controllers were devised to control marine vessels during course-changing and course-keeping maneuvers [18, 19, 32, 70, 72-79]. Some of these controllers were developed based on the adaptive control method or the optimal control methodology such as the linear quadratic regulator (LQR) and the linear quadratic tracking (LQT) techniques [80]. The drawbacks of these controllers stem from their reliance on an accurate ship model, which makes them susceptible to modeling imprecisions.

Among the nonlinear controllers that were used in controlling maritime vessels are the feedback linearization scheme and the back-stepping algorithm with feedback dominance [36]. It should be noted that the former scheme aims at cancelling all nonlinearities of the system while the back-stepping algorithm tend to exploit the "good" nonlinearities and attenuate the adverse effects of "bad" nonlinearities [78]. Some studies have demonstrated the superior performance of the back-stepping controller over conventional PID or Proportional-Derivative (PD) controllers in ship course keeping [81]. In spite of the fact that the feedback linearization technique [18, 19, 32, 77], the output feedback scheme [18, 74-76, 78] and the back-stepping

algorithm are designed to handle nonlinear systems, their shortcomings stem from the fact that they are all model-based schemes. As a consequence, these techniques become vulnerable to modeling imprecision and external disturbances, which ultimately lead to considerable degradation in their performances.

Fuzzy logic controllers have also been implemented to compensate for both heading and surge speed of marine vessels [66, 82-87] These controllers require the development of a rule-base that is founded on expert's knowledge of the plant and a time consuming procedure to fine-tune the gains. However, fuzzy logic controllers tend to be robust to modeling imprecision and external disturbances, which make them suitable for maritime applications. The main drawback of these techniques is associated with the difficulty to prove their asymptotic stability.

Self-organizing fuzzy logic controllers [87-98] represent an advanced version of fuzzy logic algorithms. Their structures include a self-tuning algorithm which varies the inputs and/or outputs of the controller according to the closed-loop performance of the system. The shortcomings of self-organizing fuzzy logic controllers are once again related to the lack of proofs of stability for the closed-loop systems.

Nonlinear robust controllers based on the variable structure systems (VSS) theory are very well suited for applications whereby the plant model is not fully known, and the system is subjected to considerable external disturbances [99-103]. Numerous studies have demonstrated the robustness of these schemes to structured and unstructured uncertainties along with external disturbances when the overall effects of uncertainties and disturbances remain below a specified upper bound [30, 102-107]. Sliding mode controllers (SMC) are based on the variable structure systems theory. Their design involves the selection of an attractive manifold that leads

to the desired performance of the controlled system in terms of either tracking, regulation or stabilization [102, 103, 108, 109]. The Lyapunov stability theory is used to determine the gain for the switching term that will ensure the convergence of the system to the attractive manifold [108]. Therefore, the asymptotic stability of the closed-loop system is always guaranteed if the effects of modeling imprecisions and disturbances remain below a specified upper bound. These characteristics of the SMC would allow it to provide robust tracking performance of marine surface vessels in spite of significant modeling imprecision and external disturbances.

Some studies suggested the use of a high gain for the switching element in the SMC control signal in an attempt to shorten the reaching phase to the attractive manifold [109-112]. The rationale is to minimize the period during which the closed-loop system would be susceptible to modeling uncertainties and external disturbances. Although this approach yields rapid and robust tracking characteristics of the SMC, it is more likely to increase chattering in the control signal. This will raise the likelihood of exciting the un-modeled higher order dynamics of the system [103, 110, 111].

To address the vulnerability of the closed-loop system during the reaching phase, a stepwise moving sliding surface (MSS) technique has been introduced by Choi in [109] and [112]. Initially, the MSS is defined to pass through the initial errors. Then, the MSS will go through stepwise rotation and/or translation towards a desired manifold. The coefficients of the MSS were fuzzy-tuned based on tracking errors. The advantage of this approach is its ability to maintain the system's representative point in the $(e, \dot{e})$ plane within a close proximity to the MSS. However, the stepwise rotation and/or translation of the MSS will continuously dislodge the system's

representative point from the switching surface. This approach was later refined by Bartoszewicz [113] who proposed to rotate the MSS in a continuous rather than a stepwise fashion.

Other studies aimed at combining the advantages of both the sliding mode methodology and the fuzzy logic approach. This was done in two different approaches. In the first one, the fuzzy inference systems (FIS) was implemented to tune online the gains of the sliding mode controller [107, 111, 112, 114]. In the second approach, the tuning mechanism of a Takagi-Sugeno fuzzy logic controller incorporated switching functions based on sliding surfaces [20, 115, 116]. Khaled and Chalhoub [20] devised a self-tuned controller that does not require an accurate model of the plant or a rule-based FIS. Its asymptotic stability is guaranteed by selecting the upper bound parameter in the switching term of the controller to always exceed the combined effects of modeling imprecision and external disturbances. The robustness of the controller and its capability of adapting to environmental conditions have been demonstrated through digital simulations. It should be emphasized that the overwhelming majority of advanced control techniques have only been validated by digital simulations. This is particularly true in maritime applications where the experimental validation of control and guidance schemes of marine surface vessels is scarce [19, 20, 24, 29, 30, 32-38]. The brief summary provided by Fahimi and Van Kleeck [39] on experimental work of marine surface vessels demonstrates a strong need for conducting experimental validation of advanced controllers of vessels with or without guidance systems in truly uncontrolled open-sea environments.

Breivik and his co-workers [117] conducted a successful experimental study validating an integrated controller and guidance system. They used a full-scale unmanned surface vehicle (USV) to track a straight line in open-sea while moving at a high speed. The guidance system is

based on the Constant Bearing (CB) scheme, which is also labeled in the literature as the proportional navigation system. It relies on proportional rotations to line up the interceptor's velocity with the line-of-sight (LOS). It also aims at minimizing overshoot by reducing the vessel's speed as the interceptor approaches the target. The surge speed tracking is performed by implementing a feedforward controller based on a maneuver map along with a PI-controller. However, only a PI-controller was employed to compensate for the errors in the heading angle.

The experimental study performed by Ashrafiuon et al [118] used a sliding mode controller to make the mass center of a small-scale (0.45 m in length) autonomous boat track a desired trajectory in a fully controlled environment of 1.9 m by 2.6 m indoor pool. Only the translational coordinates of the mass center were fed back to the controller. Since the heading angle was ignored in the computation of the control signal then the controller would not be able to compensate for errors in the heading angle. Such an approach may yield reasonable results under the fully controlled environment of a calm sea state [39] because longitudinal hydrodynamic forces tend to stabilize the heading angle in the presence of small perturbations. However, in rough sea states that are capable of producing considerable external disturbances, this scheme may be able to accurately position the mass center while pointing the boat backward. To address this drawback, Fahimi and Van Kleeck [39] used a sliding mode controller to accurately track the desired trajectory for a "controlled" point, which is different from the boat's mass center [119]. Their experimental work involved a small boat weighing 7.8 kg and having a length of 0.8 m. Unlike the previous work, this study was conducted on a large outdoor pond in William Hawrelak Park, Edmonton, Alberta. The experiment entailed a travel distance shorter than 25 m and a desired path in the shape of the number "8". The experimental data revealed that that the sliding

mode control signals tend to saturate for a long period of time whenever the initial tracking errors are large, which can have a destabilizing effect on the controlled system. To overcome this problem, a waypoint PD-controller was implemented to reduce the initial tracking errors below a certain threshold before activating the sliding mode controller. The controlled boat performed well during calm and windy days. It should be stressed that all these studies have incorporated nominal models of the boat in their controller design.

In the current study, the sliding mode methodology has been employed to devise a heading and a surge displacement controller. The main focus is to experimentally validate the robustness of the controller to environmental disturbances and modeling imprecision. In fact, the dynamics of the boat were ignored in determining the gains of the controller. The control signals were computed based on estimated rather than measured state variables of the system. A brief review of the literature on state observers is provided in the subsequent sub-section.

State Observers

Autonomous operation of ships would eliminate catastrophic maritime accidents caused by human errors, especially, under severe weather conditions [31]. However, autonomous vessels require the implementation of advanced controllers that require system's state variables to be available either through measurements or estimation. Many studies that have been reported in the literature preferred estimated over measured state variables of the system due to the adverse effect of observation spillover on structural controllers [105, 120].

In the current study, the state variables that are needed for the computation of the control signals pertain to the global coordinates of the ship (X and Y) and the heading angle, ψ, along with their time derivatives. Generally, both X and Y are directly measured using a global

positioning system (GPS). The time rate of change of the heading angle, $\dot{\psi}$, can be obtained by an on-board Gyro compass system [78, 121, 122]. Therefore, $\dot{X}, \dot{Y}\ and\ \psi$ are not measured. It should be emphasized that some state variables cannot be determined by simple differentiation of measured signals without magnifying the noise level. Moreover, the integration of $\dot{\psi}$ necessitates an accurate knowledge of the initial value of ψ, which is not known. Thus, the required state variables must be estimated by a nonlinear robust observer that can yield accurate estimates in spite of significant modeling imprecision and external disturbances [35, 107, 123-127].

Luenberger observers can provide accurate estimation of the state variables for linear time-invariant systems with fully known plant structure and parameters [128-134]. Some studies aimed at extending their use to nonlinear systems [135] while others coupled them with the gain scheduling technique in order to apply them on systems with varying parameters [136]. The drawbacks of the Luenberger observers stem from their inabilities to deal with modeling imprecisions and/or external disturbances [137]. Similarly, Kalman filters have been developed to estimate state variables of stochastic linear plants in the presence of measurement noise [138-143]. These observers also require exact knowledge of the plant dynamics.

An adaptive state observer (ASO) has also been devised to estimate the state variables of a system with structured uncertainties [144]. Other studies have provided a systematic approach for designing an asymptotically stable adaptive nonlinear observer for Lipschitz nonlinear systems [145]. These techniques tend to be computationally intensive since they estimate both system parameters and state variables of the plant.

Several nonlinear observers have also been presented in the literature for systems satisfying the Lipschitz conditions [146-154]. The observer developed by Bestle and Zeitz [155] converts the nonlinear dynamical equations of the plant to the observable canonical form by using a nonlinear time-variant transformation matrix. However, the main issue in implementing such an observer is in the difficulty of generating such a transformation matrix.

Since the dynamics of the ship are not fully known and the vessel may experience significant external disturbances then only robust nonlinear observers can be useful for the current work. A promising class of nonlinear observers, capable of handling modeling uncertainties and external disturbances, has been developed based on the variable structure systems (VSS) theory [104, 105, 127, 156-159]. Similar to sliding mode controllers, these observers do not require exact knowledge of the dynamics of the system. The convergence of the estimated state variables to the actual ones is guaranteed as long as the upper bounds on the modeling imprecision are known. Kfoury and Chalhoub Ref. [160] enhanced the capabilities of these observers to handle constrained systems whose dynamics are governed by a set of highly nonlinear differential-algebraic (D-A) equations. The observer is formulated based on the sliding mode methodology and yields accurate estimates of all the state variables including the superfluous ones.

The capability of sliding mode observers in yielding accurate estimates of the state variables of marine vessels in the presence of considerable modeling imprecisions and external disturbances have been demonstrated through digital simulations in Ref. [161]. The robust and accurate estimation characteristics of sliding mode observers were validated experimentally in Ref. [162]. This was done without accounting for the dynamics of the vessel in the formulation of the observer in order to generate a model-less nonlinear observer.

A self-tuning fuzzy sliding mode observer was presented in Ref. [163] by combining the advantages of the variable structure systems (VSS) theory and the self-tuning fuzzy logic scheme [164]. The self-tuning state estimator does not require exact knowledge of the plant or the construction of a rule-based expert fuzzy inference system (FIS). For asymptotic stability of the observer, the upper bounds of the modeling imprecision and external disturbances must be known or conservatively estimated. The convergence of the estimation process is guaranteed by ensuring that the tuning parameters satisfy inequality conditions stemming from the negative definiteness requirement of the time derivatives of Lyapunov-like functions. The observer has been applied to estimate the state variables of an under-actuated marine surface vessel and its validity has also been proven in digital simulations.

In the current study, a sliding mode observer has been implemented to provide online estimation of the state variables that are needed for the computation of the control signals.

Guidance Systems

A plausible approach for tracking a specified trajectory with an under-actuated marine surface vessel is to couple the controller with a guidance system. The under-actuation of the vessel is attributed to the fact that only two actuators are available to control its three degrees of freedom. The actuators are the propeller and the rudder while the degrees of freedom are the surge and sway displacements along with the heading angle. The propeller provides the thrust needed to control the surge speed while the rudder is mainly used for controlling the sway displacement and the heading angle [19, 29]. Given the under-actuated configuration of the vessel, the tracking maneuvers cannot successfully be accomplished by specifying to the controller the desired surge speed and heading angle as functions of time. Under this setting, the

ship can drift away from its desired trajectory even though the controller may be successful in yielding the desired heading angle and surge speed. This is because environmental disturbances stemming from wave excitations, sea currents and wind loads can induce substantial drifts in the sway direction in spite of the controller being able to maintain the desired surge speed and orientation of the ship. Thus, a more viable approach would be to determine the desired heading angle based on the instantaneous cross-track error, which is defined to be the distance between the current position of the ship and its desired trajectory. Such a scheme will enable the rudder action to simultaneously compensate for the drift in the sway motion while yielding the desired handing angle of the vessel. It will also lead to a smooth and fast convergence of the vessel to its desired trajectory. Therefore, by fully integrating the guidance system with the controller, the former will provide the desired heading angle while the latter will ensure that the actual heading angle and surge speed converges to their desired values. It should be emphasized that the guidance system should be devised in a manner to guide the ship irrespective of the magnitude of the cross-track error. Moreover, guidance systems have the potentials of causing a serious tracking problem that lead the ship to track its desired trajectory while pointing backward [19, 29, 74, 75]. Therefore, these schemes should have a provision in their design to prevent the occurrence of such a problem.

There are three classical guidance laws for tracking a target, namely, the line-of-sight (LOS), the pure pursuit (PP), and the constant bearing (CB). The LOS technique is a three-point guidance scheme, it is comprised of a stationary reference point, a pursuer and a target (see Figure 0-1) [117, 165]. The objective of this method is for the pursuer to converge to the straight-line path that exists between the static reference point and the target. In the case of way point navigation

in maritime applications, the reference point will be the n^{th} waypoint and the target will be the $(n+1)^{th}$ waypoint. The marine vessel will converge to the desired trajectory until it reaches its target at which point the $(n+1)^{th}$ waypoint becomes the reference point and the $(n+2)^{th}$ waypoint becomes the new target (see Figure 0-1) [165].

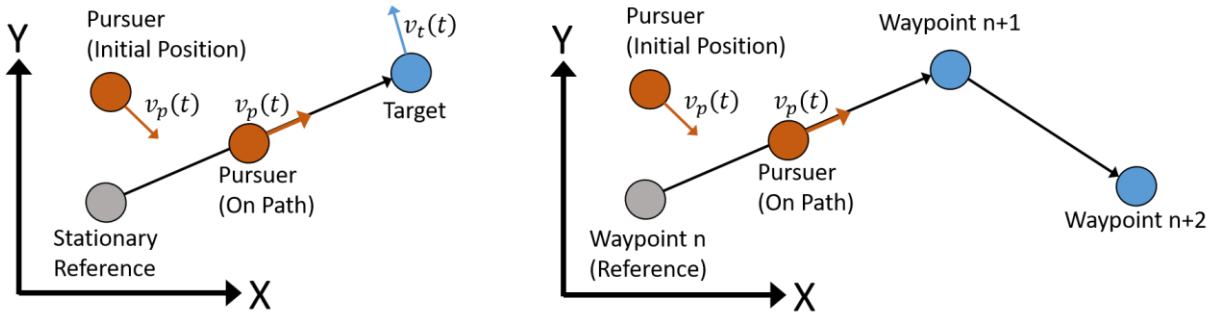

Figure 0-1 Left: LOS guidance scheme, Right: LOS guidance scheme for waypoint navigation, ($v_p(t)$ = velocity of the pursuer at time t, $v_t(t)$= velocity of the target at time t)

The pure pursuit (PP) guidance is a two-point guidance scheme where the pursuer being always on the line-of-sight between itself and the target [117]. Instead of trying to follow a reference path, as with the LOS technique, this scheme guides the pursuer along the instantaneous shortest distance between itself and the target (see Figure 0-2). In particular, if the target is stationary, the PP scheme will perform similarly to the LOS technique once the pursuer has reached the reference trajectory.

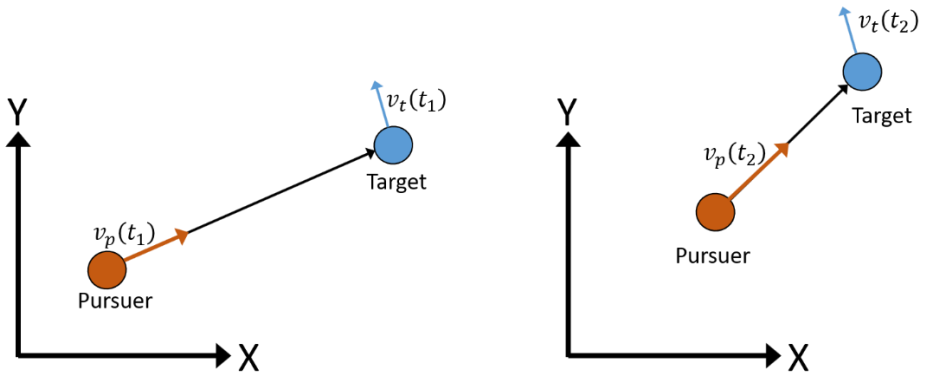

Figure 0-2 Left: Pure Pursuit guidance scheme at t_1, Right: Pure Pursuit guidance scheme at t_2, ($v_p(t)$ = velocity of the pursuer at time t, $v_t(t)$= velocity of the target at time t)

The constant bearing (CB) approach is also a two-point guidance scheme; however, it differs from the PP scheme in that the pursuer's velocity vector is defined by its two components. The first one, $v_t(t)$, is defined to be a co-directed vector with the same magnitude and orientation as the target's velocity vector. The second component will be aligned with the line-of-sight between the pursuer and the target (see Figure 0-3). As a consequence, the line-of-sight will maintain a constant direction causing the pursuer to perceive the target at a constant bearing. It should be noted that CB guidance becomes equivalent to the PP guidance system whenever the target is stationary [117].

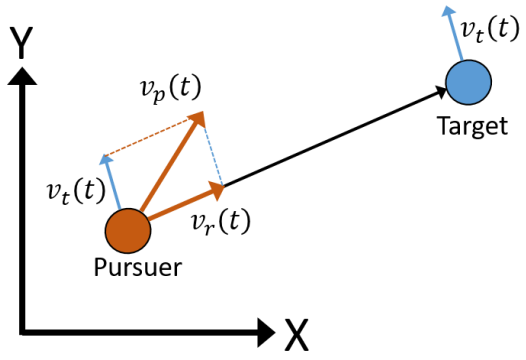

Figure 0-3 Constant Bearing Scheme, ($v_p(t)$ = velocity of the pursuer at time t, $v_t(t)$= velocity of the target at time t, $v_r(t)$= velocity along the line-of-sight at time t)

The guidance scheme that will be used in the current work will build upon the most up-to-date version of the LOS system as it applies to marine surface vessels. Therefore, a brief review of the latest developments in the LOS system will now be presented.

A guidance system, based on the line-of-sight (LOS) concept, has been reported in the literature [19, 21, 24, 25, 29]. The initial design employed a circle centered at the mass center of the vessel with a constant radius, R. The drawback of this design is due to the failure of this scheme to provide guidance whenever the cross-track error becomes larger than R. Moreira et al [19] introduced a guidance scheme that varies R linearly with the cross-track error [19]. This approach will always provide a suitable desired value for the heading angle that will ensure convergence of the vessel to its desired trajectory regardless of the magnitude of the cross-track error. Khaled and Chalhoub [30] presented a modified version of this guidance system by exponentially varying the radius of LOS with the cross-track error [30]. The rationale is to improve the convergence rate of the vessel to its desired trajectory beyond what is currently achievable by existing guidance systems.

Under harsh environmental conditions, the LOS guidance systems may not be able to eliminate the drift in the sway direction. Bibuli et al [166] experimentally validated an Integral Line-of-Sight (ILOS) guidance scheme. Their work was conducted on an 0.9 m long and 0.75 m wide Unmanned Semi-Submersible Vehicle (USSV) equipped with four DC brushless motors that are coupled to 4-bladed propellers. The integral action in the ILOS was added to enhance the robustness of the sway motion to environmental disturbances. A Proportional-Derivative (PD) controller was used to control the heading angle of the vessel.

Chalhoub and Khaled [164] presented a guidance system that varies the radius of line-of-sight (LOS) exponentially with the cross-track error and has a built-in feature to continually monitor both the cross-track error and its time derivative in order to detect and correct for the drift in the motion of the marine vessel. The capability of this scheme in eliminating the drift motion in the sway direction has been successfully demonstrated in digital simulations.

Collision Avoidance

A substantial research work has been done on obstacle avoidance in the field of robotics. To benefit from the existing literature, the previous work on obstacle avoidance has been reviewed and briefly summarized in the subsequent subsections.

Potential Fields

The "Potential fields" method has been developed for autonomous path planning and obstacle avoidance for robotic manipulators and mobile robots. This scheme creates artificial repulsive or attractive forces based on whether the object encountered by the robot is an obstacle or target. The force is defined to be proportional to the distance between the robot and the object, which allows the field to project the attractive force over large distances while slowing

the robot as it approaches its target in order to prevent overshoot. Repulsive forces will be reduced over distance to limit the effect of an obstacle. The resultant of all attractive and repulsive forces will be used to determine the desired velocity vector of the robot (see Figure 0-4) [167, 168]. The simplicity of this method has made it popular for this application, however it has limitations that complicate its implementation. The sum of all forces may create a resultant force with zero magnitude; this, creating a trap-situation causing the robot to stop. This can occur, for example, with closely spaced or U-shaped obstacles (see Figure 0-5). Narrow corridors can also cause instability by simultaneously inducing repulsive forces from opposite sides resulting in oscillations [168, 169].

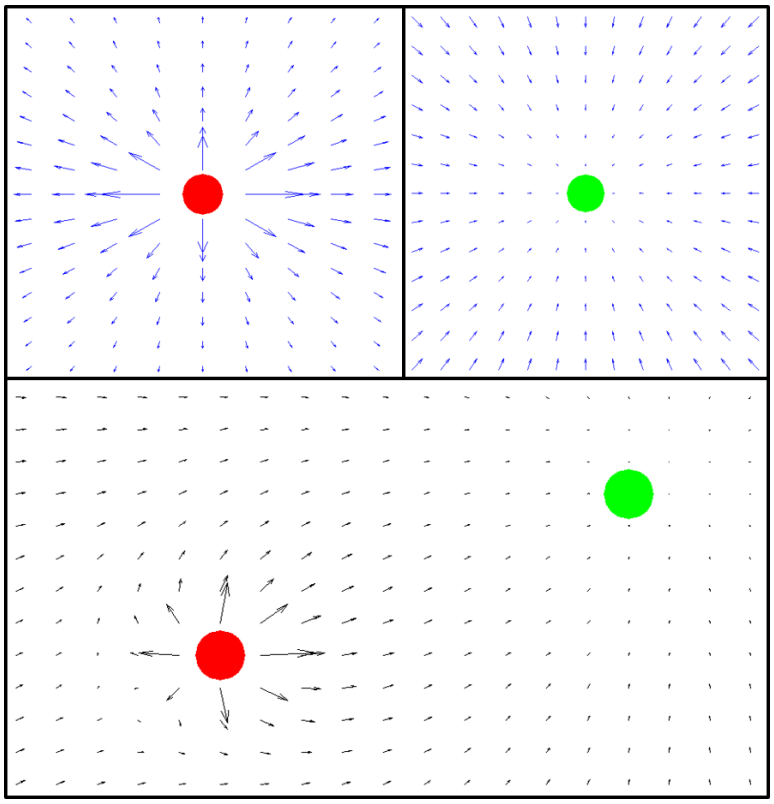

Figure 0-4 Top Left: Obstacles have repulsive forces, Top Right: Targets have attractive forces, Bottom: Forces are summed to generate the potential field

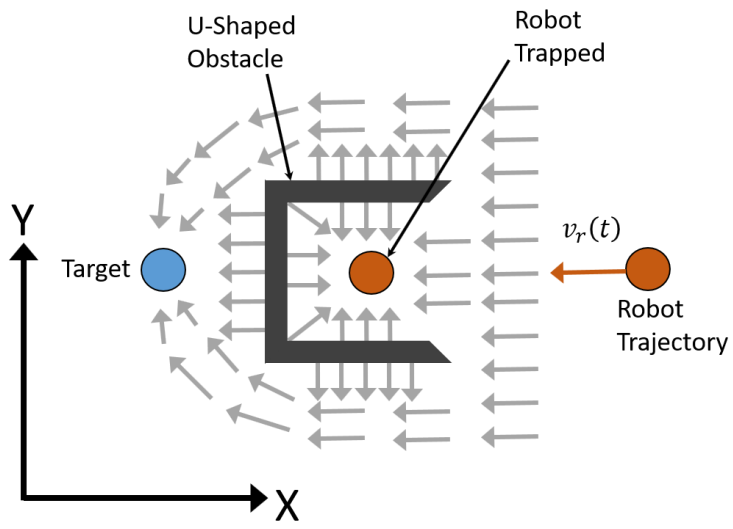

Figure 0-5 U-shaped obstacle can create a trap situation, (v_r = velocity of the robot at time t)

Dynamic Window Approach

Dynamic window approach (DWA) is a reactive collision avoidance scheme which computes control commands directly in velocities space (see Figure 0-6). DWA aims at determining potential translational and rotational velocity vectors achievable within one control cycle from the robot's current position and velocity. The admissible trajectories are then identified by excluding all trajectories that result in an undesirable event, such as a collision. The desired or optimal trajectory for the control cycle is selected by minimizing or maximizing a cost function that considers factors such as target distance, target direction and safety. Note that velocity vectors that may result in a collision in the future will remain acceptable if the robot retains the ability to turn or stop before a collision occurs [170-173].

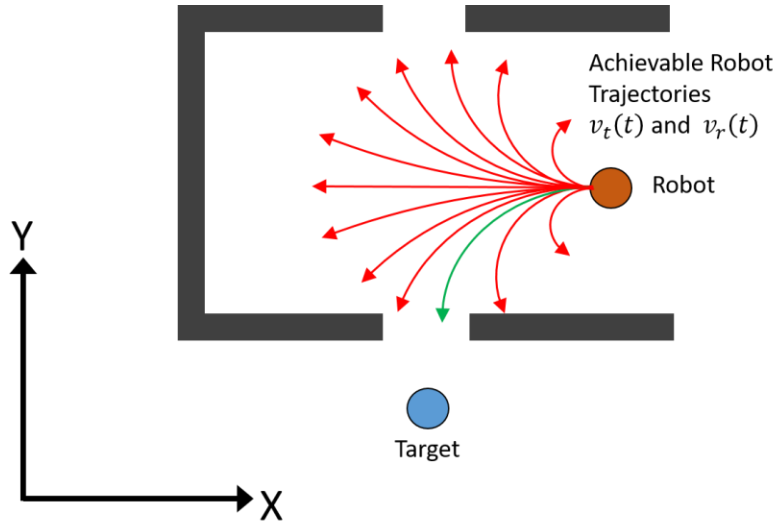

Figure 0-6 Dynamic Window Approach: Arrows represent sets of translational (v_t) and rotational (v_r) velocities that are achievable by the robot. Red arrows are undesirable or non-optimal trajectories; the green arrow is the optimal trajectory.

One disadvantage of the DWA method stems from the fact that a car or a single impeller boat, requiring a forward translational motion to achieve desired rotational velocity, can become trapped in its maneuver inside a corner, around a U-shaped obstacle or in close vicinity to an obstacle. Moreover, this scheme does not have any provision in its formulation to slow down the robot as it approaches the desired path, a narrow corridor or the final goal; thus, resulting in the robot overshooting its target or desired trajectory [170-173].

Velocity Obstacles

The velocity obstacles (VO) approach is a collision avoidance scheme developed for dynamic environments (see Figure 0-7). The method relies on current position and velocity vectors of the robot and all visible obstacles to identify the “collision velocity vectors" that will result in a collision between the robot and one or more of the obstacles in the future should the current information remains the same. Any velocity vector that does not belong to the set of “collision velocity vectors” will guide the robot in a collision-free path. Once the physical limitations of the

robot along with its current position and velocity vectors are known then realistic paths of the robot from its current position can be drawn by curved lines as illustrated in Figure 0-7. The initial velocity vector $V^{(i)}{}_A$ corresponding to the i^{th} trajectory would result in the relative velocity vector $V^{(i)}{}_{A/B.}$ If the latter is located in zones I or III then the robot will pass behind or in front of the moving obstacle, respectively. On the other hand, should $V^{(i)}{}_{A/B}$ be located in zone II then the robot would be on a collision path with the moving obstacle. Note that the robot and the moving obstacle would move away from each other if $V^{(i)}{}_{A/B}$ is located in zone IV. The admissible velocity vectors will constitute a subset of all collision-free velocity vectors that are achievable by the robot. This subset is then segregated into groups based on whether they avoid the obstacle by passing behind, in front, travel parallel to or move away from the obstacle [174, 175]. The group from which the desired velocity vector is selected would be left to a separate system, such as a global planning technique. The inherent flexibility of this scheme allows for smooth integration with path planning algorithms and make this method well suited to work within rule based environments such as at sea where Collision Regulations, the international regulations for preventing collisions at sea (COLREGS) must be followed [176, 177].

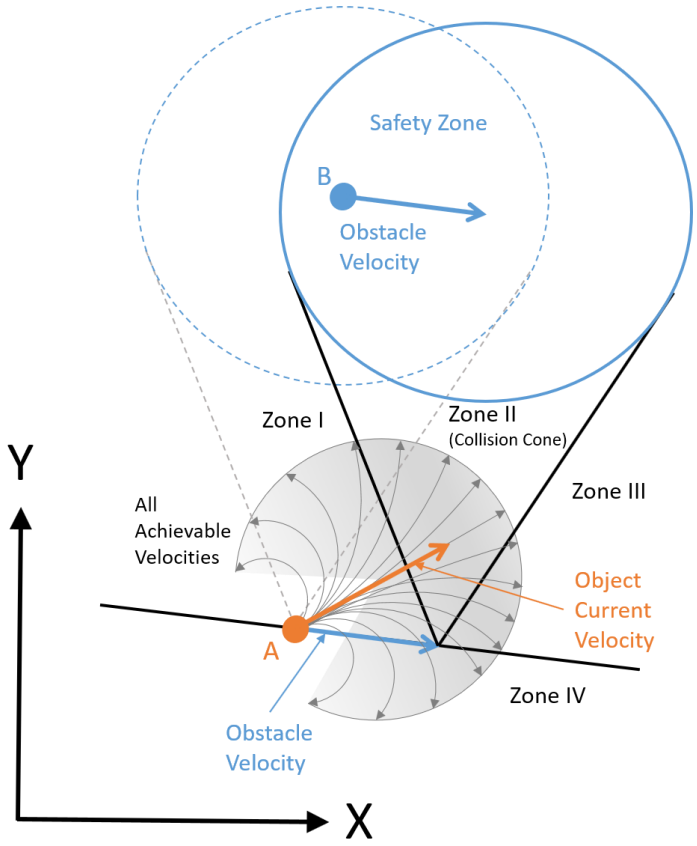

Figure 0-7 Velocity obstacles for a single target. Zone I represents velocities that will pass behind the obstacle, Zone II represent velocities that will encroach on the safety zone, Zone III represents velocities that will pass in front the obstacle, Zone IV represents velocities that will move parallel to or move away from the obstacle

Implementation of any of the schemes discussed above would require accurate information about the environment in which the robot is operating. In a simulation setting, the environment is well known and fully controlled. Moreover, the simulated sensor data is assumed to be perfect, which is not the case in any real-life applications. Therefore, any of these systems must account for sensor inaccuracies. Dealing with highly accurate sensors and low noise, a safety buffer built-in the calculations would usually be sufficient. However, inaccurate and noisy sensors will require complex schemes to overcome the sensor limitations. It is worth noting that any calculation

scheme needed to enhance sensor data will result in higher computational overhead and create latency in the system.

The collision avoidance system used in the current study builds on the velocity obstacles (VO) approach that was originally developed for mobile robots. It has been modified herein to incorporate the COLREGS rules of maritime navigation and was integrated with the LOS navigation system.

Dissertation Overview

A successful autonomous operation of a marine surface vessel would require a holistic approach encompassing a navigation system, robust nonlinear controllers and observers. The purpose of the current study is to experimentally validate such a holistic approach on an under-actuated 16 ft tracker boat in a completely uncontrolled real-world setting of the open-water in Lake St. Clair, Michigan. A successful validation of the proposed holistic approach mandates that the controlled marine vessel exhibits robust tracking characteristics in the presence of considerable external disturbances and modeling imprecision.

The contribution of the current work stems from the fact that theoretical development of advanced control algorithms and nonlinear observers has greatly surpassed the experimental work in this field. The intent of the current study is to make a significant stride towards bridging the gap between the experimental validation and theoretical advancements in this field.

The formulation of the robust nonlinear controller and observer along with the LOS guidance system is presented in the next Chapter. The enhancement of the LOS guidance scheme to avoid collision with stationary and moving obstacles has been done herein by integrating the guidance system with a modified version of the velocity obstacles (VO) scheme, which incorporates the

COLREGS rules of maritime navigation. The current obstacle avoidance system is described in Chapter 3. Subsequently, the experimental results used in the validation of the fully-integrated LOS guidance system with a sliding mode controller and observer are presented in Chapter 4. The feasibility of the proposed LOS system with obstacle avoidance features is demonstrated in digital simulations results in Chapter 5.

Finally, the work is summarized, and its main results and contributions are highlighted in Chapter 6. Furthermore, prospective research topics dealing with fully autonomous maritime navigation are proposed.

CHAPTER 2 FORMULATIONS FOR CONTROLLER, OBSERVER AND GUIDANCE SYSTEM

Autonomous operation of under-actuated marine surface vessels requires a holistic approach that would encompass a navigation system, a controller and an observer. Given the unpredictable nature of open-sea operations of marine vessels and the ensuing external disturbances, the controller and the observer must be robust to structured and unstructured uncertainties of the ship along with environmental disturbances. Moreover, the under-actuated configuration of the vessel can be dealt with by integrating the controller/observer of the ship with the guidance system. The formulations pertaining to the controller, observer and guidance system are presented in this Chapter.

The guidance system is relied on to provide the desired heading angle that will ensure convergence of the under-actuated ship to its specified trajectory; thus, yielding simultaneous compensation for both heading angle and sway motion with a single control action. Consequently, the trajectory tracking problem is now reduced to the control of the surge speed and the heading angle for which two control variables are readily available, namely, the propeller thrust and the rudder angle.

Hybrid Control Strategy Used in the Experimental Work

The structure of a hybrid control strategy for the under-actuated 16 ft tracker boat that was used in the current experimental work was developed in Ref. [162]. This strategy entails five controllers that are being managed by a main supervisory algorithm. Two controllers are dedicated for tracking and maneuvering operations based on feedback signals representing the actual surge motion and heading angle of the vessel. Another two controllers were devised for either point-to-point (PTP) or prescribed throttle angle and heading angle control tasks. Feedback

signals for these controllers are obtained from optical encoders mounted on their respective servomotors. The fifth controller is a "recovery" controller, which is only activated in the case of unforeseen mishaps either by the supervisory algorithm or the user. Its main function is to drive back the throttle arm to its neutral position while reducing the propeller thrust to zero in a controlled manner. The supervisory algorithm orchestrates the functioning of these controllers to successfully perform the specified control tasks while ensuring a safe operation of the marine vessel. Its role entails activating the appropriate controllers and triggering the recovery controller when needed.

The supervisory algorithm is coded to be as versatile as possible in MATLAB\Simulink\Stateflow chart. At its highest level, it provides the user with the capability of invoking the "recovery" controller if he/she wishes to abort the experiment. In addition, it allows the user to select whether to run PTP, prescribed profiles for the angular displacements of both the throttle arm and the rudder, or tracking a desired trajectory for the marine vessel.

Once the hybrid control strategy is activated, a "Stateflow" chart will take over the decision-making process and synchronize the operation of the various components of the system. Beyond this point, the user's input is limited to the push-button emergency switch that has the capability of aborting the boat maneuver. Every process initiated by the system will activate a specific state element in the Stateflow chart. The active state will then trigger its respective controller. As a safety measure, all active state elements will continuously monitor pre-defined events that may be induced by critical operations. Once any of these events occur, a system shutdown flag will be raised and both surge motion and steering maneuvers go into a recovery mode. Safe operation envelopes for both throttle handle and steering wheel angular displacements have been set to

$[\theta_{min}^{throttle}, \theta_{max}^{throttle}]$ and $[\theta_{min}^{steering}, \theta_{max}^{steering}]$, respectively. Critical operating conditions are declared whenever one or both of these intervals of angular displacements are breached.

The recovery strategy has been designed to get the boat into a safe state without putting the crew at risk during the process. For instance, instead of suddenly turning off the propeller's thrust, a predefined deceleration profile has been employed in order to minimize the surge of water at the stern and the sudden jerking motion that could throw an unsuspecting crew member off-board. Additionally, the recovery control action for the heading DC servomotor will assign a zero command voltage in order to halt any rotation maneuver and lock the steering wheel in place. The rationale behind this choice of action stems from the fact that the loss of throttle thrust will lead to a loss in steering capability.

Nominal MSV Model Used in Controllers Design

The nonlinear dynamics of the ship are not fully known. They are represented by the following nominal equations:

$$\ddot{\bar{x}}_i = \hat{f}_s(\dot{\bar{x}}_i, \bar{x}_i) + \hat{b}_1(\bar{x}_i)v_{c_s} \qquad (0\text{-}1)$$

$$\ddot{\psi} = \hat{f}_h(\dot{\psi}, \psi) + \hat{b}_2(\psi)v_{c_h} \qquad (0\text{-}2)$$

where $\bar{x}_i, \dot{\bar{x}}_i \; and \; \ddot{\bar{x}}_i$ denotes the actual surge displacement, speed and acceleration of the boat along the i^{th} segment of the desired trajectory, respectively. Similarly, $\psi, \dot{\psi}, and \; \ddot{\psi}$ are the heading angular displacement, velocity and acceleration of the vessel, respectively. $\hat{f}_s(\dot{\bar{x}}_i, \bar{x}_i)$, $\hat{f}_h(\dot{\psi}, \psi)$, $\hat{b}_s(\bar{x}_i)$ and $\hat{b}_h(\psi)$ are the best available approximations of the actual $f_s(\dot{\bar{x}}_i, \bar{x}_i)$, $f_h(\dot{\psi}, \psi)$, $b_s(\bar{x}_i)$ and $b_h(\psi)$ terms, respectively. The input gains are considered to be bounded by [103]

$$\hat{b}_1 = \sqrt{b_{1_{min}}\, b_{1_{max}}} \qquad \hat{b}_2 = \sqrt{b_{2_{min}}\, b_{2_{max}}} \tag{0-3}$$

$$\beta_1 = \sqrt{\frac{b_{1_{max}}}{b_{1_{min}}}} \qquad \beta_2 = \sqrt{\frac{b_{2_{max}}}{b_{2_{min}}}} \tag{0-4}$$

$$\beta_1^{-1} \leq b_1^{-1}\hat{b}_1 \leq \beta_1 \qquad \beta_2^{-1} \leq b_2^{-1}\hat{b}_2 \leq \beta_2 \tag{0-5}$$

where $\boldsymbol{b_{s_{max}}, b_{s_{min}}, b_{h_{max}}}$ $\boldsymbol{and}$ $\boldsymbol{b_{h_{min}}}$ are assumed to be known.

By defining the state vector as

$$\underset{\sim}{x}^T \triangleq \left[x_1 = \overline{x}_i, x_2 = \psi, x_3 = \dot{\overline{x}}_i, x_4 = \dot{\psi}\right] \tag{0-6}$$

equations (0-1) and (0-2) can be represented by the following state vector equation:

$$\dot{\underset{\sim}{x}} = \hat{\underset{\sim}{f}}(\underset{\sim}{x}) + \hat{b}(\underset{\sim}{x})\, \underset{\sim}{u} \tag{0-7}$$

Where

$$\hat{\underset{\sim}{f}}(\underset{\sim}{x}) \triangleq \begin{pmatrix} \dot{\overline{x}}_i \\ \dot{\psi} \\ \hat{f}_s \\ \hat{f}_h \end{pmatrix} \qquad \hat{b}(\underset{\sim}{x}) = \begin{bmatrix} 0 & 0 \\ 0 & 0 \\ \hat{b}_1 & 0 \\ 0 & \hat{b}_2 \end{bmatrix}$$

$$\underset{\sim}{u} = \begin{pmatrix} v_{c_s} \\ v_{c_h} \end{pmatrix}$$

The above state equation will then be used for designing the surge displacement and heading controllers.

Surge Displacement and Heading Controllers

The errors in the surge displacement and heading angle are defined as follows

$$e_1 \triangleq \overline{x}_i - \overline{x}_{i_d} = x_1 - x_{1_d} \tag{0-8}$$

$$e_2 \triangleq \psi - \psi_d = x_2 - x_{2_d}$$

Where x_{i_d} is the desired value for the i[th] state variable. The sliding surfaces are given by

$$s_i(\dot{e}_i, e_i) = \dot{e}_i + \lambda_i e_i \qquad i = 1,2 \tag{0-9}$$

By implementing the sliding mode methodology, the entries of the control vector can be written as

$$\mathrm{u_i} = \mathrm{u_{i_{eq}}} - \frac{\mathrm{k_i}}{\hat{\mathrm{b}}_\mathrm{i}} \mathrm{sgn(s_i)} \quad \mathrm{i} = 1,2 \tag{0-10}$$

Set $\dot{s}_i = 0$ for $i = 1 \; and \; 2$, one would obtain

$$u_{i_{eq}} = \frac{1}{\hat{b}_i}\left(-\hat{f}_{i+2} + x_{(i+2)_d} - \lambda_i \dot{e}_i\right) \qquad i = 1,2 \tag{0-11}$$

By satisfying the sliding conditions, the k_i gains for $i = 1 \text{ and } 2$ can be expressed as

$$\mathrm{k_i} \geq \beta_\mathrm{i}(\eta_\mathrm{i} + \mathrm{F_i}) + |\beta_\mathrm{i} - 1|\left|\hat{\mathrm{f}}_{\mathrm{i+2}} + \lambda_\mathrm{i}\dot{\mathrm{e}}_\mathrm{i} + \mathrm{x}_{(\mathrm{i+2})_\mathrm{d}}\right| \quad \mathrm{i} = 1,2 \tag{0-12}$$

where η_s and η_h are control parameters. F_i represents the i[th] upper bound on the modeling uncertainties:

$$\mathrm{F_i} \geq \left|\mathrm{f_{i+2}} - \hat{\mathrm{f}}_{\mathrm{i+2}}\right|_{\mathrm{sup}} \qquad \mathrm{i} = 1,2 \tag{0-13}$$

Generally, the $sgn(s_i)$ is replaced by a saturation function $sat\left(\frac{s_i}{\phi_i}\right)$, where ϕ_i is the thickness of the boundary layer surrounding the i^{th} sliding surface.

General Procedure for Designing a Sliding Mode Observer

Robust and autonomous operation of marine vessels requires advanced control schemes that can handle different sea states and harsh environmental conditions without relying on precise dynamic models of the vessel. These controllers generally need all state variables to be readily available. Due to the limited number of sensors used in this work, a nonlinear robust observer,

namely, a sliding mode observer (SMO) [161] has been used to accurately estimate the state variables in the presence of both structured and unstructured uncertainties.

This Section presents a general procedure for designing a nonlinear sliding mode observer. The robust performance of such an observer, in accurately estimating the state variables of the vessel in spite of considerable modeling imprecision and external disturbances, has already been experimentally validated in a completely uncontrolled real-world setting of the open-water in Lake St. Clair, Michigan in Ref. [162]. The SMO formulation is included herein for completeness of the reported work.

In this study, the SMO was implemented to estimate the global positioning X and Y coordinates of the boat and their time derivatives. The estimated $X, Y, \dot{X}, \dot{Y}$ values are then used to deduce information about the heading angle and its time derivative. Let the state vector equation of the observer be given by

$$\dot{\underset{\sim}{x}}_o = \underset{\sim}{f}_o(\underset{\sim}{x}_o, \underset{\sim}{u}) \qquad (0\text{-}14)$$

where $\underset{\sim}{x}_o^T = [X, Y, \dot{X}, \dot{Y}]$ and $\underset{\sim}{f}_o^T = [\dot{X}, \dot{Y}, f_{o_3}, f_{o_4}]$. Since the f_{o_i} terms are not known then they are approximated by their nominal $\hat{f}_{o_i}$ expressions. The structure of the SMO is expressed as follows [161]

$$\dot{\hat{x}}_{o_i} = \hat{x}_{o_{i+2}} - K_{o_i} \mathrm{sgn}(s_{o_i}) \qquad i = 1 \text{ and } 2 \qquad (0\text{-}15)$$

$$\dot{\hat{x}}_{o_{i+2}} = \hat{f}_{o_{i+2}}(\underset{\sim}{\hat{x}}_o, \underset{\sim}{u}) - K_{o_{i+2}} \mathrm{sgn}\left(s_{o_j}\right) \qquad (0\text{-}16)$$

The sliding surfaces are chosen to be:

$$s_{o_i} = \hat{x}_{o_i} - x_{o_{i_m}} = \tilde{x}_{o_i} \qquad i = 1 \text{ and } 2 \qquad (0\text{-}17)$$

where $x_{o_{i_m}}$ is the measured i^{th} state variable. The estimation error equations become

$$\dot{\tilde{x}}_{o_i} = \tilde{x}_{o_{i+2}} - K_{o_i}\mathrm{sgn}(s_{o_i}) \qquad i = 1 \text{ and } 2 \tag{0-18}$$

$$\dot{\tilde{x}}_{o_{i+2}} = \Delta f_{o_{i+2}} - K_{o_{i+2}}\mathrm{sgn}\left(s_{o_j}\right)\ i = 1 \text{ and } 2 \tag{0-19}$$

The K_{o_i} gains for i=1 and 2 are determined by satisfying the following sliding conditions:

$$\frac{1}{2}\frac{d}{dt}(s_{o_i}^2) \leq -\eta_{o_i}|s_{o_i}| \qquad i = 1 \text{ and } 2 \tag{0-20}$$

As a result, one gets

$$K_{o_i} \geq \eta_{o_i} + |\tilde{x}_{o_{i+2}}|_{\text{upper bound}} \qquad i = 1 \text{ and } 2 \tag{0-21}$$

The remaining gains of the SMO are determined by ensuring that the time derivatives of the following Lyapunov functions are negative definite:

$$V_1 = \frac{1}{2}\tilde{x}_{o_{i+2}}^2 \qquad i = 1 \; and \; 2 \tag{0-22}$$

which yields

$$K_{o_{i+2}} \geq \frac{F_{o_{i+2}}K_{o_i}}{|\tilde{x}_{o_{i+2}}|_{\text{desired\_accuracy}}} \quad \text{for} \quad i = 1 \text{ and } 2 \tag{0-23}$$

where the $\Delta f_{o_{i+2}}$ terms are substituted by their upper bounds $F_{o_{i+2}} = |\hat{f}_{o_{i+2}} - f_{o_{i+2}}|_{sup}$ for i=1 and 2.

Formulation of the Guidance System

The surge, sway and yaw motions must be controlled for a marine vessel to accurately track its desired trajectory. However, under-actuated vessels would only have two control variables, namely, the propeller thrust, F_{th}, and the rudder torque, T_{rud} to control the surge speed or displacement and the rudder angle-of-attack, respectively. Through the integration of the controller with the guidance system, T_{rud} will be able to compensate for both the sway motion and the heading angle.

The guidance system is based on the concepts of the variable radius line-of-sight (LOS) and the acceptance circle around the waypoints [19]. It assigns the desired heading angle, ψ_d, which aims at reducing the cross-track error, d, and orienting the ship to ensure rapid convergence to the desired trajectory (see Figure 0-1). The latter is usually defined by a set of waypoints connected with straight segments. This is illustrated in Figure 0-1 where (x_k, y_k) and (x_{k+1}, y_{k+1}) represent the coordinates of two consecutive waypoints on the desired trajectory and the current position of the vessel is given by (x, y).

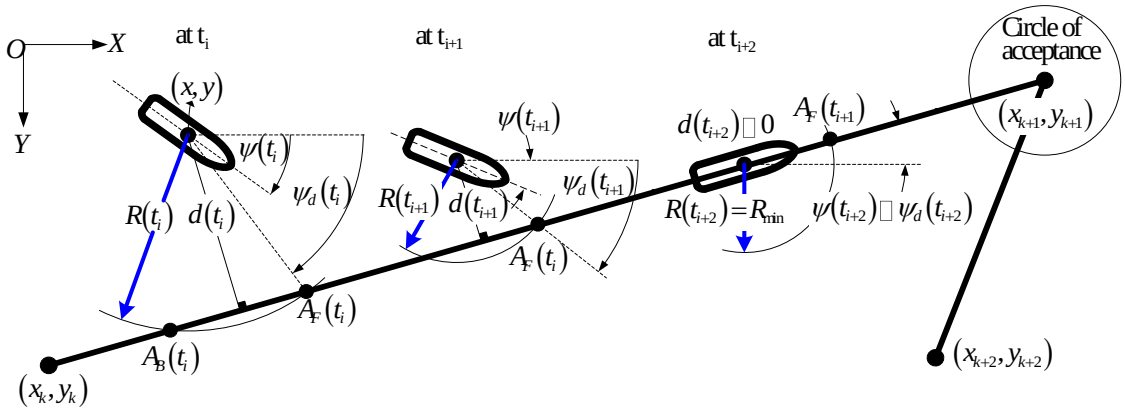

Figure 0-1 LOS Guidance scheme as it applies to marine surface vessels

The guidance system introduces a circle of radius, R, centered at (x, y). Original designs considered the radius to be constant and equal to αL_{ship}, which is a multiple of the ship length. When the ship is in close proximity to its desired path, the circle will intersect (x_k, y_k) and (x_{k+1}, y_{k+1}) segment at two points A_B and A_F (see Figure 0-1). The LOS is defined by the line starting from the current vessel position, (x, y), and ending at A_F. The angle between the LOS and the reference X-axis is considered to be ψ_d. A marine vessel moving along the direction of LOS will ultimately converge to the desired trajectory. However, guidance systems relying on a constant radius will fail to assign numerical values for ψ_d whenever d is greater than R. To

overcome this drawback, Moreira et al. Ref. [19] selected R to be $d + L_{ship}$; thus, varying the radius linearly with d. This will enable the guidance system to provide appropriate values for ψ_d irrespective of the magnitude of d.

Moreover, the guidance system is designed to switch from the consecutive pair of waypoints, $\{(x_k, y_k), (x_{k+1}, y_{k+1})\}$, to the succeeding pair $\{(x_{k+1}, y_{k+1}), (x_{k+2}, y_{k+2})\}$ whenever the ship enters a circle of acceptance centered at (x_{k+1}, y_{k+1}) and having a radius that has been chosen for the present work to be $2.2L_{pp}$ (see Figure 0-1).

Summary

This Chapter describes in detail the hybrid control strategy used in the current experimental work. Moreover, it provides an overview of the formulation for the surge displacement and heading angle controller, the nonlinear state observer and the guidance system. These formulations have been implemented using MATLAB\Simulink and Stateflow charts in the experimental validation of the robust performance of the integrated controller/observer/guidance system in the uncontrolled open-water environment of Lake St. Clair, Michigan.

In the next Chapter, an overview of the proposed collision avoidance scheme will be presented in detail.

CHAPTER 3 COLLISION AVOIDANCE

The LOS navigation system described in Section 0 has been modified in this study to expand its capabilities to avoid collision with stationary and moving obstacles. This was done by integrating the LOS guidance scheme with a modified version of the velocity obstacles (VO) technique while incorporating the COLREGS rules of maritime navigation.

The LOS navigation system employs waypoints that are chosen by a human operator to avoid known stationary obstacles such as land masses, shallow regions, navigation buoys, etc. Although, the collision avoidance system will have the ability to avoid such obstacles, the current study focuses on dynamic obstacles.

Rationale for Selecting the Velocity Obstacle Scheme

There are two different paradigms for implementing a collision avoidance system. The first one is to integrate collision avoidance into the guidance system where the desired trajectory is changed to avoid the collision. The second one temporarily overrides the guidance system to avoid the collision of the vessel with an obstacle and relinquishes the control back to the guidance system once the danger of a collision subsides. The selection of the paradigm for implementing the collision avoidance system strongly depends on the chosen guidance system. For example, the "Potential Fields" method allows for a natural integration of the guidance and collision avoidance schemes in a single system since there is no specific path defined. It uses a velocity vector field to direct the vessel around obstacles and toward its final destination. On the other hand, a waypoint navigation system prescribes a desired path for the vessel. To incorporate obstacle avoidance features in such a system would require the introduction of additional temporary waypoints to guide the vessel around an obstacle. However, these new waypoints

would only be an initial best guess and may not necessarily be sufficient or may cause excessive deviations from the original desired path should the obstacle change its speed or direction. Therefore, a temporary overriding of the waypoint guidance system would be the preferred paradigm in this case.

Since the waypoint navigation system is utilized in the current work then the overriding paradigm has been selected for the implementation of the collision avoidance method. The latter was chosen to be the "Velocity Obstacle (VO)" scheme since it possesses the desired capabilities needed for the task at hand. The VO approach greatly differs from the "Constant Bearing (CB)" scheme, which ensures convergence of the pursuer to its target by assigning the magnitude and orientation of the first component of the pursuer's velocity vector to be the same as those of the target's velocity vector while aligning the second component with the line-of-sight between the pursuer and the target. Instead, the VO scheme creates a safety zone around each obstacle and determines the relative velocities that would allow the vessel to pass the obstacle on the outskirts of the safety zone. Any relative velocity vector that would guide the vessel outside of the safety zone would prevent collision between the vessel and the obstacle. This technique has worked well since it predicts where the obstacle is going to be and reacts accordingly.

Velocity Obstacle Avoidance System

The Velocity Obstacle method generates a circular safety zone around each obstacle. Then, a collision cone is generated by defining its vertex at the current vessel's position and its sides are made tangential to the circular safety zone as shown in Figure 0-1. If the tip of the relative velocity vector between the vessel and the obstacle lies within the collision cone, then an infringement of the safety zone will occur should the current information remains the same.

Otherwise, the vessel will clear the obstacle without violating its safety zone. These two cases are illustrated in Figure 0-1.

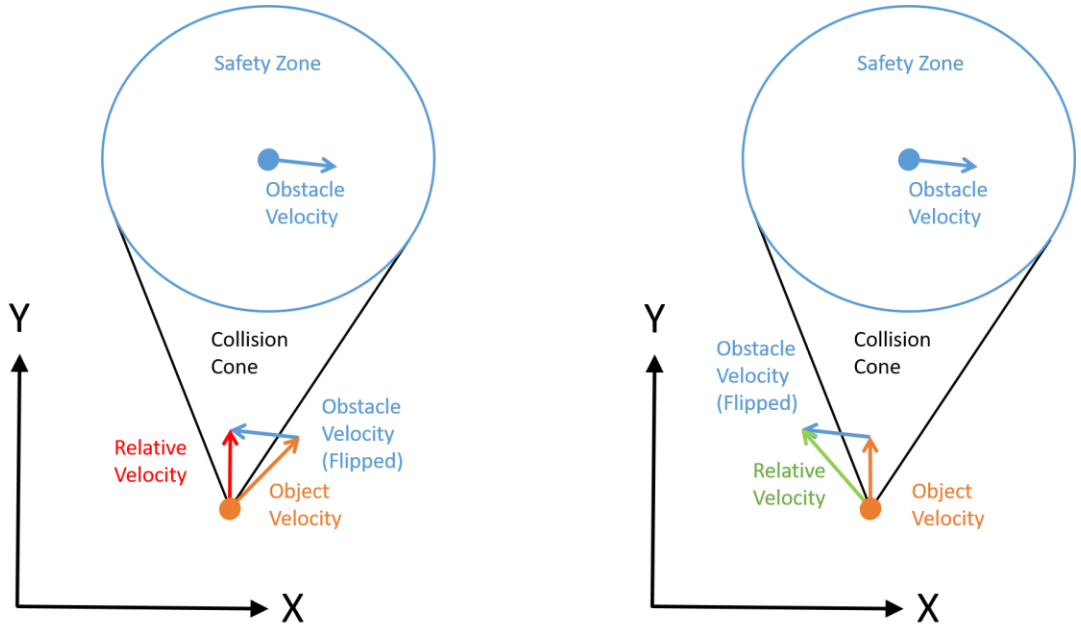

Figure 0-1 Left: Velocity obstacles showing a relative velocity that will result in a violation of the safety zone. Right: Velocity obstacles showing a safe relative velocity.

This method can be simplified by transposing the obstacle velocity vector onto the primary vessel current position and relocating the vertex of the collision cone to the tip of the transposed obstacle velocity vector. This will eliminate the need for computing the relative velocity vector between the vessel and the moving obstacle. Instead, the encroachment of the safety zone can now be determined based on whether the tip of the primary vessel's velocity vector is located within or outside of the collision zone. This is illustrated in Figure 0-2.

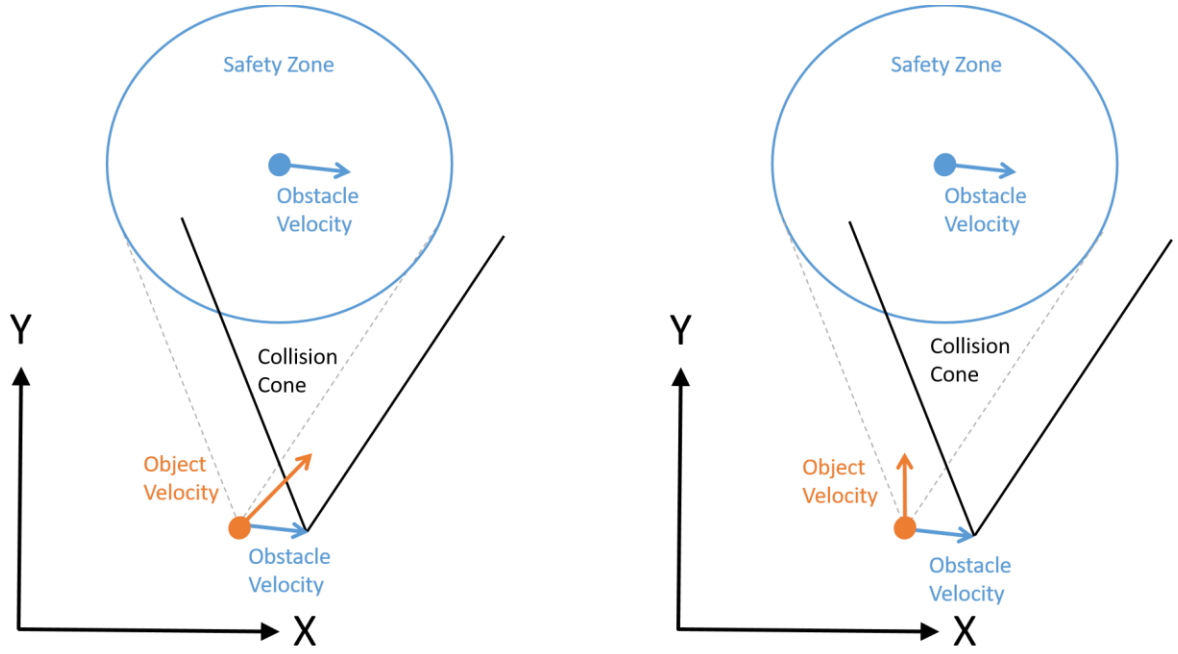

Figure 0-2 Left: Velocity obstacles showing a shifted collision cone and vessel velocity that will result in a violation of the safety zone. Right: Velocity obstacles showing a safe vessel velocity.

The physical limitations of the primary vessel would limit the admissible variations that can be made to the current velocity vector. The tips of the admissible velocity vectors corresponding to maximum and minimum vessel's speeds would form a contour whose intersection with the collision cone defines the subset of admissible velocity vectors that would lead to an encroachment of the safety zone surrounding the obstacle. The remaining area enclosed by the contour defines the tips of admissible velocity vector that would lead to a collision-free path whereby the vessel will either pass behind or in front of the moving obstacle. The area enclosed by the contour is referred to as the "reach window" since it signifies the set of velocity vectors achievable by the vessel.

In the presence of multiple obstacles, a collision cone will be generated for each obstacle (see Figure 0-3). The vessel will be able to avoid collision with all obstacles by ensuring that its velocity vector does not infringe on any of the collision cones.

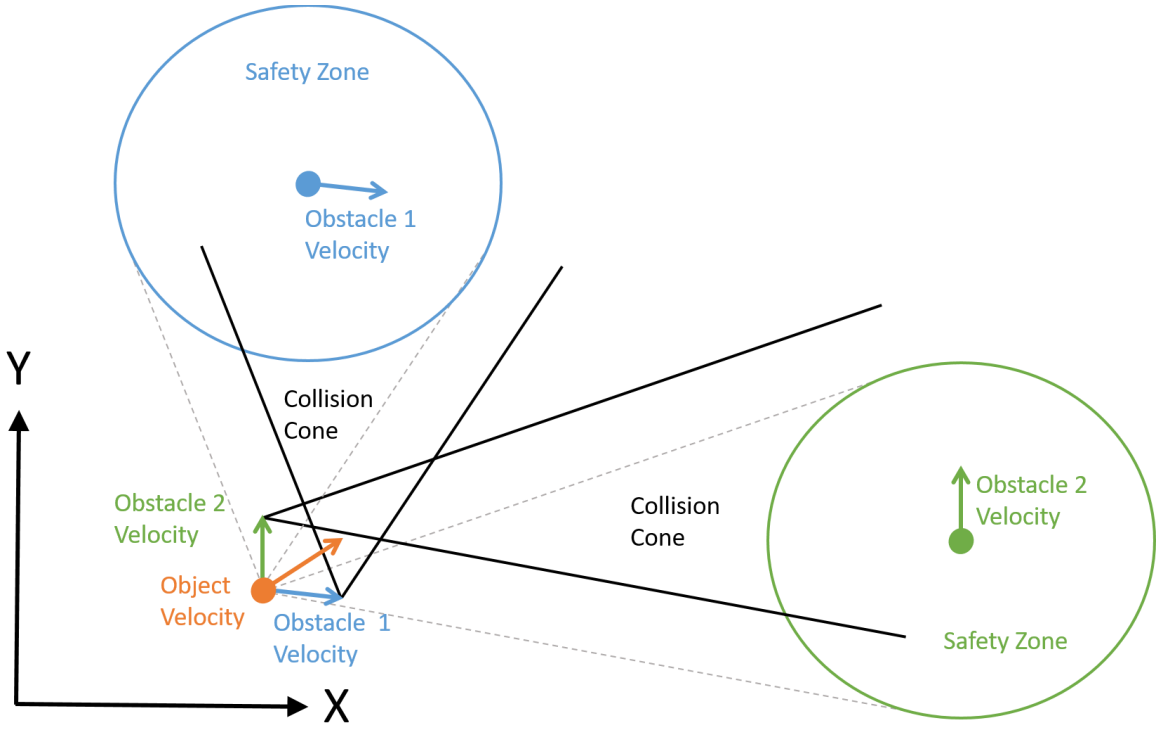

Figure 0-3 Velocity obstacles with shifted collision cones for two obstacles. The vessels current velocity will result in a collision with obstacle 1 but not obstacle 2.

Current Implementation of Velocity Obstacle Scheme

In the current work, the overriding paradigm of the guidance system has been selected to avoid any infringement on the collision cones. In addition, it was also determined that the smallest variations to the velocity vector commanded by the guidance system would lead to the least deviations from the overall desired path of the vessel. As a consequence, the new velocity vector commanded by the VO collision avoidance system should have its tip on the portions of the collision cone edges that are located within the contour. Any velocity vector having its tip within the contour but further away from the edges of the collision cones would result in unnecessary large deviations from the overall desired course of the vessel (Figure 0-4).

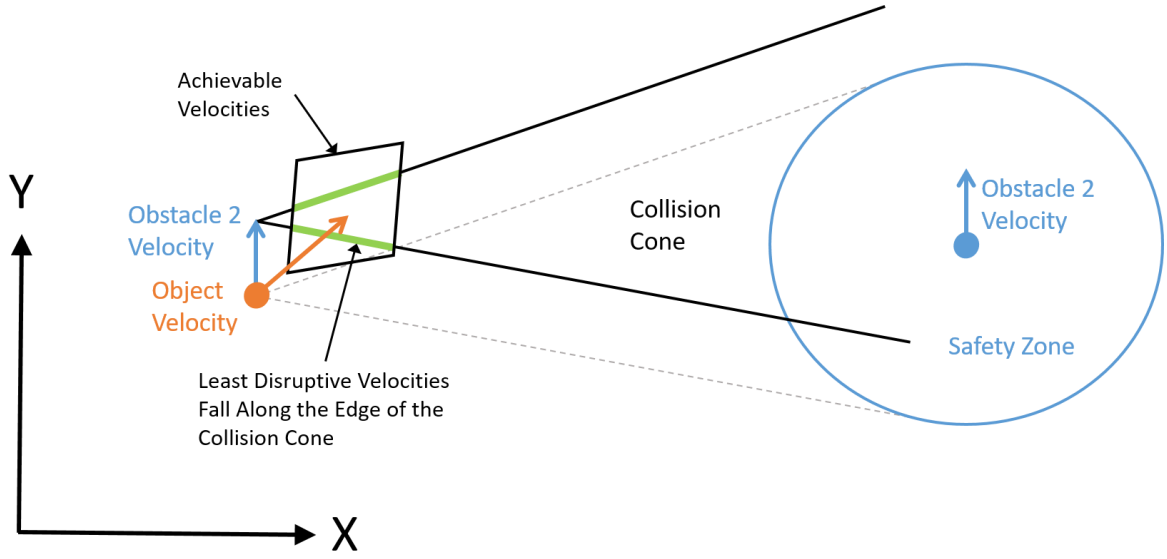

Figure 0-4 New velocities that will avoid a violation of the safety zone and be the least disruptive to the current velocity will fall on the edges of the collision cone.

Another important consideration in the implementation of the VO collision avoidance scheme is the adherence to the International Regulations for Preventing Collisions at Sea 1972 (COLREGs). According to these regulations, if the vessel has the right of way then it should maintain its course and speed. On the other hand, if the obstacle has the right of way then the vessel must yield, which means that it has to pass behind the obstacle. These rules significantly impact the outcomes of the VO system. Note that in order to avoid a collision without any consideration to the COLREGs rules, the vessel can either pass in front of or behind the obstacle, or the vessel can turn to move parallel to or away from the obstacle. With the limitations imposed by the COLREGs rules, the vessel must pass behind the obstacle. Thus, it will never be allowed to speed up and pass in front of the obstacle.

To avoid encroaching on the safety zone of an obstacle, the vessel can either change speed, direction or a combination of both. However, changing the speed of a marine surface vessel can have a significant impact on its performance. Small marine surface vessels operate in different

modes that are associated with their speeds. At slower speeds, the boat will be at "displacement speed", which causes the vessel to displace large body of water while moving. At medium or transition speeds, the bow of the boat will be much higher than the stern. This configuration is generally least efficient and difficult to operate. At high speeds, the vessel will be at "planning speed", which causes the vessel to skim the free surface of the water with only the rear portion of the vessel displacing water. Because of these phenomena, the slower the vessel moves the greater the effect of waves and currents would be. Moreover, the shape of the hull has a strong effect on the boat ride and the manner in which external forces induced by wave excitations, wind, etc. would impact the vessel's performance. To avoid these additional complexities, the vessel's speed was kept constant throughout the obstacle avoidance maneuver.

It should be emphasized that this approach of collision avoidance can certainly provide guidance to evade multiple obstacles simultaneously. However, in this work, multiple obstacles are handled individually based on a priority system. The closest obstacles represent the greatest threat and will be given the highest priority to be dealt with. Furthermore, this study was not intended for vessels operating in crowded areas. Instead, its main focus is on vessels operating in open water and traveling over long distances. Therefore, for a proof of concept, the main focus of this work was on evading a single moving obstacle.

Provisions incorporated in the code for COLREGs

When the obstacle avoidance scheme encounters a possible collision scenario, the situation will be analyzed to determine if the obstacle is far away to be of any concern. In this case, no action will be taken and the vessel will keep its course and speed. However, if it was determined that the obstacle is close enough to be of concern then a corrective action will be required. In

the absence of COLREGs, the corrective action can become complicated since there are no rules to follow when avoiding a collision. For instance, two vessels may try to avoid a collision by turning toward each other or each vessel may assume that the other will change course and no action is needed on its part. Actions taken in these scenarios will ultimately lead to more dangerous situations. This is the motivation behind the creation of COLREGs by The International Maritime Organization.

Basic COLREGs Implementation

Similar to rules applied on automobiles for determining the vehicle with the right of way or the vehicle that must yield to others, marine vessels have also predefined navigation rules. The International Maritime Organization published COLREGs, which defined a set of rules for navigation and safety at sea along with collision prevention. It should also be pointed out that power-driven vessels have a different set of rules than sailing vessels. For the purpose of this study, all vessels were considered to be power-driven. In addition, only COLREGs rules pertaining to collision avoidance are incorporated in the code of this study. However, these rules were suitable for human interpretation and they are not all encompassing. Many areas were left up to the discretion of the vessel's operator or his/her interpretation of the rules. As a consequence, these rules needed further clarifications in order to become suitable for coding. A case in point, a human operator will decide on what constitute a head-on collision between two vessels. This situation needs to be predefined in a computer code. If two vessels are perfectly aligned and heading towards each other will clearly represent a head-on collision situation. However, consider the case of two vessels that are slightly misaligned and heading towards each other. Would this situation still be interpreted by the code as head-on collision?

The need to define limits that were intended to be judged based on a situation has created interesting challenges and required the comprehension into the intent of these rules as much as the understanding of the letter of the rules. The interpretation of the intent appeared to have a desire to create a smooth, safe flow of traffic at sea. Therefore, the boundaries defining these different situations needed to reflect and promote this intent. It was decided that these limits needed to be defined in a single location so that they could be easily modified during testing to home in on functional values. Through running multiple simulations, the final values were established.

COLREGs are defined by multiple factors that need to be accounted for when determining an appropriate action. There is also a distinct lack of resolution in these rules that leaves things open to judgement by the human operator. The rules are generally defined by the direction in which the boat is approaching (see Figure 0-5).

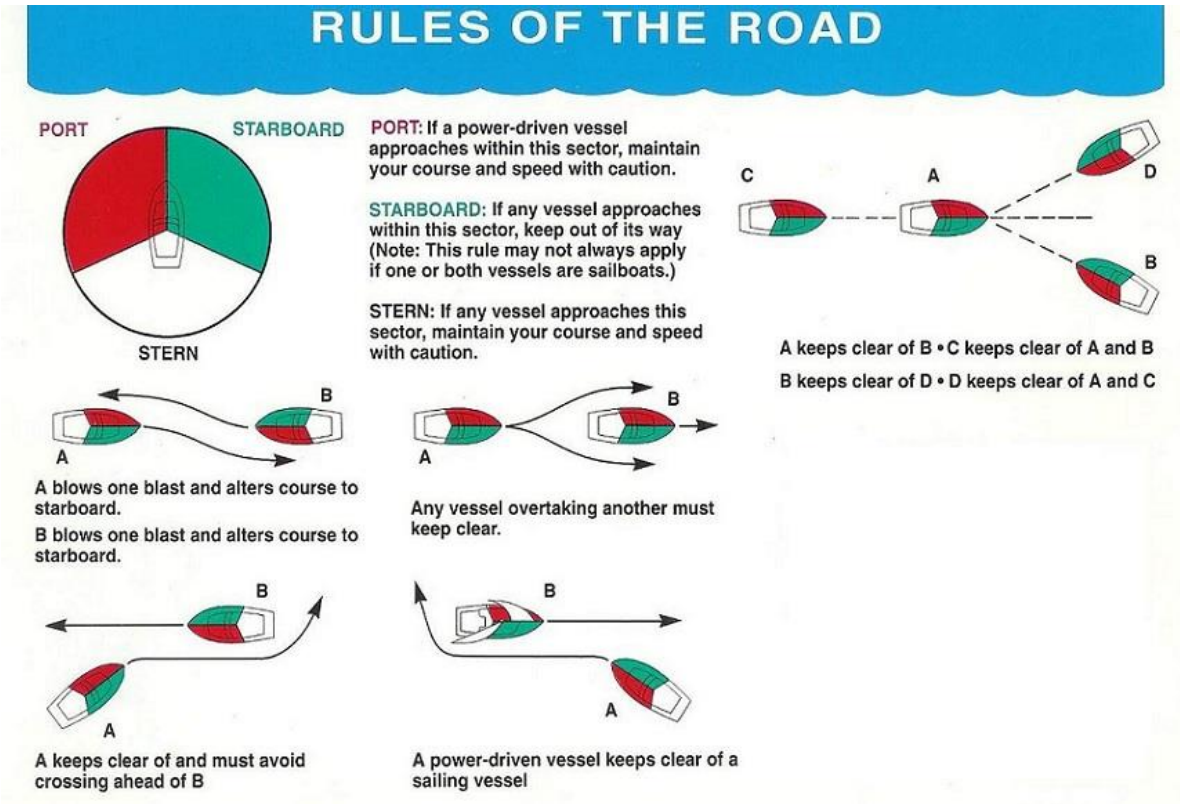

Figure 0-5 Pictorial demonstration of COLREGs Steering and Sailing Rules. Sourced from https://w.willsmarine.co.uk

There are situations in which two vessels can approach each other and neither one is required to yield to the other according to the COLREGs rules (Figure 0-6). These situations are less common and can easily be accounted for by a human operator. However, such fringe situations are not trivial when it comes to autonomous operation of the boat and had to be explicitly dealt with in the code.

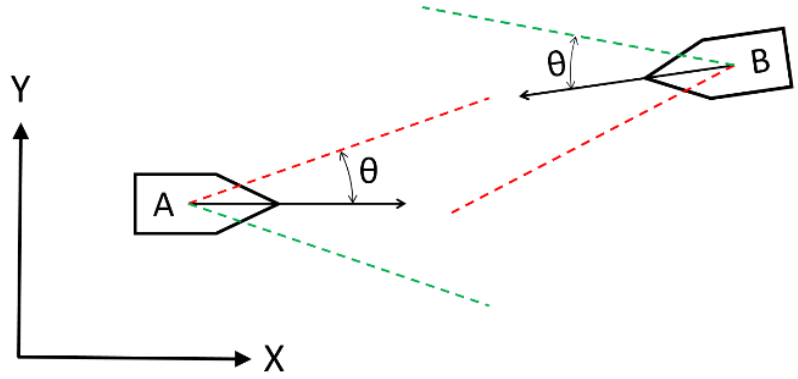

Figure 0-6 Both vessels observe the approaching vessel from the Port side meaning that both should maintain their course and speed.

There are also situations that are not clearly defined. Rule 14 section (a) of COLREGs for a Head-On Situations states "When two power-driven vessels are meeting on reciprocal or nearly reciprocal courses so as to involve risk of collision each shall alter her course to starboard so that each shall pass on the port side of the other". This is a clear representation of how COLREGs are intended to be used by humans with a final judgement made based on a given situation. Reciprocal or nearly reciprocal is subjective and requires interpretation which may change based on other conditions. The left side of Figure 0-7 shows that these vessels should clearly alter course to starboard as to pass each other on the port side. However, the figure on the right would still need to follow the same rule which would require both vessels to cross paths. In this situation, human will most likely adjust course to port as to pass each other on starboard even though this is action is not consistent with COLREGs. This would cause the least disruption to both vessels current courses and would prevent them from crossing paths.

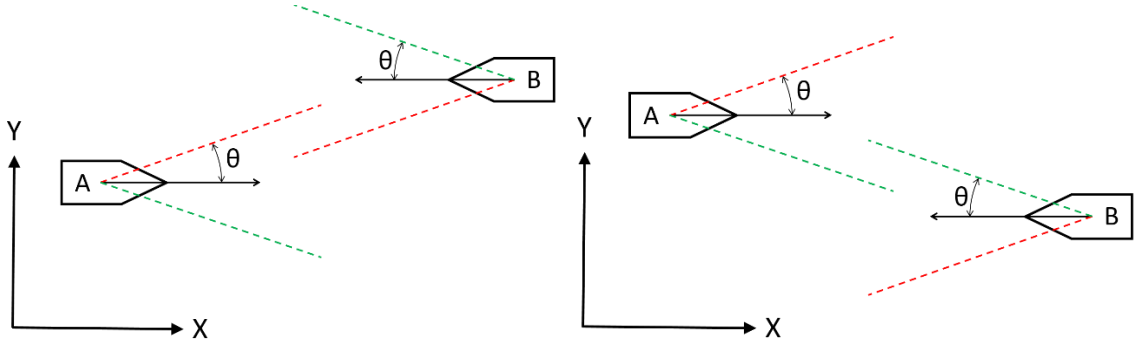

Figure 0-7 Left: These vessels should adjust to starboard to avoid encroaching safety zones. Right: Following COLREGs would require both vessels to alter course to the right resulting in the crossing of each other's path.

There are many transitional situations that are encountered during the normal operation of a marine surface vessel. If a vessel transitions from the side to the front or rear of another vessel then a smooth motion must be maintained (see Figure 0-8). A human operator would not necessarily pay attention to such a transition. Instead, a human would plan a more complete maneuver without paying attention to these transitions. The collision avoidance program needs to accomplish this maneuver by handling transitional situations seamlessly in order to mimic the behavior of the human operator.

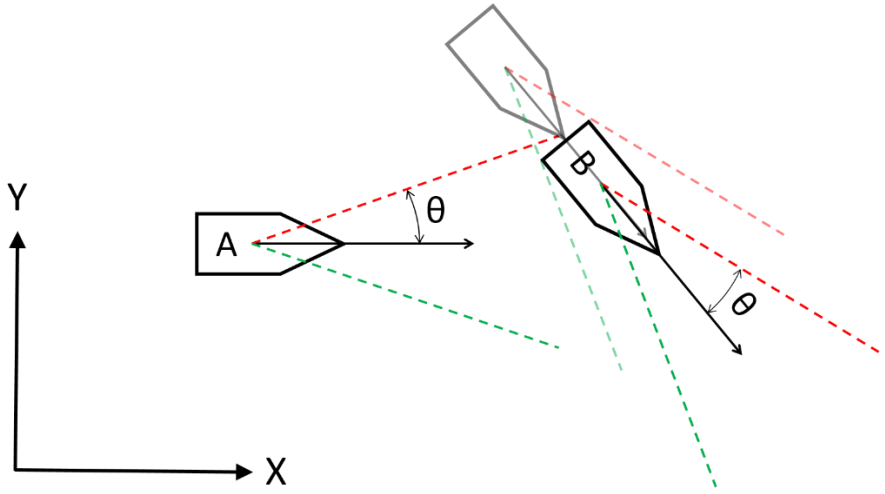

Figure 0-8 Vessel A will observe vessel B transitioning from being on the left to being in front and must maintain a smooth trajectory to prevent erratic movements.

After studying not only the rules but also their intent, three variables were recognized as being necessary to determine the appropriate corrective action of the vessel. The first one identifies the vessel approaching the primary one. The second one determines the location of the approaching vessel with respect to the primary vessel and the last one represents the angle with which the vessel is approaching the primary one. This information was calculated for all vessels within a predetermined distance from the primary vessel. It was not only used to determine the appropriate action of the main vessel but also to predict the actions of other vessels. It can be assumed with a fair amount of confidence that other vessels will adhere to COLREGs rules; thus, making their responses to a given situation reasonable and predictable.

Contingency plan when approaching vessels violate COLREGs rules

Although it can be assumed with a reasonable amount of confidence that other vessels will adhere to COLREGs, it is not always guaranteed. Therefore, contingencies had to be written in the code to account for these situations. As mentioned previously, if there is a predicted collision then there are two zones. The first one involves vessels that are far away to pose a safety concern while the second one includes vessels posing a threat and corrective actions may be required. Since it cannot be taken for granted that all vessels will obey the rules then the number of zones has now been increased to four in the case of a predicted collision. The first zone will involve vessels that are far away to be a safety concern. The second one includes vessels that are being tracked but assumed to be following COLREGs. The third one relates to vessels that do not yield in spite of the fact that they are supposed to according to the rules. The last one involves vessels that are dangerously close (Figure 0-9).

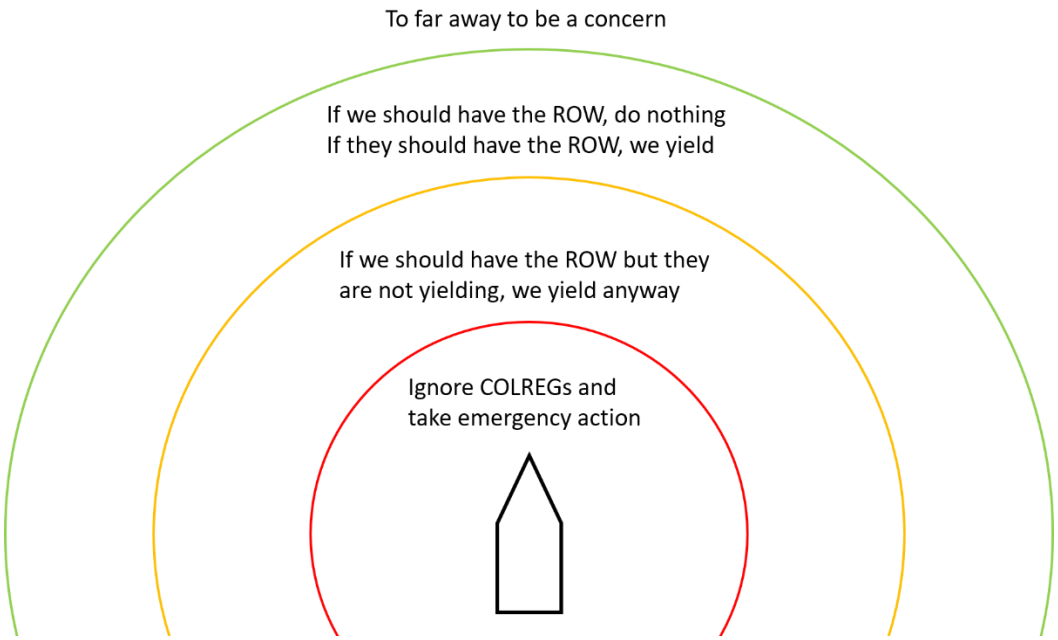

Figure 0-9 Zones have been defined to determine the appropriate course of action.

There are two reasons for ignoring far away vessels. First, these vessels do not pose safety concerns. Second, their speeds and/or directions will likely change during the long period that may take them to approach the primary vessel. Thus, any action to avoid them would most likely prove to be a wasted effort. Next, for the vessels that are being tracked but assumed to follow COLREGs, the primary vessel will yield for them if they have the right-of-way (ROW). Otherwise, the primary vessel will not take any action since it is assumed that the other vessels will adjust their courses accordingly. In the third zone, additional precautions and appropriate actions have to be taken since the primary vessel is now encountering vessels that do not follow the rules. In the fourth zone, the primary vessel has to take emergency measures because the obstacle vessel is within its close proximity. In this situation, it cannot be guaranteed that a collision will be avoided. However, actions must be taken as a last effort to avert collision. Simulation results have demonstrated that if an obstacle vessel is approaching very fast then the primary vessel would not be able to avoid encroachment into the safety zone. In this case, the collision

avoidance system would not take action because all actions would be in vain. As a result, contingencies were added in the code to take preventive action for minimizing these types of violations. Commands will be given even though the boat may not be able to achieve them. Although the encroachment of the safety zone cannot be completely avoided, it can be minimized and hopefully avoid an actual collision.

Special features distinguishing this study from previous work

As stated in the literature review section, the velocity obstacles (VO) method has been implemented for marine vessels incorporating COLREGs. However, there are two main distinctions between previous work and the current one. First, the studies that have incorporated COLREGs have only demonstrated the system's functionality in very simple situations. The performance of the system has not been proven in complex real-world scenarios. Furthermore, these studies did not provide enough details on how they accounted for the lack of granularity in COLREGs and how they overcame these shortcomings in their implementation. Therefore, the level that COLREGs has been incorporated and the performance of the system cannot be verified. Second, these studies have only considered predictable operating conditions and assumed that all vessels obey the rules. For any real-world application, it is necessary for a system to be able to account for objects that are not acting according to the rules. Whether through malice or neglect, these situations occur and must be taken into consideration. The implementation used for these experiments fully incorporate COLREGs in the collision avoidance system and accounts for obstacles that are not following the rules.

Summary

This chapter described the implementation of the collision avoidance method and how it incorporates COLREGs rules for safe navigation. Moreover, it provides a detailed discussion on how the lack of granularity in COLREGs have been accounted for in the current code. In addition, it highlights the distinctions between previous work and the current one on the implementation of COLREGs in the collision avoidance system.

In the next chapter, the experimental validation of the fully integrated controller, observer and guidance system will be presented.

CHAPTER 4 EXPERIMENTAL VALIDATION OF THE FULLY-INTEGRATED CONTROLLER/OBSERVER/GUIDANCE SYSTEM

The robustness to environmental disturbances and modeling inaccuracies of most advanced control algorithms have been demonstrated through digital simulations. While there exists much theoretical work with simulations involving the control and guidance of marine surface vessels [20, 29, 30, 32, 37], actual experimental studies are scarce [39]. The overwhelming majority of the experimental work on autonomous marine surface vessels was not conducted in truly uncontrolled real-world environments.

Although theoretical simulation is necessary, it is only the first step in proving the efficacy and robustness of this type of systems. The main focus of the current work is to experimentally validate a fully-integrated guidance system with a sliding mode controller and observer in a totally uncontrolled environment using a 16' aluminum boat with a 60 hp outboard motor operating in the open-water of Lake St. Clair, Michigan. The experimental results collected under a variety of weather conditions involving significant variations in lake temperature, wind resistance, wave height, current magnitudes and directions are presented in great detail in this chapter.

Description of the Experimental Setup

Description of the Vessel

The experimental work was conducted using a 16' aluminum Tracker Pro Guide V-16 fishing boat with a 60 horsepower Mercury outboard motor (see Figure 0-1). The experiments were conducted in the uncontrolled waters of Lake St. Clair, Michigan. The boat in its stock configuration did not have sufficient electrical power for the equipment needed to run the

experiments. Moreover, it was not equipped so that it can be controlled electronically; thus, significant structural and electrical modifications had to be made on the boat.

Figure 0-1 16' Boat used in the experimental work.

Modifications to the Vessel

Electrical Power Improvements

The power shortage on the boat was solved by adding three additional 12-volt lead acid batteries. These batteries were mounted in the bow of the boat in a storage compartment along with a battery charger that was capable of charging all three simultaneously. During charging, the two covers for this compartment were left open providing adequate ventilation to prevent overheating. These additional batteries were used for two purposes. The first one was used to provide extra power for the laptop. The computer had built in power but lacked the capacity to allow for a full day's operation. This also allowed us to plug in the Wi-Fi hotspot eliminating the need to charge it at the end of the day. The power from this battery was routed through a front panel on the boat and down into a compartment with existing wires, which allowed a panel to be added in the rear of the boat to provide two 12-volt accessory ports and two USB charging

ports. A DC to DC charging plug was purchased for our Dell XPS 13 laptop allowing the computer to run experiments for a full day.

The second pair of batteries were connected in series creating a 24-volt supply to power the rest of the equipment that was required for electronic control of the vessel. The 24-volts was directly used to power the dSpace unit which was the real-time controller of the system and the brushless motors that were added to actuate the steering and throttle of the boat.

Electronically Controlled Throttle

The throttle mechanism on the boat was intended for human operation and uses a series of cables to actuate the linkage inside the outboard motor. In order to interface with this system, an actuator had to be installed. Adding the actuator directly at the outboard proved difficult due to a lack of space inside the engine compartment and therefore it was decided to interface with the throttle handle located next to the driver's seat (see Figure 0-2). The system consisted of an arm attached to a Faulhaber brushless motor with a planetary gearhead and incremental encoder. An arm with a fork that captured the throttle arm was attached to the gear head creating the interface to the handle. This system was mounted on an X-Y table to allow for alignment with pivot axis of the throttle handle. When the vessel was under manual control, this system was backed away from the throttle handle allowing for direct manual control over the boat throttle. When electronic control was required, the mechanism was translated forward to engage the arm of the throttle.

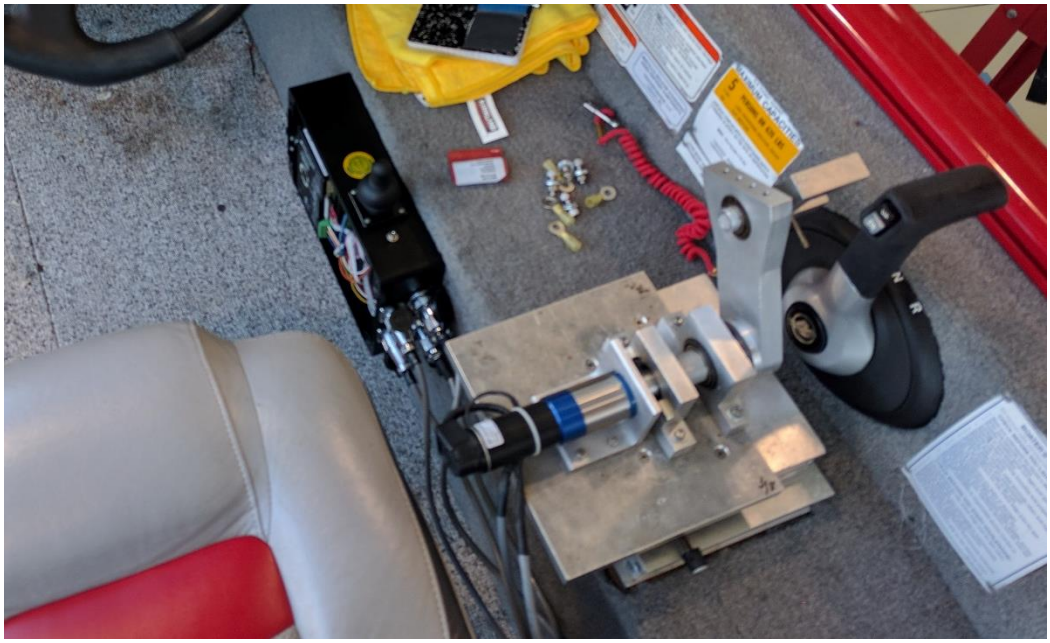

Figure 0-2 Actuator that enabled electronic control of the throttle

Electronically Controlled Steering

To allow for electronic control over the steering, it was first considered to use the steering wheel of the boat. During this investigation, it was observed that that this system had an undesirable amount of backlash which created excessive inaccuracy in the system. Therefore, a system had to be designed and built that would enable steering by directly connecting a point on the outboard motor to the boat (see Figure 0-3). The base of this system was attached to the deck of the boat with a bearing and a hinge while the dynamic end of the mechanism was attached to a pin mounted on the front of the outboard using a ball joint (see Figure 0-4). These passive joints allowed for enough degrees of freedom to prevent bending while still constraining the system. The joint that engages the pin at the front of the outboard motor is locked in place with a hairpin cotter pin to prevent detachment while in operation. When this pin is removed the system can slide off the pin allowing for easy disengagement and release.

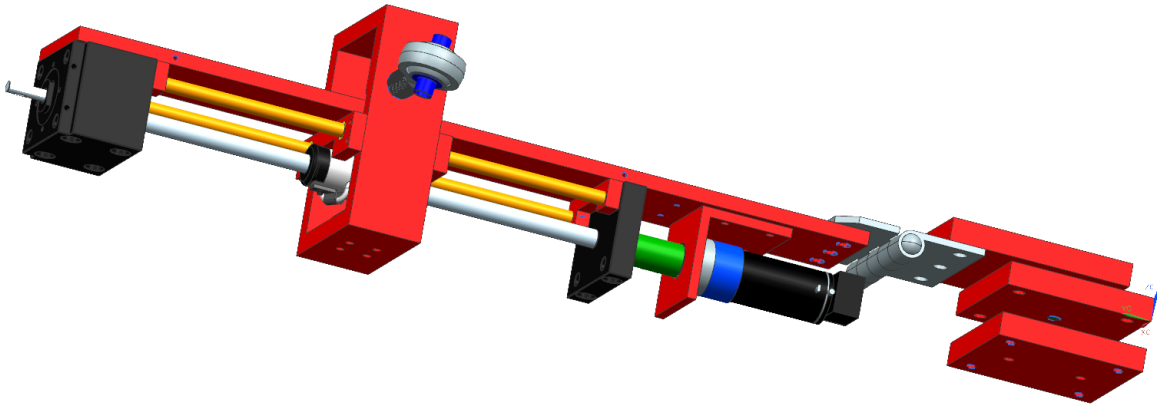

Figure 0-3 3D model of the steering mechanism

Figure 0-4 Actuator that enables electronic control over the steering

Drive by Wire

When these two systems are engaged, the person driving the boat can no longer manually operate the controls. To avoid the need to continuously engage and remove these systems it was decided to incorporate a drive by wire system. This was accomplished by adding a joystick next to the driver's seat allowing the person operating the boat to have control with either the traditional boat controls or by the joystick (see Figure 0-5). This joystick was read by an Arduino Uno which then translated its output into a +/- 5-volts signal which is readable by the motor drivers.

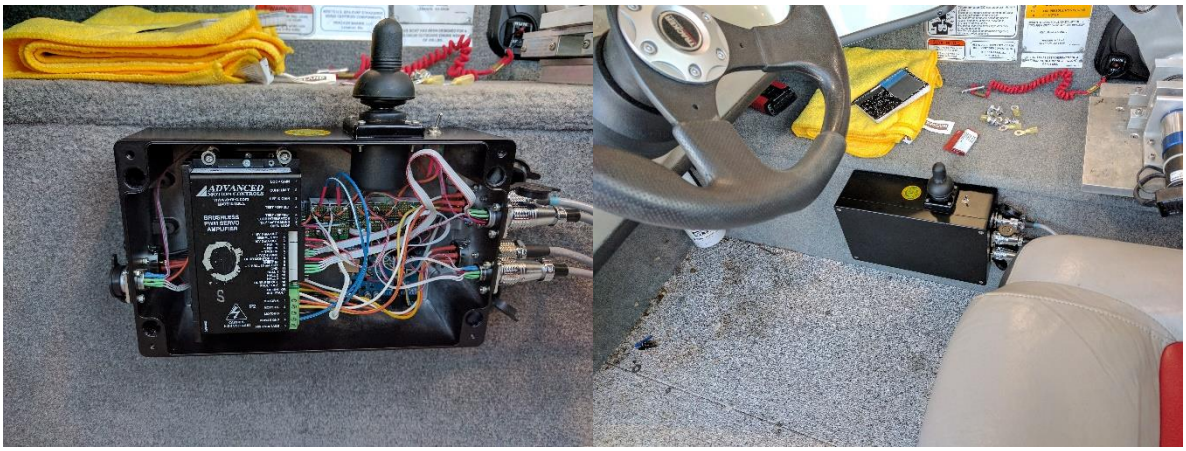

Figure 0-5 Drive by wire system

The system needed the ability to be controlled by both the drive by wire system and the dSpace unit and therefore a method for switching between these two systems needed to be designed (see Figure 0-6). A series of relays were added allowing a simple manual switch to control this transition with a single point of input. This not only gave the boat operator an input method for switching between the two systems but has also added an independent system to detach the dSpace unit in the case of an undesirable event. This system was housed inside an aluminum project box with a water tight seal around the lid to protect it from the environment. This box also acted as a pass through for the encoder signals from the motors and managed the power going to them.

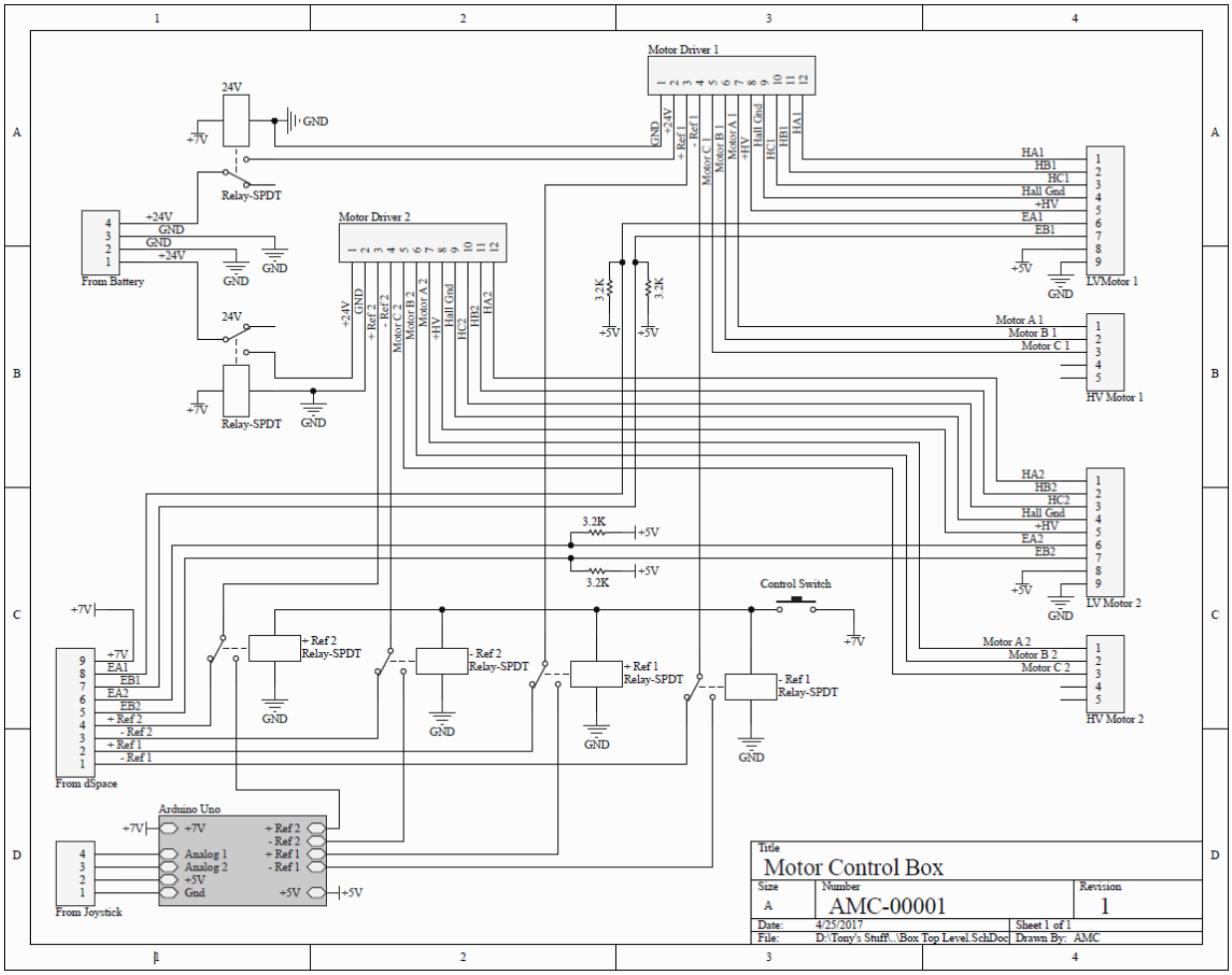

Figure 0-6 Electrical schematic of the control box that housed the drive by wire system and the motor drivers

Real-Time ECU and Communications Unit

As with the drive by wire system, the dSpace unit, wireless router, and power management needed to be protected from the environment. These components were mounted inside a Pelican 1620 Protector Case, which is waterproof and has wheels that allowed for easy transport (see Figure 0-8). The case was modified to permit communication from inside of the box to the outside. A total of ten waterproof connectors were added, more than the current communication needs, accounting for future expansion as the project progresses. It was also

decided to mount the GPS on top of the box which consolidated the entire autonomy kit into one unit (see Figure 0-7) opening the opportunity to use the kit on other vehicles in the future.

Figure 0-7 Pelican Case with mounted GPS creating a complete autonomy kit

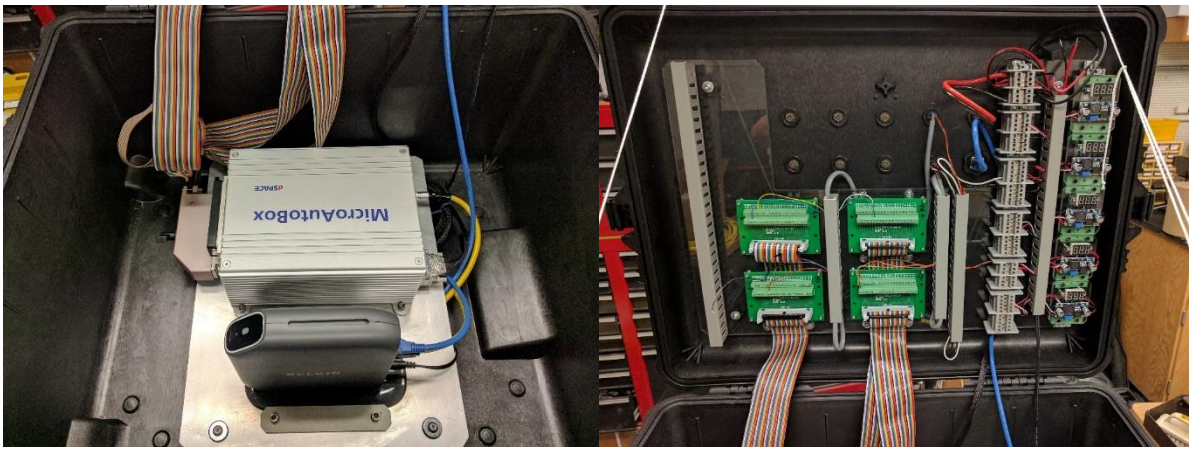

Figure 0-8 Inside of the Pelican case that protects the autonomy kit

dSpace MicroAutoBox II

A dSpace MicroAutoBox II 1401/1513 is the brains of the autonomy kit. It is an in-vehicle prototyping ECU designed for real-time applications. It has a compact and robust design that has been specifically designed for use in real-world conditions. The system has a 900 MHz processor, 16 MB of memory and is equipped with multiple communication interfaces including Serial, CAN,

CAN FD, LIN, K/L Line, FlexRay, and Ethernet. There are also thirty-two 16-bit analog inputs, eight 16-bit analog outputs, and forty-eight digital IO pins which allowed the unit to be customized to fit our application. The unit directly reads the output from the GPS, the two encoders that were attached to the throttle and steering actuators and provides the control signals to the motor drivers allowing for closed-loop control.

The MicroAutoBox II is programmed through a laptop computer using MATLAB, Simulink, and Stateflow charts through the Real-Time Interface (RTI) software that is also available through dSpace. The software is equipped with a library of I/O modules that connect with blocks in the Simulink library allowing the units capabilities to be programmed graphically in a Simulink model. This software is then used in tandem with MATLAB and a C compiler to convert these programs into real-time firmware and load it onto the ECU.

The RTI software also provides a customizable graphical user interface (GUI) which runs on a laptop computer. Therefore, an operator can interact with the unit during an experiment through virtual buttons, switches, and input boxes (see Figure 0-9). This eliminates the need to build a dashboard with physical controls thus streamlining the prototyping phase even further. During testing, there is a need to start and stop tests, adjust values, engage a software emergency stop, etc. which is all performed through this interface.

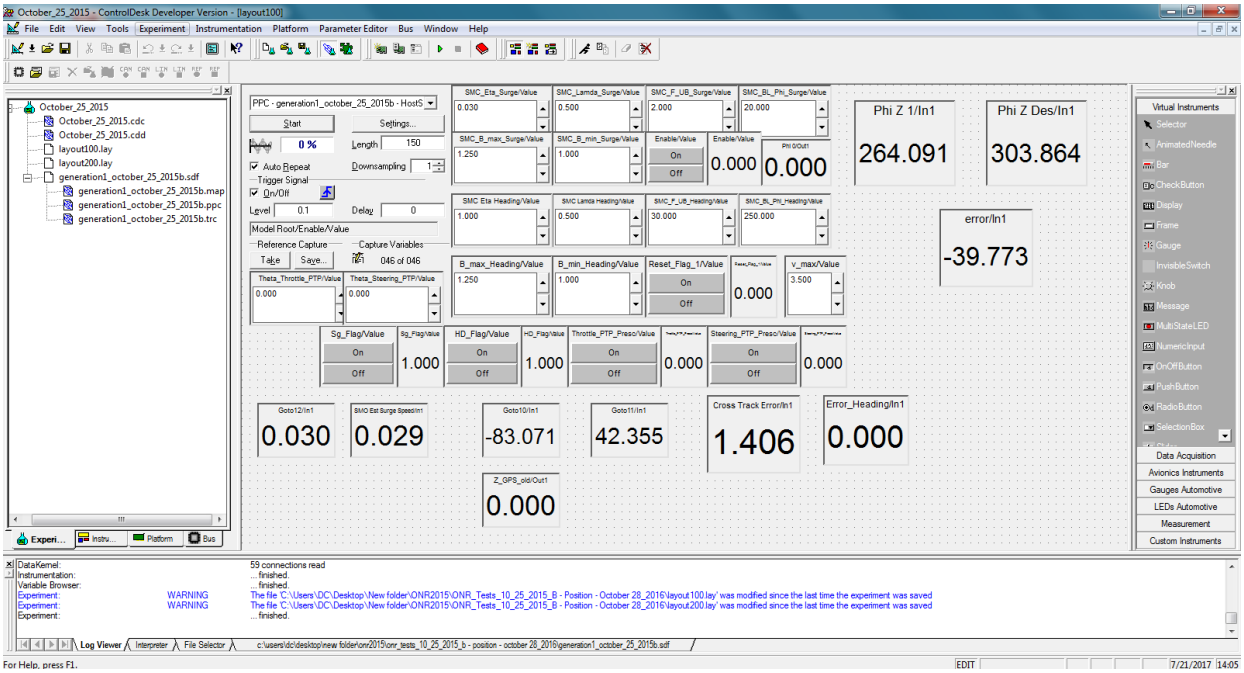

Figure 0-9 dSpace Real-Time Interface GUI

GPS, Wireless Router, and Voltage Regulators

For this portion of the work, the only sensor providing information about the surrounding environment was a Hemisphere V101 differential GPS, which has a horizontal accuracy of less than a meter under ideal conditions. The data obtained from the GPS was then used to estimate all other state variables. When this work first began, there was also a Crista IMU which allowed the system to know the heading angle of the boat before the test began. Aligning the axes of the GPS and IMU proved to be problematic resulting in errors between the two units. Since small alignment errors created substantial performance problems, it was decided to eliminate this sensor since the heading could be calculated from the GPS data alone once the vessel began moving under power. As mentioned previously, the GPS was mounted on top of the Pelican case that housed the rest of the autonomy components meaning that the entire case needed to be mounted in a central point of the boat to minimize errors in the overall system.

The connection between the laptop computer and the MicroAutoBox II is handled through an ethernet connection. This can be achieved through a direct wired connection or can be configured to communicate over a network. A direct connection would have required permanently attaching an ethernet cable to the boat which was undesirable since it was unknown how well it would tolerate being parked outside in a boat well all summer. This meant that the ethernet cable would have to be temporarily routed across the floor of the boat creating a safety concern. To eliminate this concern, this connection was made wirelessly since there was no predicted negative impact on performance. It was therefore decided to configure the connection over a network since this allowed the communication to be performed through a Wi-Fi connection. A Belkin N600 wireless router was connected to the dSpace MicroAutoBox II via an ethernet cable. The laptop was then connected to the local area network (LAN) allowing interaction between the two units without the need for a physical connection.

There is a 24-volt power source provided to the Pelican case which is used to power the dSpace MicroAutoBox II. However, the GPS, router, encoders, Arduino and other components required a variety of different voltage levels. Five adjustable switching voltage regulators were added inside of the case to provide these different voltage levels along with power distribution blocks. This permitted easy attachment of multiple devices to each voltage source and allowed for future modifications or expansion.

Experimental results

The aim of this Subsection is to provide experimental validation of the robust performance of the fully integrated guidance and controller-observer system. Note that the guidance system has been described in Sub-Section 0. The heading and surge displacement controllers are

presented in Sub-Section 0. While the sliding mode observer (SMO) is included in Sub-Section 0. The experimental results have been generated in the uncontrolled environment of Lake Saint Claire, Michigan. In each test, the operation of the marine surface vessel was continually monitored by a high level supervisory code, which will disable both surge and heading controllers and activate a "recovery" strategy in case of an impending dangerous situation. All experimental results of this Section have been generated on the same day where the local air temperature on the lake was $56^o F$ and the wind direction was 118^o east-southeast (ESE). Moreover, the wind speed was 5.5 kts (6.4 mph) and wind gust was 6 kts (6.9 mph). The dominant wave height was under 2.0 ft. The results of two experiments are presented herein. Note that all tests in the current work were conducted by setting the dynamics of the nominal model to zero, which translates into completely neglecting the dynamics of the marine surface vessel in the computation of the control signals as well as in the estimation of the required state variables. Therefore, the fully integrated guidance and controller-observer system was tested in the current work in a model-less configuration, whereby all information provided from the vessel's nominal model have been ignored.

In the first experiment, the desired trajectory consisted of three segments connecting the following waypoints:

$\mathrm{A}(X_1 = 0\ m, Y_1 = 0\ m)$ $\mathrm{B}(X_2 = 200\ m, Y_2 = -200\ m)$

$\mathrm{C}(X_3 = 0\ m, Y_3 = -400\ m)$ $\mathrm{D}(X_4 = 200\ m, Y_4 = -600\ m)$

This is depicted in Figure 0-10. The behavior of the boat near waypoint A reveals that it was initially pointing away from the desired trajectory (see Figure 0-11). As a consequence, the boat had to turn around in order to converge to the first segment of the desired trajectory. This is

clearly shown in Figure 0-12 shown that the cross-track error, d, dropped from around 15 m to less than 2 m during the period when the boat was tracking the first segment of the desired trajectory. The spike in the cross-track error at $t = 83\ sec.$ stems from the fact that the boat entered the acceptance circle centered at the second waypoint B that has a radius 15 m. As a result, the guidance system will shift its tracking focus from the first to the second segment of the desired trajectory. It should be pointed out that the initial spike dropped down to zero in 4 secs at which time the boat has crossed the second segment or its extension. However, the cross-track error grows back to 13.7 m as the boat maneuvers around the second waypoint B to align itself with the second segment of the desired trajectory. Figure 0-10 to Figure 0-12 demonstrate the robustness and good tracking characteristics of the integrated guidance and controller/observer system by overcoming the large cross-track error induced at the beginning of each segment and converging the boat to the desired trajectory in spite of the fact that both controller and observer were implemented in a model-less configuration and in the presence of considerable environmental disturbances. Figure 0-12 reveals that the cross-track error was reduced and maintained within $2m$ for all three segments of the desired trajectory. Moreover, the response pattern of the boat was similar for all segments of the desired trajectory, which crisscrossed the lake and subjected the boat to significantly different wave excitations, currents and wind loads. Figure 0-13 illustrates the desired heading angle specified by the guidance system. It also demonstrates the robustness of the heading controller in forcing the actual heading angle to converge to the desired one. Figure 0-14and Figure 0-15 represent the desired and actual time derivatives of the heading angle. Figure 0-16 shows the heading control signal, $u_{Heading}$, and the sliding surface, $s_{Heading}$. The ultimate goal of the heading controller is to

reduce $s_{Heading}$ to zero and maintain it at that value. As a result, the error in the heading angular displacement will be driven to zero; thus, causing the actual heading angle to converge to its desired value. However, due to structured and unstructured uncertainties along with external disturbances, the system will be pushed away from the sliding surface $s_{Heading} = 0$. In its attempt to drive the system back towards $s_{Heading} = 0$, the heading controller has applied a control signal that is out-of-phase with $s_{Heading}$ (see Figure 0-16). Such a corrective action is consistent with those of controllers that are derived based on the variable structure systems theory. Furthermore, Figure 0-16 reveals segments where the heading control voltage is saturated. It should be emphasized that a saturated command control voltage of the heading drive mechanism does not necessarily mean that the rudder is now locked in place and has reached its maximum rotational limits. Actually, it only indicates that the ball-bearing screw is now spinning at its maximum rotational speed, which causes the tiller arm that is connected to the outboard motor through a bracket to move at its maximum forward or backward speed. Consequently, the rudder would now be turning at its maximum angular velocity, which keeps on increasing the steering torque of the boat in spite of the fact that the control command voltage of the heading drive mechanism has already been saturated for a period of time. This argument is confirmed in Figure 0-17, which shows that the tiller arm was operating throughout the test within its allowable linear displacement range of $\pm\, 0.070m$.

Figure 0-18 illustrates the surge displacement and velocity profiles along the segments of the boat's desired trajectory. The desired surge speed profile along the i^{th} segment connecting the (X_i, Y_i) and (X_{i+1}, Y_{i+1}) waypoints has an acceleration phase, a constant cruising speed phase and a deceleration phase. The acceleration phase starts when the boat exits the acceptance circle

surrounding the (X_i, Y_i) waypoint and ends when the surge speed reaches the cruising speed. Beyond that point, the boat will maintain a constant cruising speed until it enters the acceptance circle surrounding the (X_{i+1}, Y_{i+1}) waypoint. At that point, the deceleration phase begins and ends when the surge speed reaches a specified maneuvering speed. Beyond that point, the boat will maintain a constant maneuvering speed until it exits the circle of acceptance surrounding the (X_{i+1}, Y_{i+1}) waypoint. This speed profile has been adopted for all other segments except for the first and last segments of the desired trajectory. In the first segment, the boat will start from an initial speed dictated by the environmental conditions of the boat. While the maneuvering speed of the last segment is usually set to zero. It should be pointed out that for short transition periods between the i^{th} and $(i+1)^{th}$ segments the boat may shift from a deceleration to an acceleration phase without going through a cruising phase (see Figure 0-18). In the current work, the desired surge speed profile has been generated online based on the boat position relative to the waypoints of the desired trajectory.

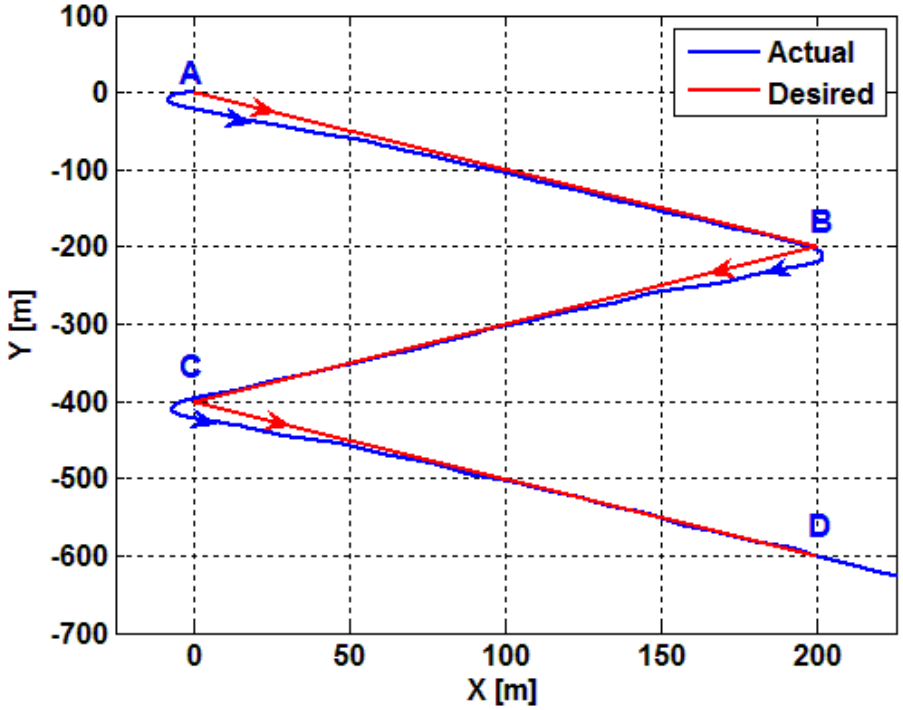

Figure 0-10: Desired and actual trajectories

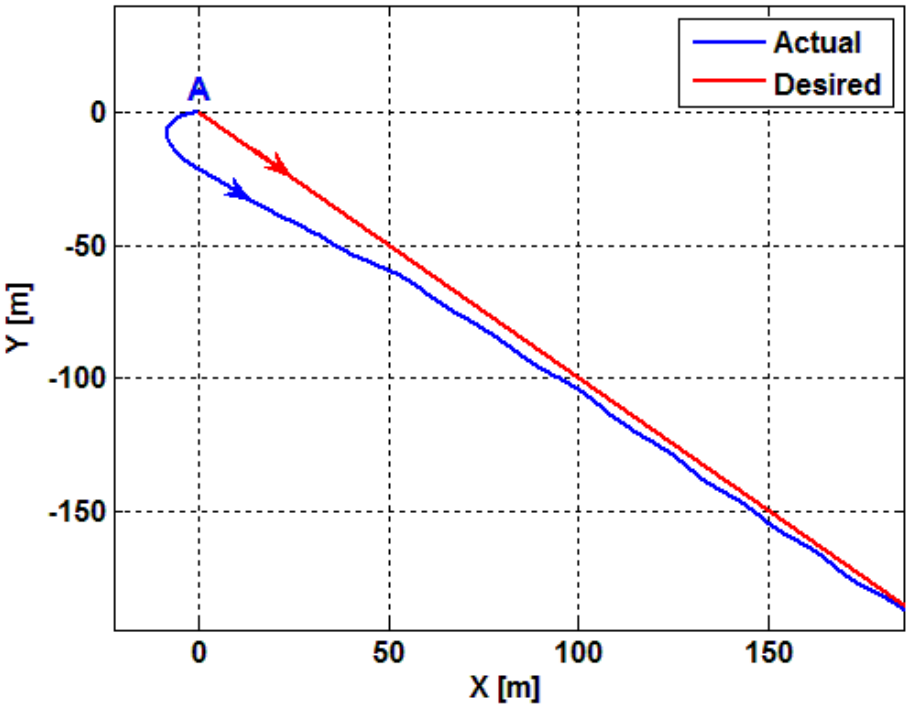

Figure 0-11: First segment of the desired and actual trajectories

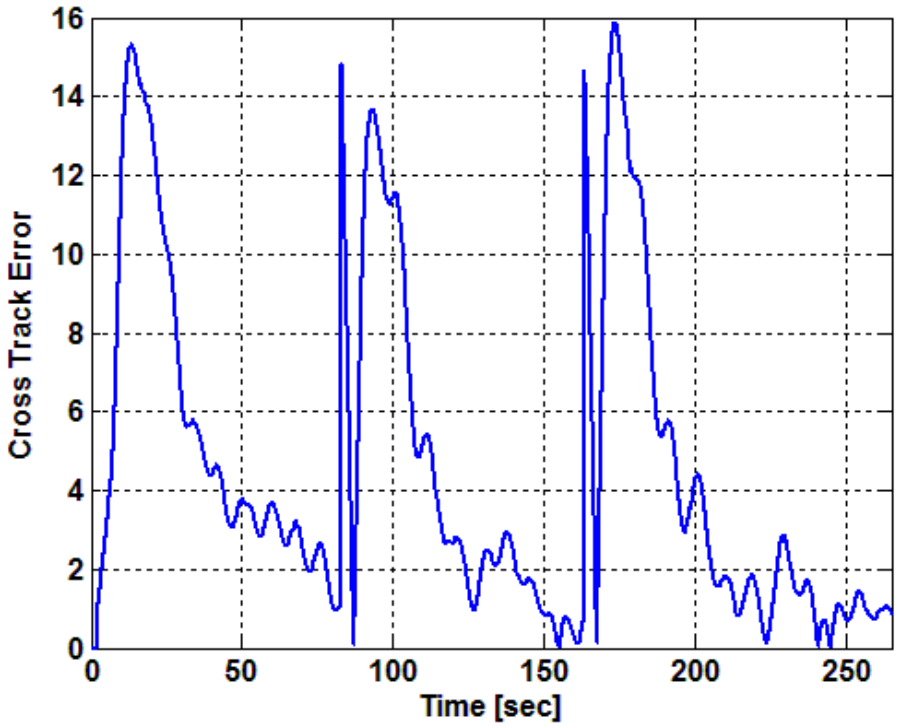

Figure 0-12: Cross-track error

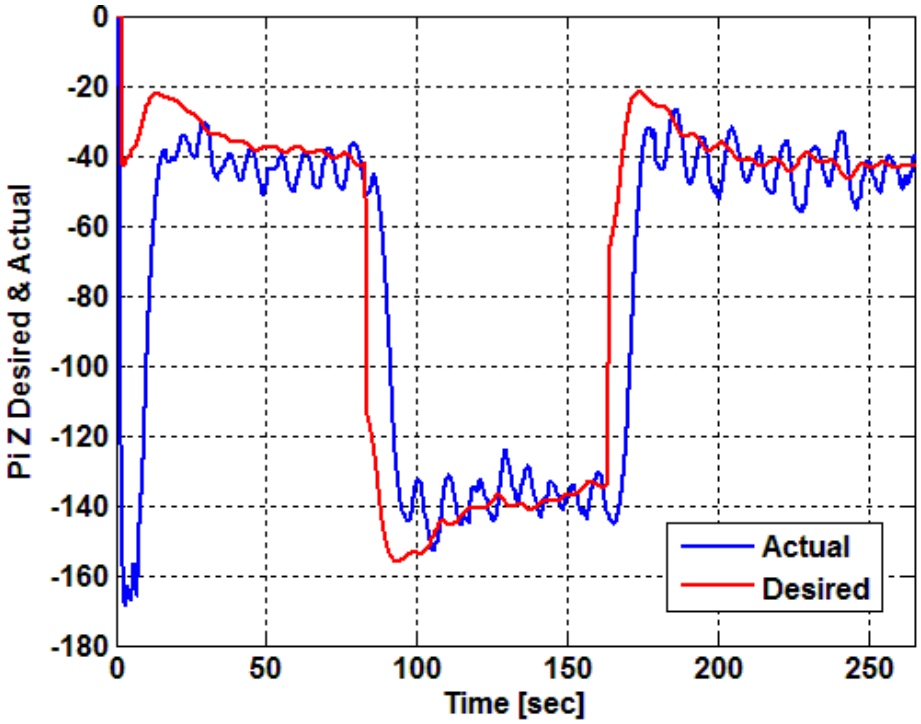

Figure 0-13: Desired and actual heading angle of the boat

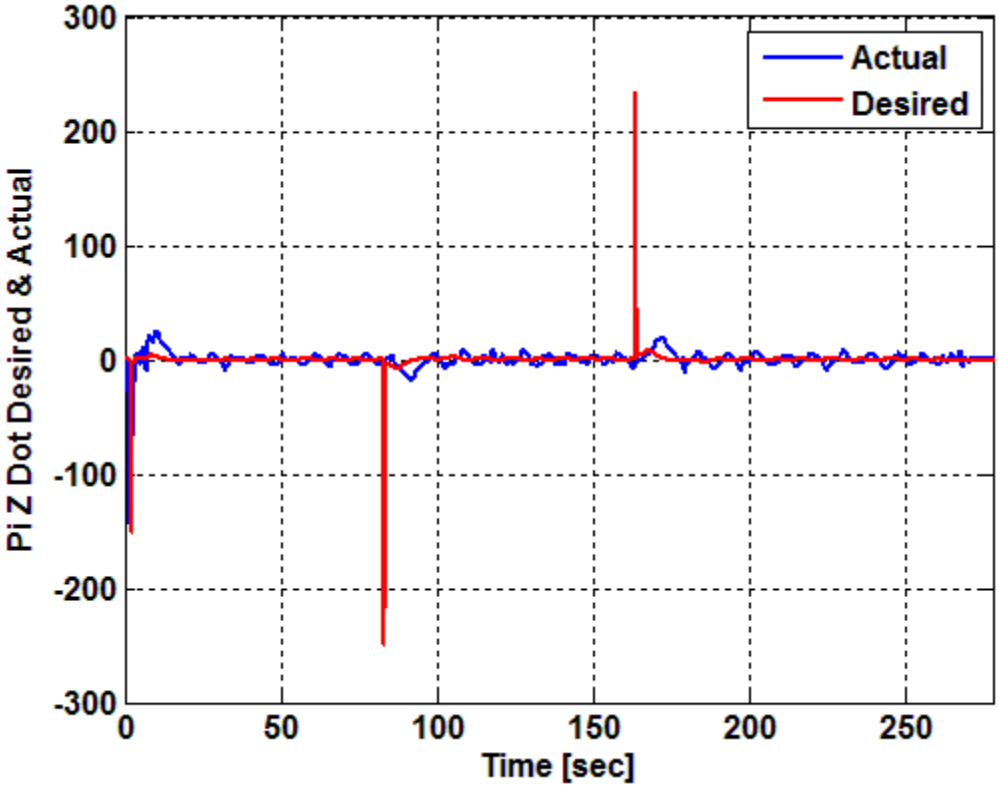

Figure 0-14 Actual and desired time derivatives of the heading angle

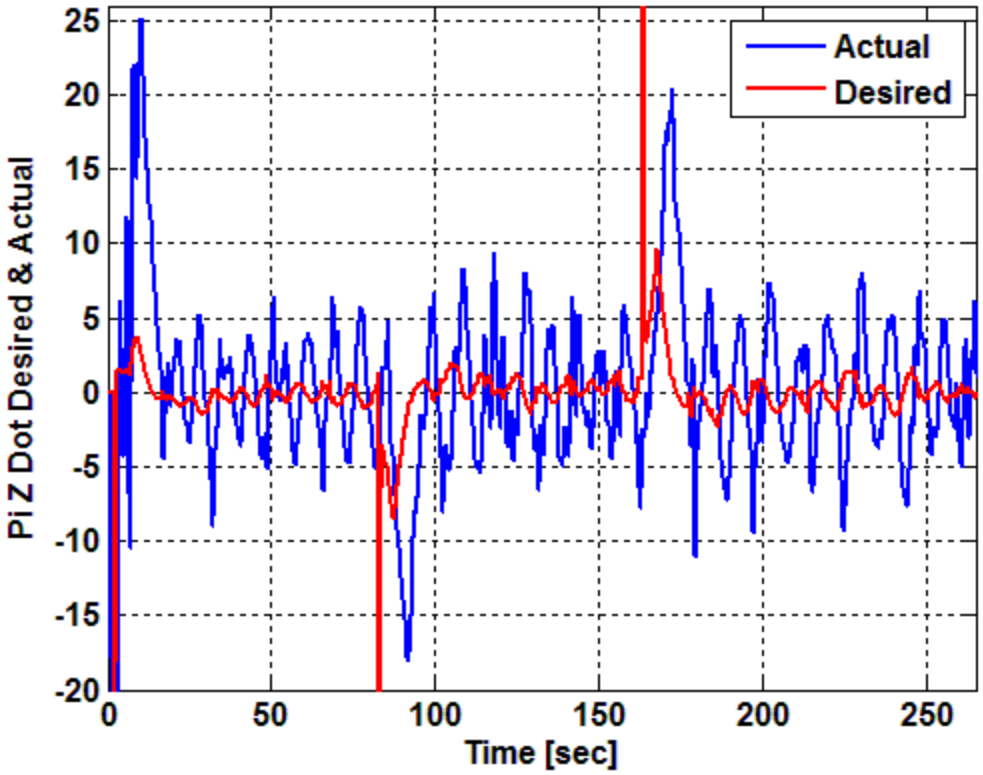

Figure 0-15 A close-up view of the actual and desired time derivatives of the heading angle

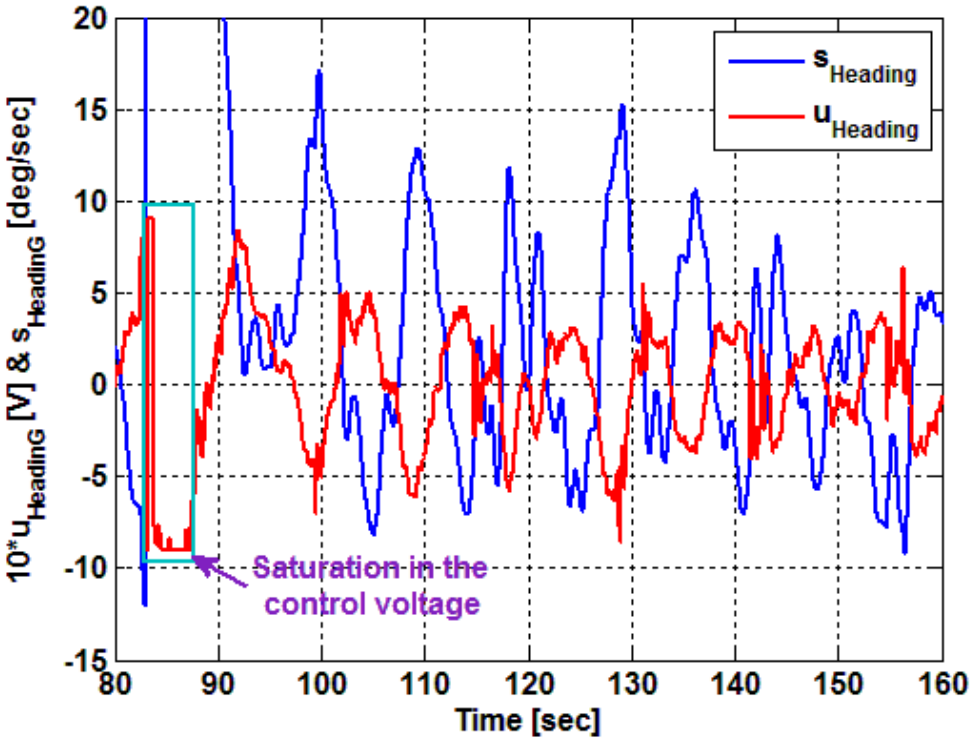

Figure 0-16 Close-up view of the heading sliding surface and a 10x magnified control signal

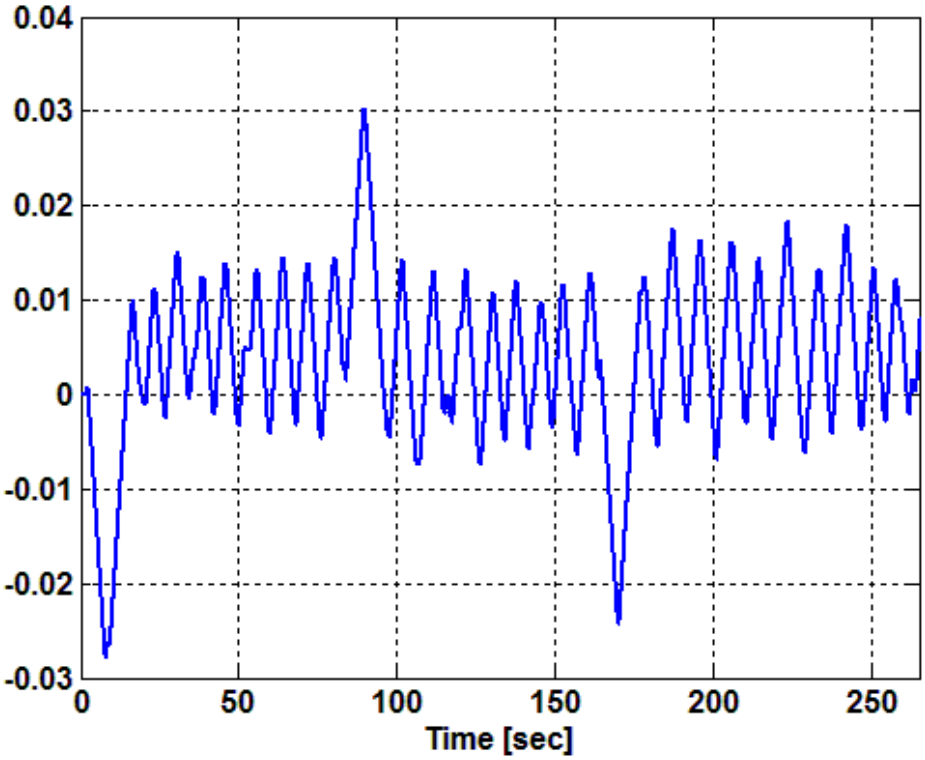

Figure 0-17 Steering mechanism linear displacement

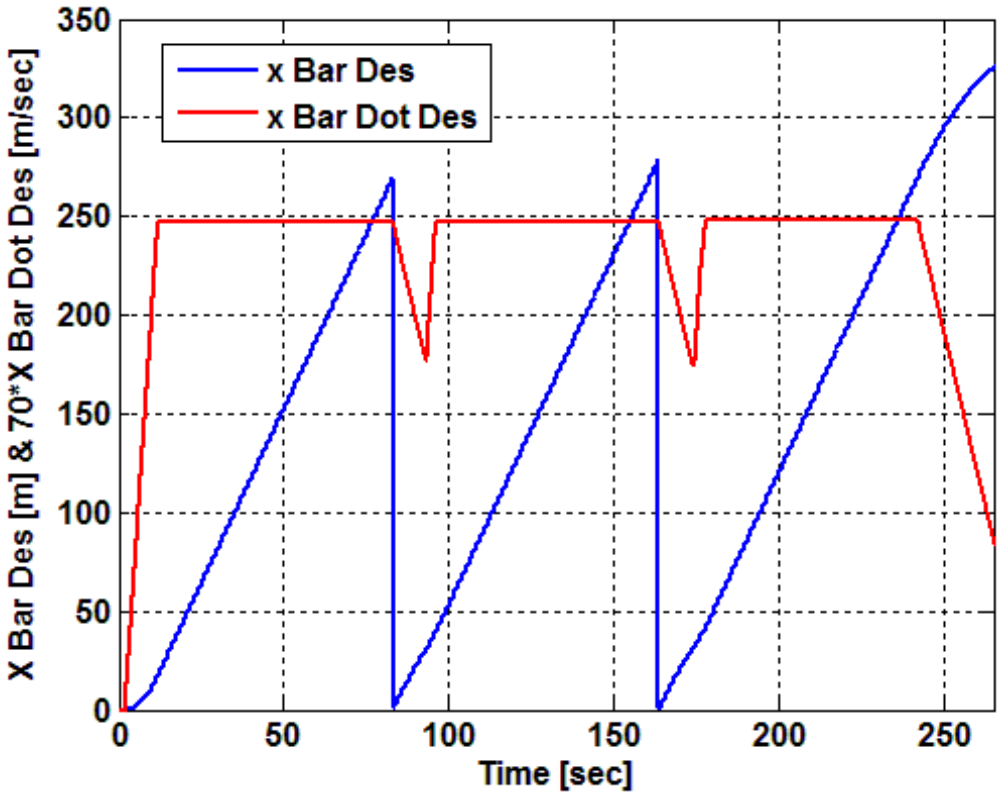

Figure 0-18: Specified surge displacement and 70x magnified surge speed along the segments of the desired trajectory

The surge displacement along the segments of the desired trajectory has been generated in the present work by integrating online the surge speed profile depicted in Figure 0-18. Note that the desired surge displacement had to be reset to zero whenever the boat enters the acceptance circle surrounding the waypoint at the end of the segment that is being tracked by the boat (see Figure 0-18). This procedure was followed in the present work except for the last segment where the surge displacement was allowed to increase beyond the boat's point of entry into the acceptance circle surrounding the last waypoint.

Figure 0-19 reveals a rapid convergence of the actual surge displacement to the desired one in spite of neglecting the system's dynamics in the controller and observer formulations and carrying out the experiment in the presence of considerable environmental disturbances. These

results serve to experimentally validate the good tracking characteristic and the robustness of the surge displacement controller.

Figure 0-20 and Figure 0-21 illustrate the surge controller command signal, u_{Surge}, and the sliding surface, s_{Surge}. Note that the objective of the surge controller is to reduce s_{Surge} to zero and maintain it at that level. This will ensure that the error in the surge displacement along the segment of the desired trajectory to be driven to zero. However, the large wave excitations, wind and currents have a tendency to push the boat away from the sliding surface $s_{Surge} = 0$; thus, causing s_{Surge} to become different than zero. Therefore, to bring the system back towards $s_{Surge} = 0$, the surge controller assigned a control signal that is out-of-phase with s_{Surge} (see Figure 0-20 and Figure 0-21). Such a pattern is similar to the one exhibited by the heading controller command signal (see Figure 0-16).

Throughout this experiment, only the data from the Hemisphere V101 Compass Global Positioning System (GPS) receiver was used. Any information pertaining to the heading angle was deduced from the GPS data and the time rate of change of the heading angle generated by the Crista Inertial Measurement Unit (IMU) was ignored. The optical encoders of the servomotors were only used by the recovery controller in case of emergency.

In performing the present work, we noticed that the GPS data may be lost momentarily while conducting an experiment or the GPS may yield unrealistic numbers resulting in huge spikes in the data record. These anomalies in the data had to be dealt with by writing a considerable code to detect online missing data points and replacing them with the last good data point that was received prior to losing data. Moreover, the same code would continually check for unrealistic spikes in the GPS data and replacing them by data points that were received prior to the spikes.

The modified X and Y GPS data are referred to herein as “filtered” data. They played the role of measured data, which are required by the model-less sliding mode observer (SMO). The latter was used to accurately estimate the required state variables that are needed by both the guidance system and the controller. The code first cleans up the data by replacing bad data points with good data points that were last received. Once the GPS resumes sending good data points then the code would pass them on to the observer. As a result, the modified or “filtered” GPS data would now exhibit step discontinuities, which yield large impulses in the time derivatives of these signals; thus, causing the controller to react to large impulses that do not represent any physical phenomenon pertaining to the dynamic behavior of the boat. Therefore, such signals are not suitable to be used in the computation of the control signals. As far as the observer is concerned, the displacement discontinuities are treated as disturbances. Moreover, the estimated displacement converged to the modified GPS data within 1.5 sec, which proves the robustness of the nonlinear observer. This explanation is confirmed by the plots in Figure 0-22 to Figure 0-25, which demonstrate that the estimated $\dot{X}_{estimated}$ and $\dot{Y}_{estimated}$ signals are not prone to large impulses or spikes that appeared by taking the time derivative of the filtered GPS data. Therefore, the estimated variables $X_{estimated}$, $Y_{estimated}$, $\dot{X}_{estimated}$ and $\dot{Y}_{estimated}$ are used in the current work for the computation of the control signals and by the guidance system to determine the desired heading angle and the surge displacement along the segments of the desired trajectory.

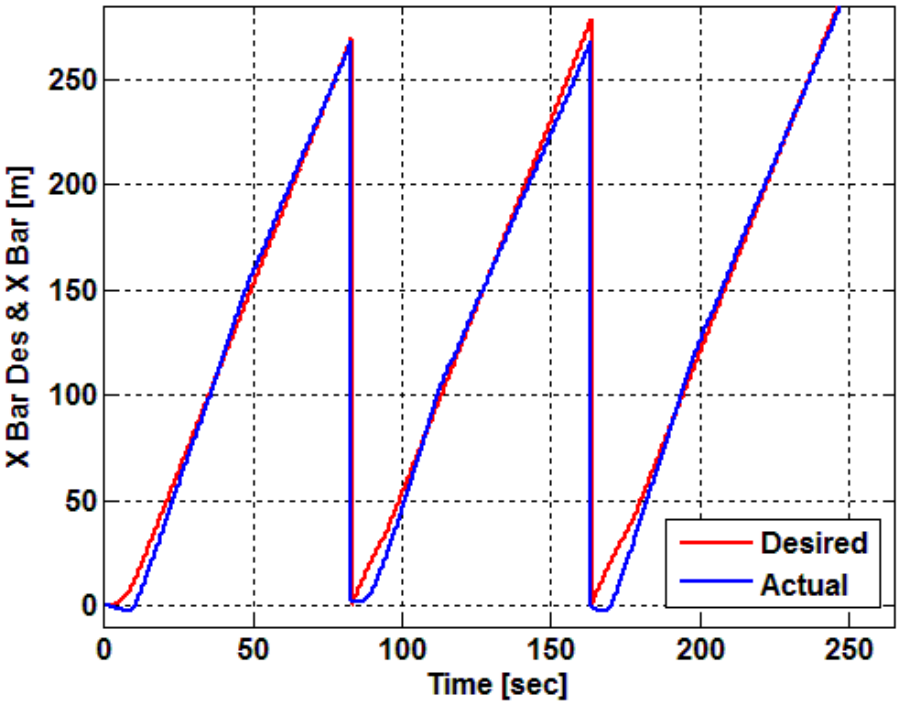

Figure 0-19: Desired and actual surge displacement along the segments of the desired trajectory

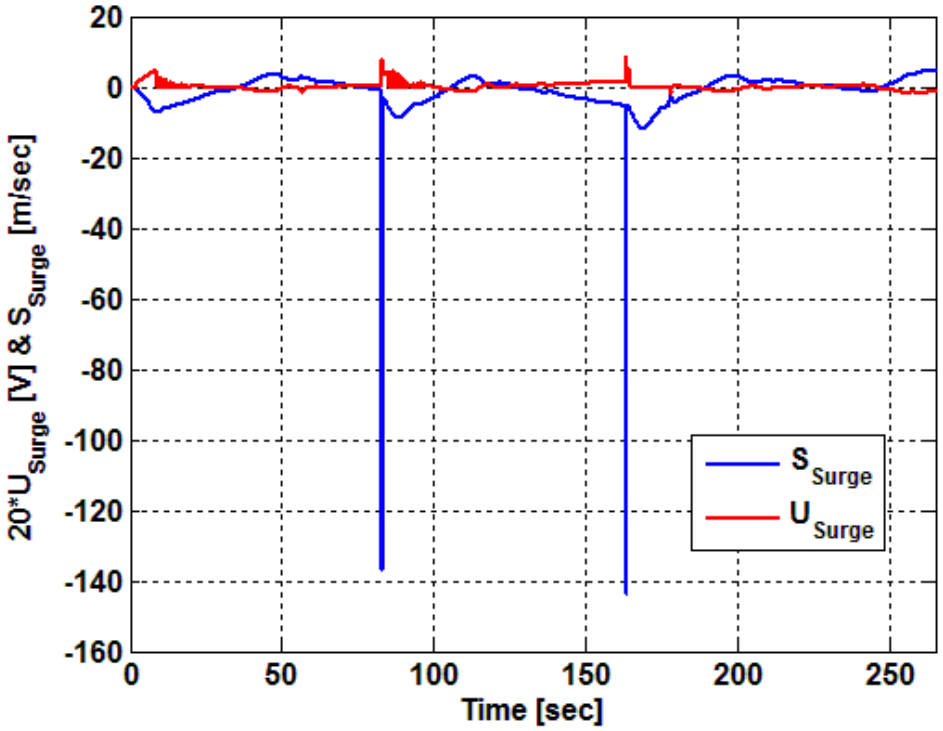

Figure 0-20 Surge sliding surface and a 20x magnified control signal

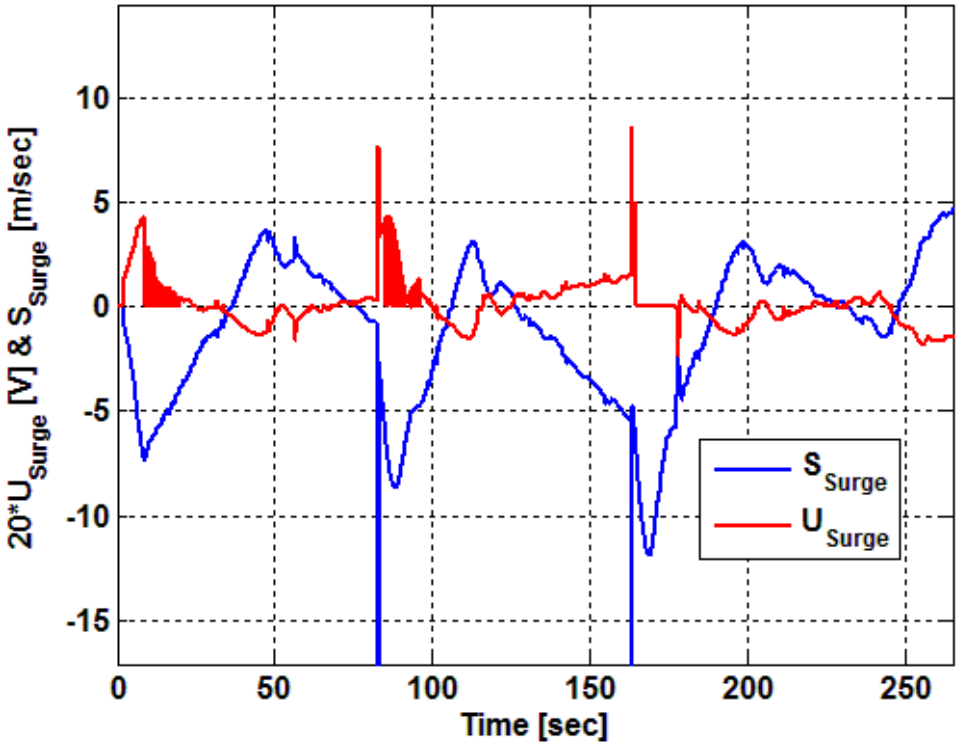

Figure 0-21 Close-up view of the surge sliding surface and the 20x magnified control signal

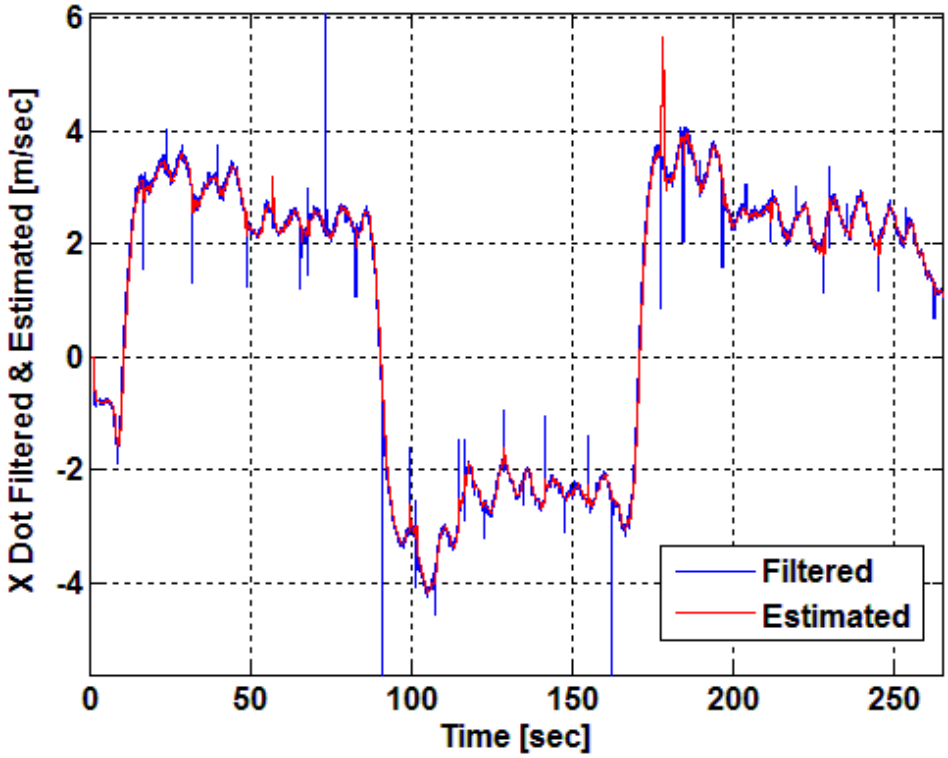

Figure 0-22: Close-up view of the filtered and estimated $\dot{X}$ of the boat

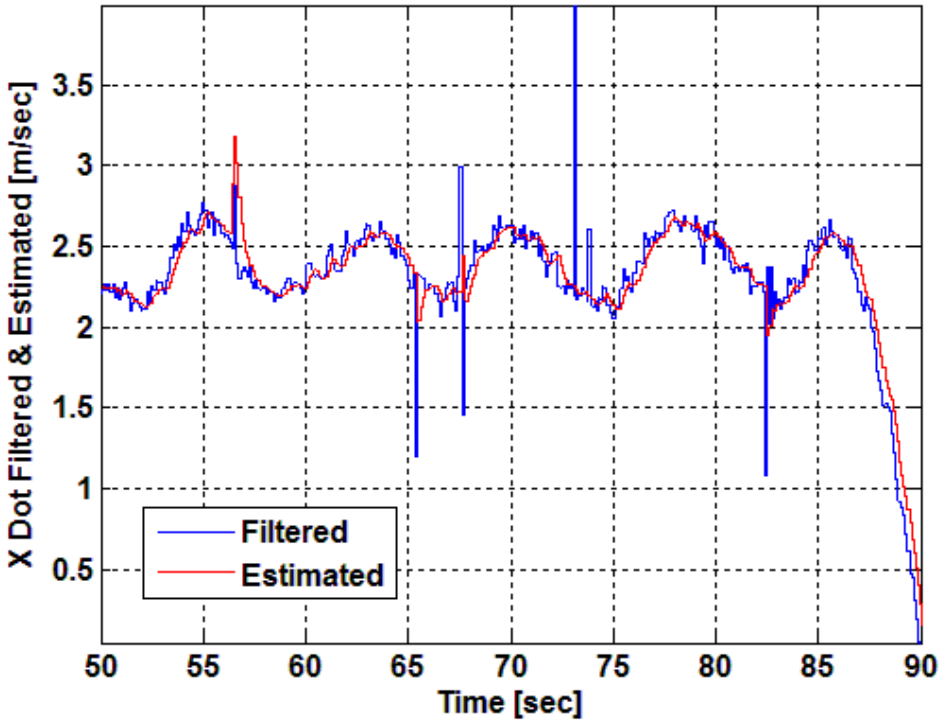

Figure 0-23: Zoomed-in view of the filtered and estimated $\dot{X}$ of the boat

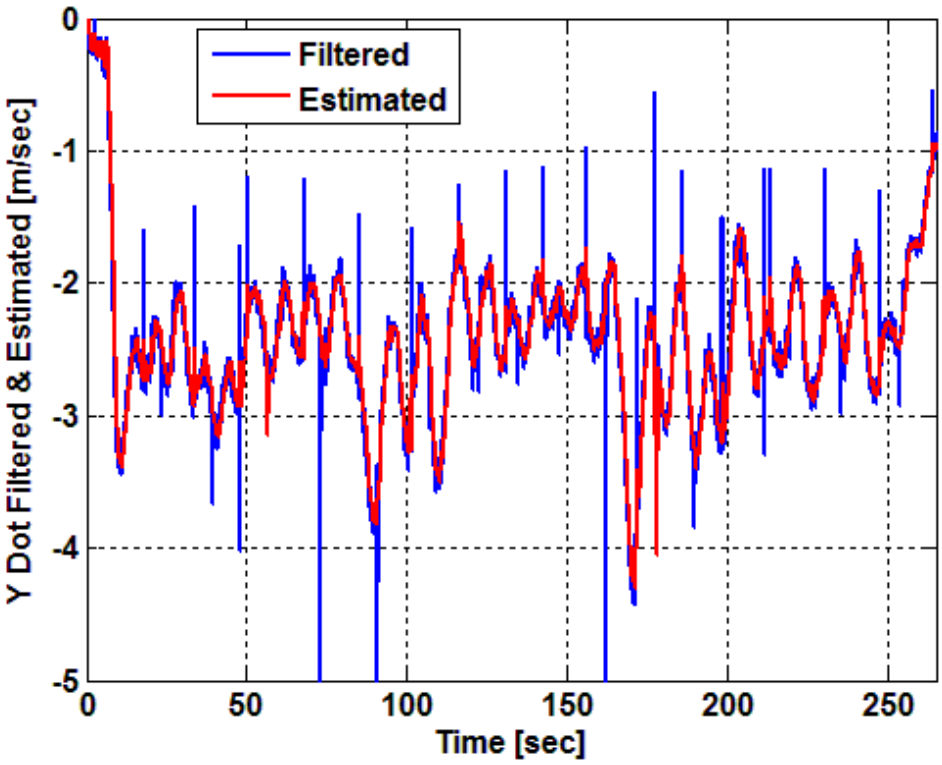

Figure 0-24: Close-up view of the filtered and estimated $\dot{Y}$ of the boat

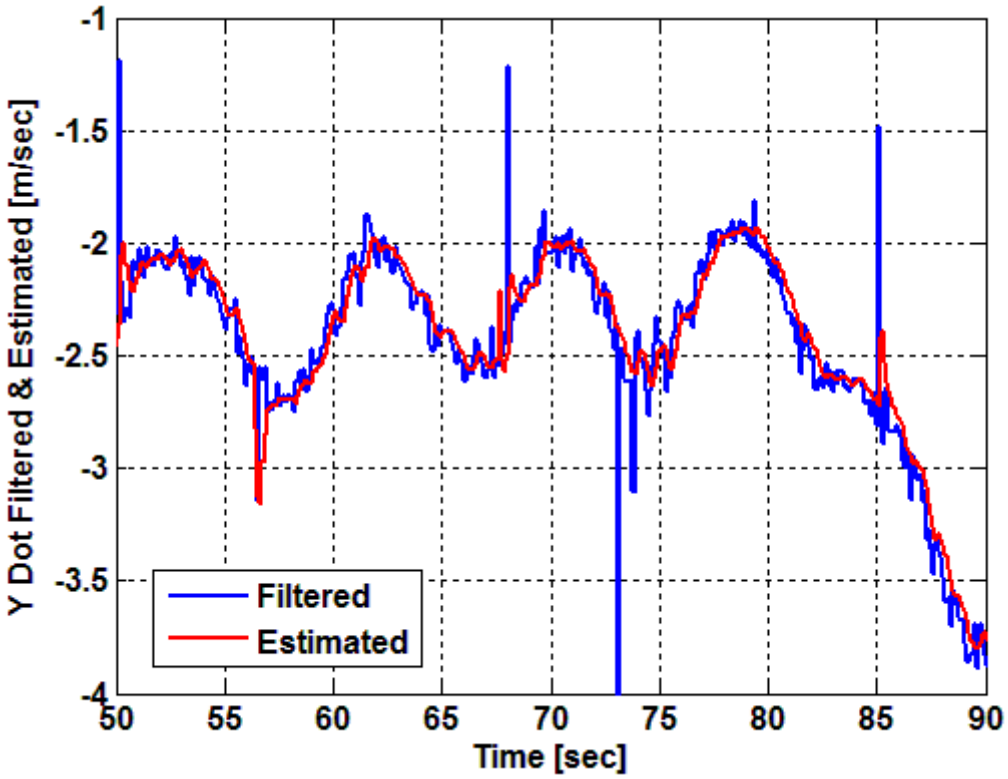

Figure 0-25: Zoomed-in view of the filtered and estimated $\dot{Y}$ of the boat

The results of a second experiment have also been included herein to demonstrate the repeatability and consistency in the performance of the fully integrated guidance and controller/observer system. The second experiment was conducted under similar environmental conditions as the first one that was described earlier. Again, it should be recalled that the dynamics of the marine surface vessel have been ignored in the computation of the control signals as well as in the estimation of the required state variables.

In the second experiment, the desired trajectory consisted of three segments connecting the following waypoints:

$\mathrm{A}(X_1 = 0\ m, Y_1 = 0\ m)$ $\mathrm{B}(X_2 = 100\ m, Y_2 = 250\ m)$

$\mathrm{C}(X_3 = 100\ m, Y_3 = 500\ m)$ $\mathrm{D}(X_4 = 0\ m, Y_4 = 750\ m)$

Figure 0-26 and Figure 0-27 reveal that the boat initial orientation in the vicinity of waypoint A was almost perpendicular to that of the desired trajectory. Therefore, the boat had to make a steep maneuver to re-align itself with the first segment of the desired trajectory (see Figure 0-27). Figure 0-28 illustrates that the cross-track error was kept most of the time within $2m$; thus, demonstrating the robustness and good tracking characteristic of the integrated guidance and controller/observer system. These results were achieved in the presence of considerable environmental disturbances and in spite of the fact that both controller and observer were implemented in a model-less configuration.

Figure 0-29 and Figure 0-30 show the desired heading angle specified by the guidance system. They also demonstrate the robustness of the heading controller in forcing the actual heading angle to converge to the desired one. Figure 0-31 and Figure 0-32 represent the desired and actual time derivatives of the heading angle.

Figure 0-33 to Figure 0-35 show the heading control signal, $U_{Heading}$, and sliding surface, $S_{Heading}$. As in the first experiment, the heading controller applied a control signal that is out-of-phase with $S_{Heading}$. Such a corrective action is consistent with those generated by controllers that are based on the variable structure systems theory. Figure 0-36 shows that the tiller arm was operating throughout the test within its allowable linear displacement range of $\pm\ 0.070m$.

Figure 0-37 illustrates similar pattern for the desired surge displacement and velocity along the segments of the desired trajectory as in the first experiment. Figure 0-38 reveals a rapid convergence of the actual surge displacement to the desired one in spite of neglecting the system's dynamics in the controller and observer formulations and carrying out the experiment in the presence of considerable environmental disturbances. These results serve to

experimentally validate the good tracking characteristic and the robustness of the surge displacement controller.

Figure 0-39 and Figure 0-40 illustrate the surge controller command signal, U_{Surge}, and the sliding surface, S_{Surge}. As in the first experiment, the surge controller assigned a control signal that is out-of-phase with S_{Surge}. Such a pattern is similar to the one exhibited by the heading controller command signal (see Figure 0-35).

Figure 0-41 to Figure 0-43 demonstrate the capability of the nonlinear observer in accurately estimating both X and Y coordinates of the boat. Figures Figure 0-44 to Figure 0-49 prove that the estimated $\dot{X}_{estimated}$ and $\dot{Y}_{estimated}$ signals are not prone to large impulses or spikes exhibited in the time derivatives of the filtered GPS data. Therefore, the estimated variables $X_{estimated}$, $Y_{estimated}$, $\dot{X}_{estimated}$ and $\dot{Y}_{estimated}$ are used in the current work for the computation of the control signals and by the guidance system to determine the desired heading angle and the surge displacement along the segments of the desired trajectory.

The results of both experiments reveal a close adherence of the actual trajectory to the desired one. This was accomplished in spite of the sharp turns in the desired trajectory and the large initial errors in both the surge position and the heading angle due to the initial position and orientation of the boat relative to the desired trajectory. Note that the guidance system was relied on in these experiments to provide online values for the desired surge displacement and the heading angle. The objectives of the surge and heading controllers were to ensure that the actual surge displacement and the heading angle accurately track their desired values. The results experimentally validate the robustness and the good tracking characteristics of the model-less

and fully-integrated guidance and controller-observer system in spite of considerable environmental disturbances.

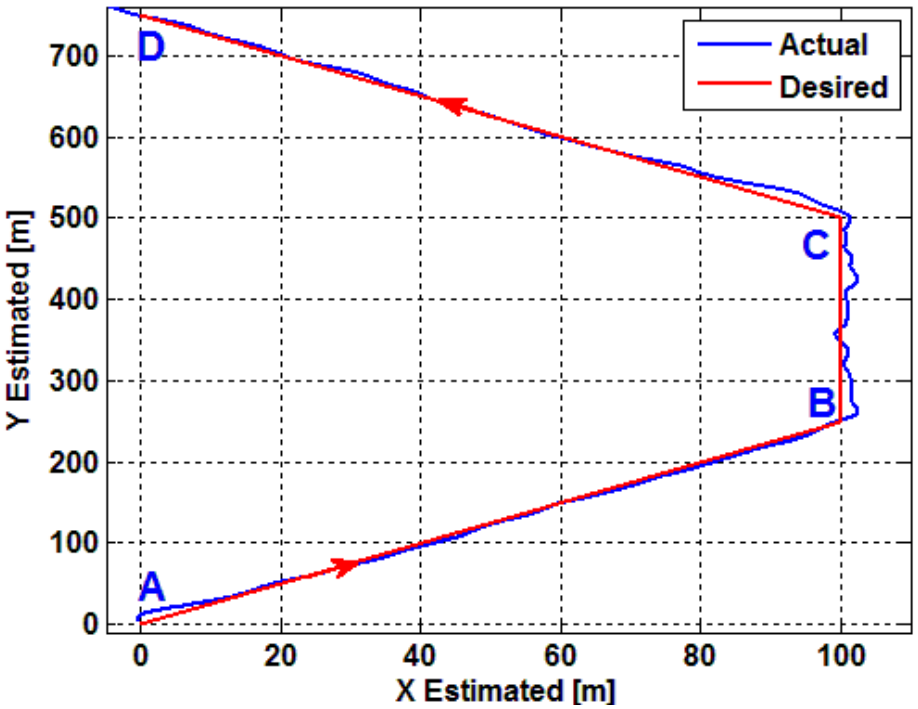

Figure 0-26 Desired and actual trajectories of the boat

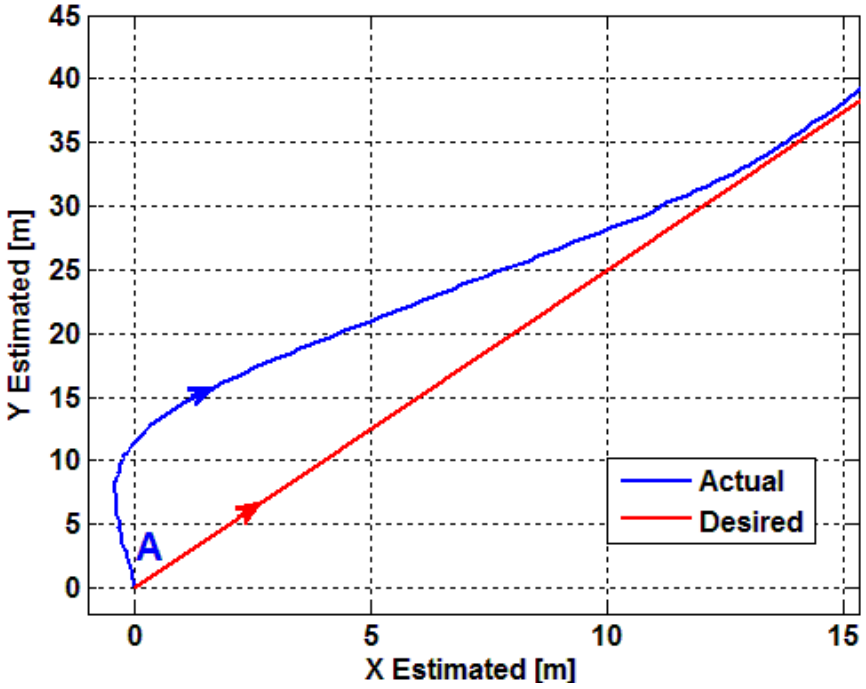

Figure 0-27 A close-up view of the first segment of the desired and actual trajectories of the boat

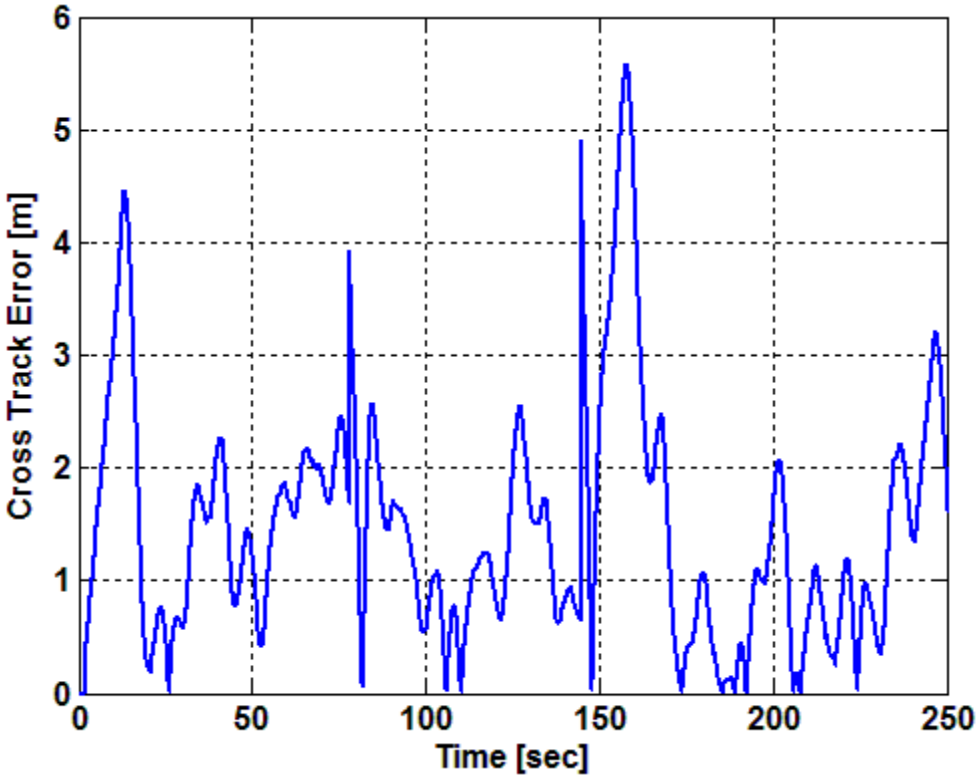

Figure 0-28 Cross track error

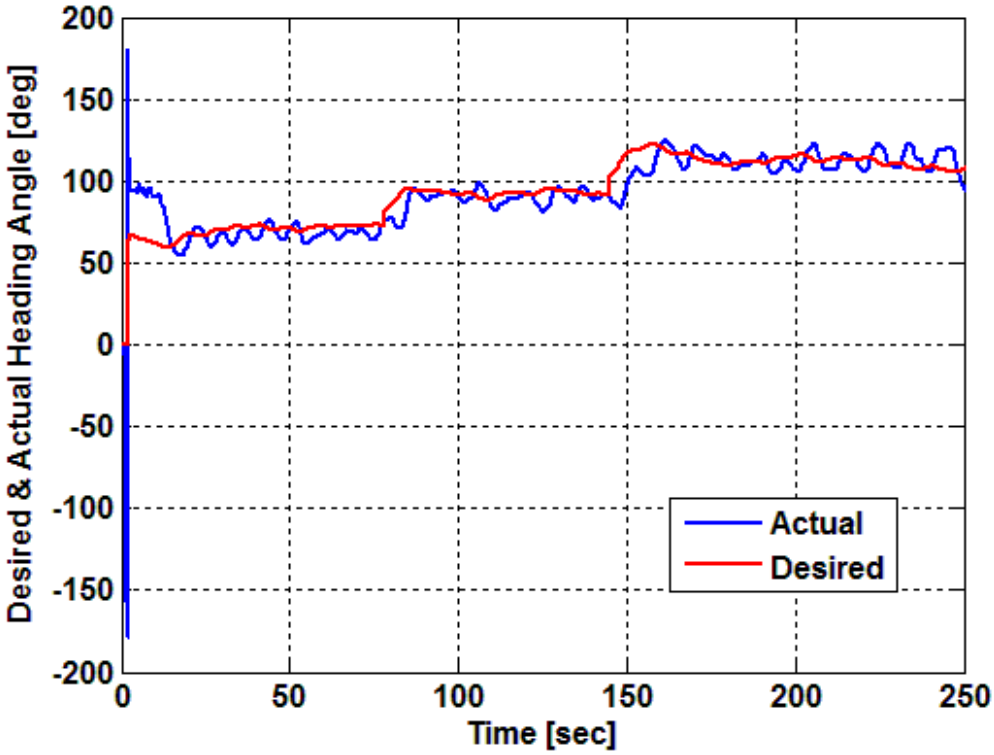

Figure 0-29 Desired and actual heading angle of the boat

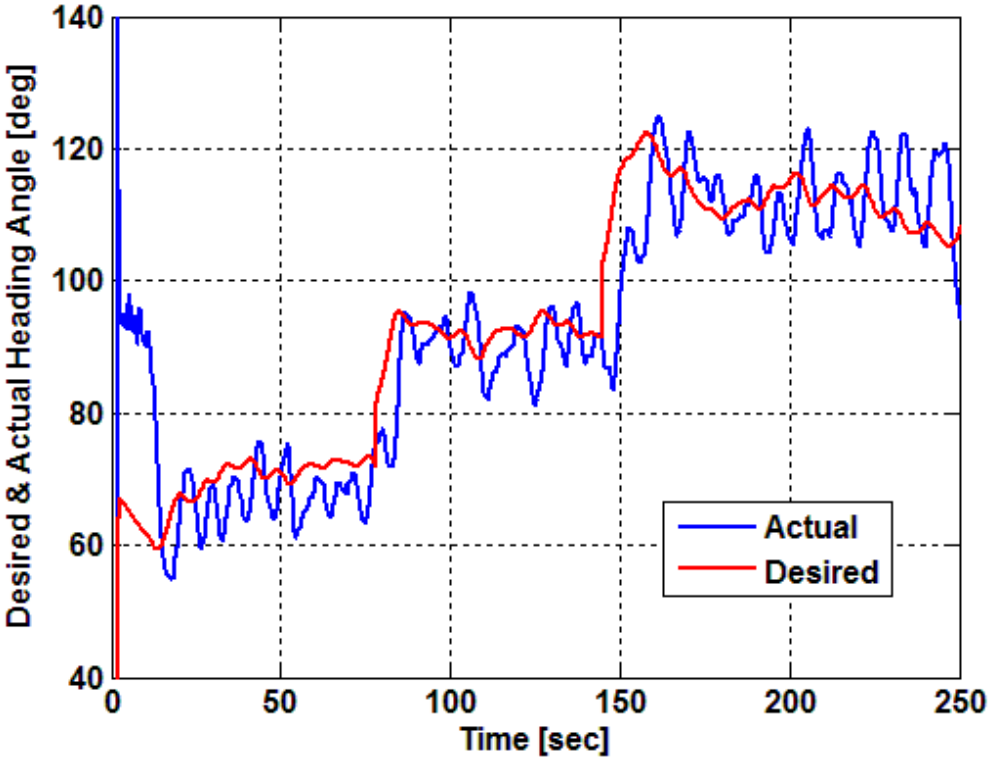

Figure 0-30 Desired and actual heading angle

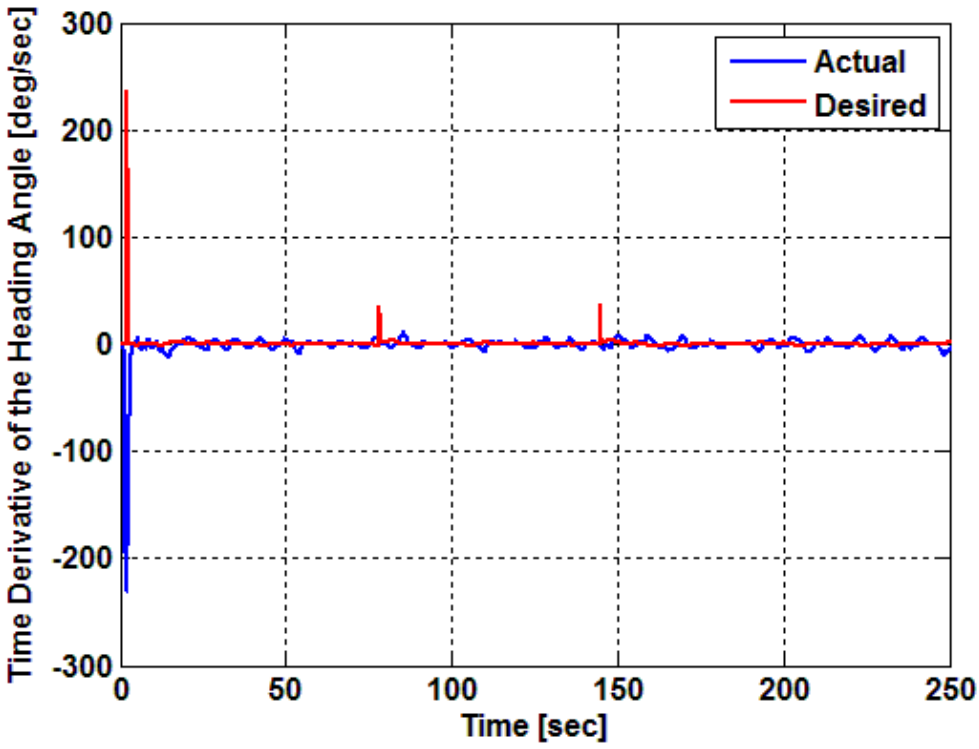

Figure 0-31 Actual and desired time derivative of the heading angle

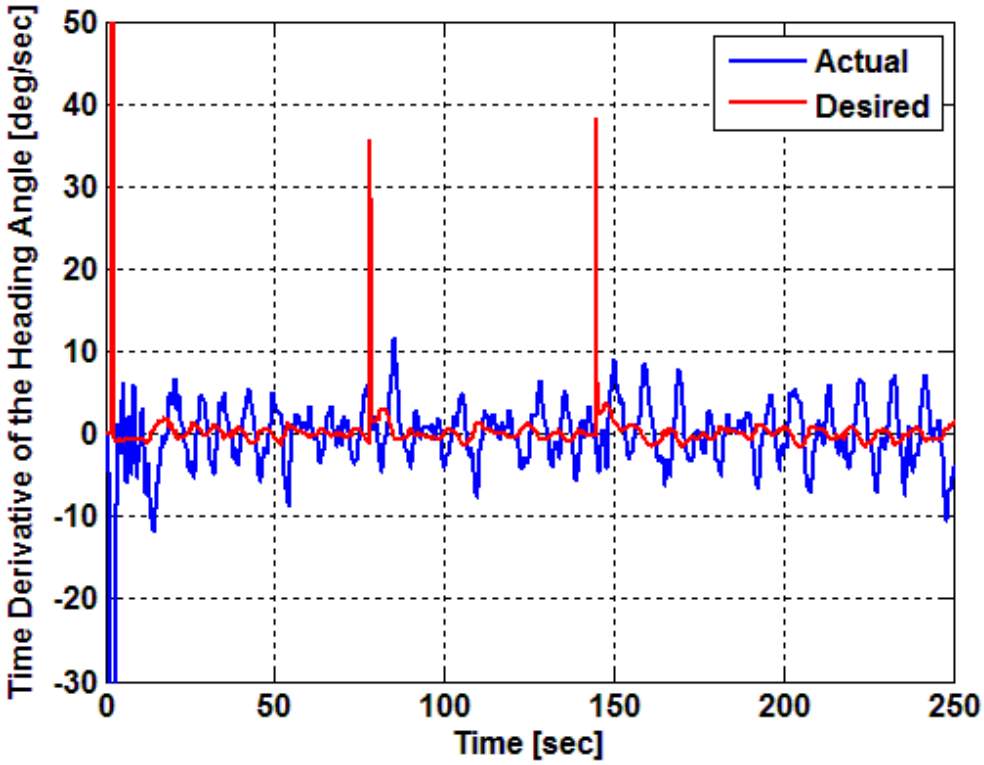

Figure 0-32 A close-up view of the actual and desired time derivative of the heading angle

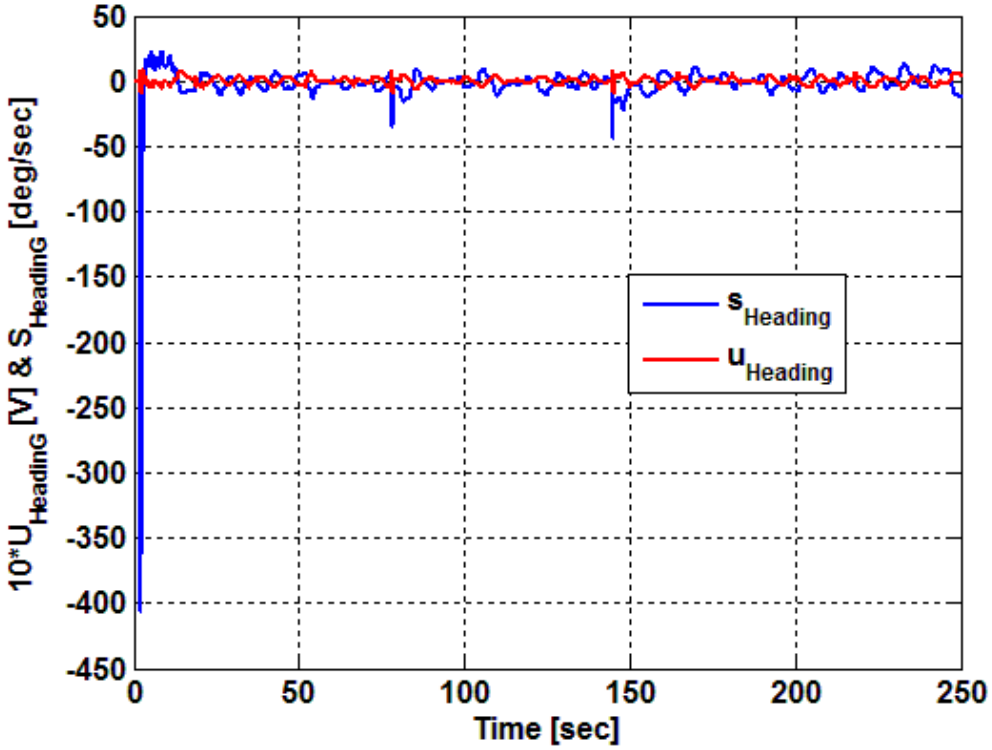

Figure 0-33 Heading sliding surface and a magnified control signal by a factor of 10

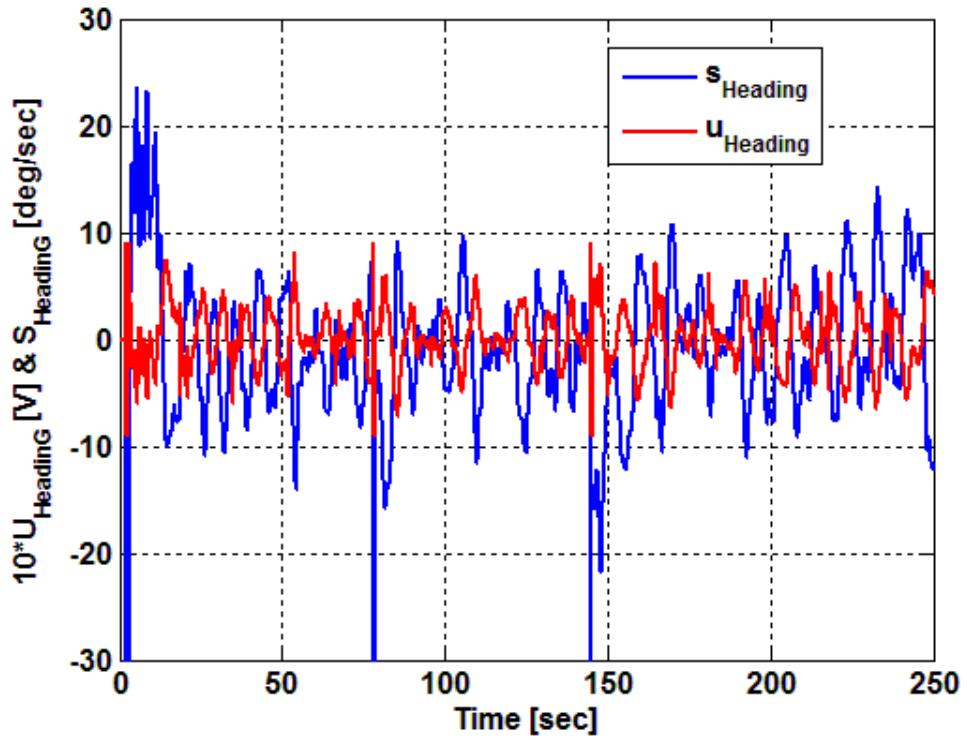

Figure 0-34 A close-up view of the heading sliding surface and a magnified control signal by a factor of 10

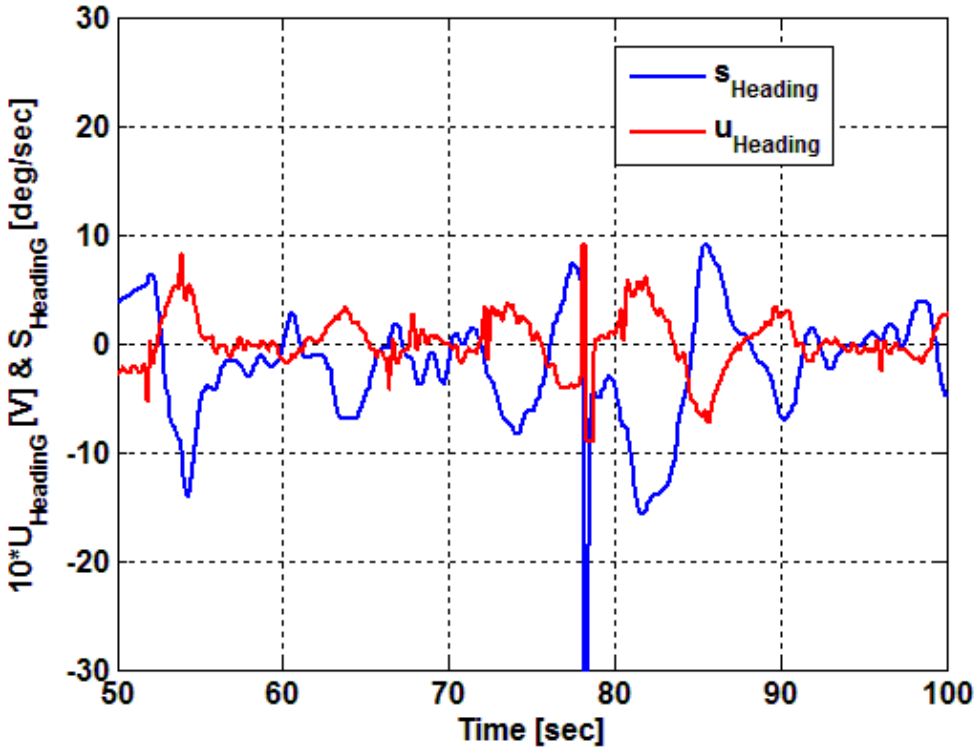

Figure 0-35 A zoomed-in view of the heading sliding surface and a magnified control signal by a factor of 10

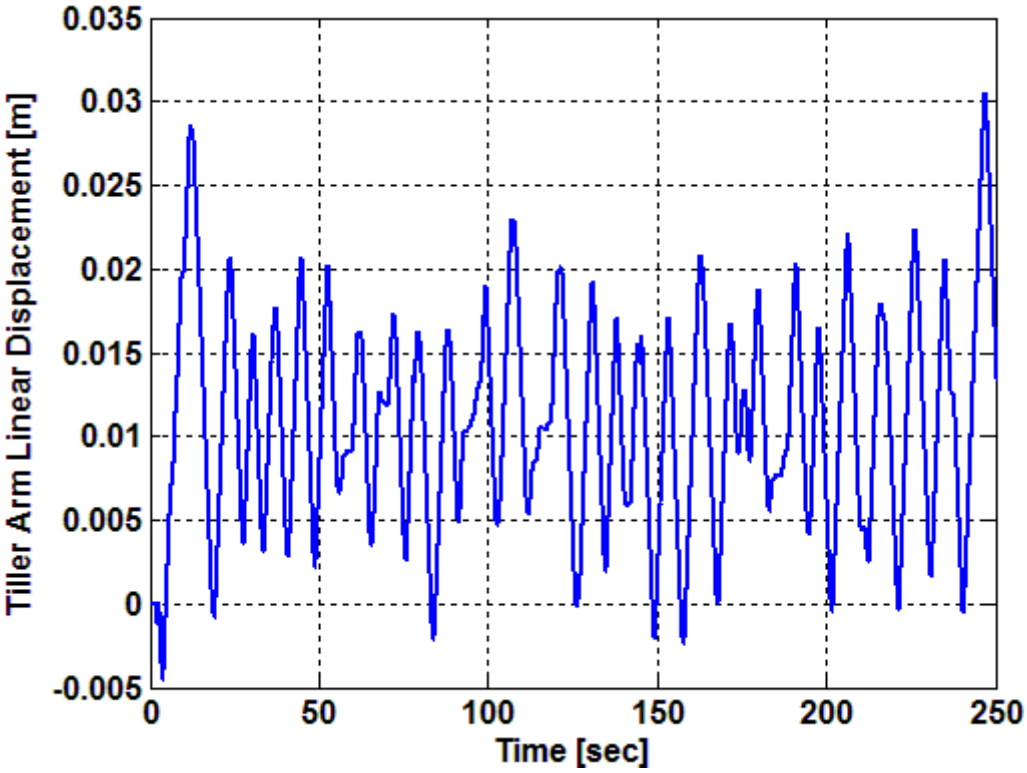

Figure 0-36 Tiller arm linear displacement

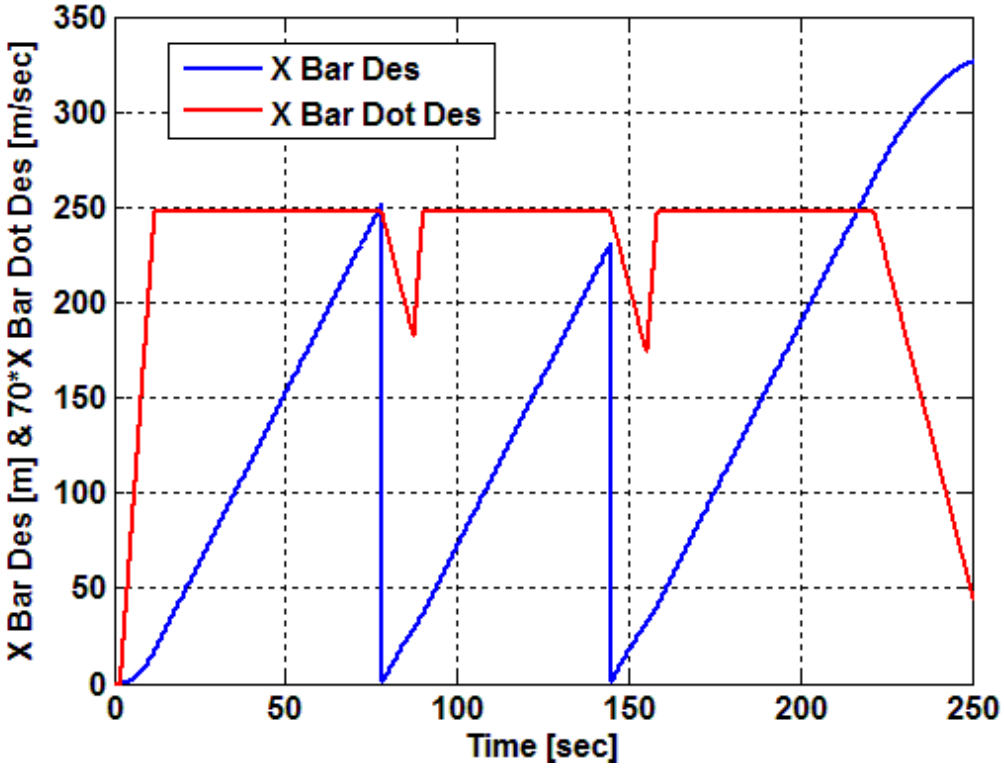

Figure 0-37 Specified surge displacement and magnified surge speed by a factor of 70 along the segments of the desired trajectory

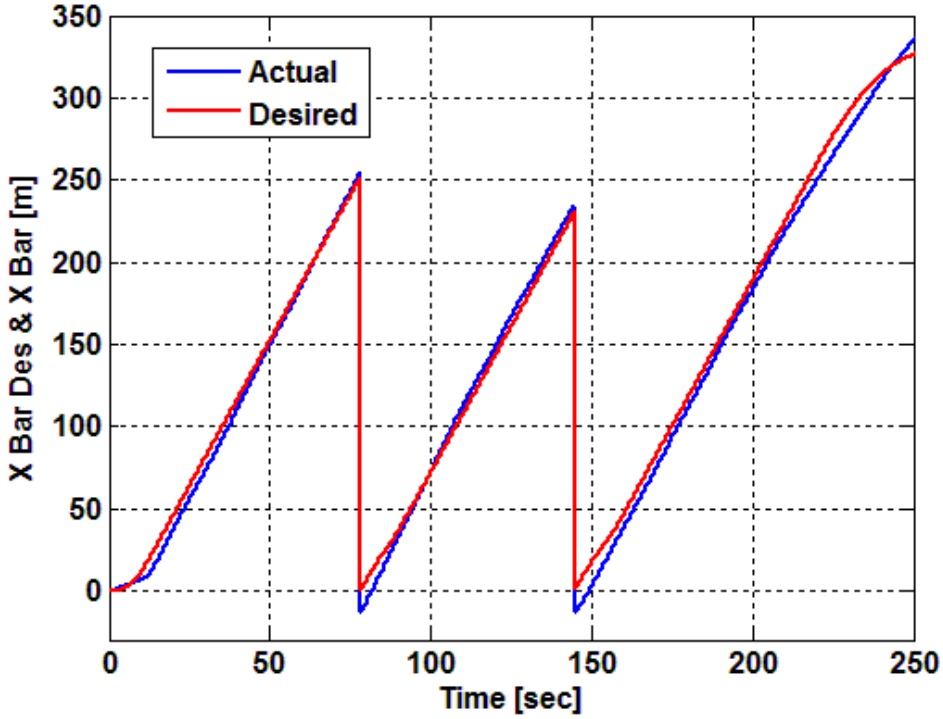

Figure 0-38 Desired and actual surge displacement along the segments of the desired trajectory

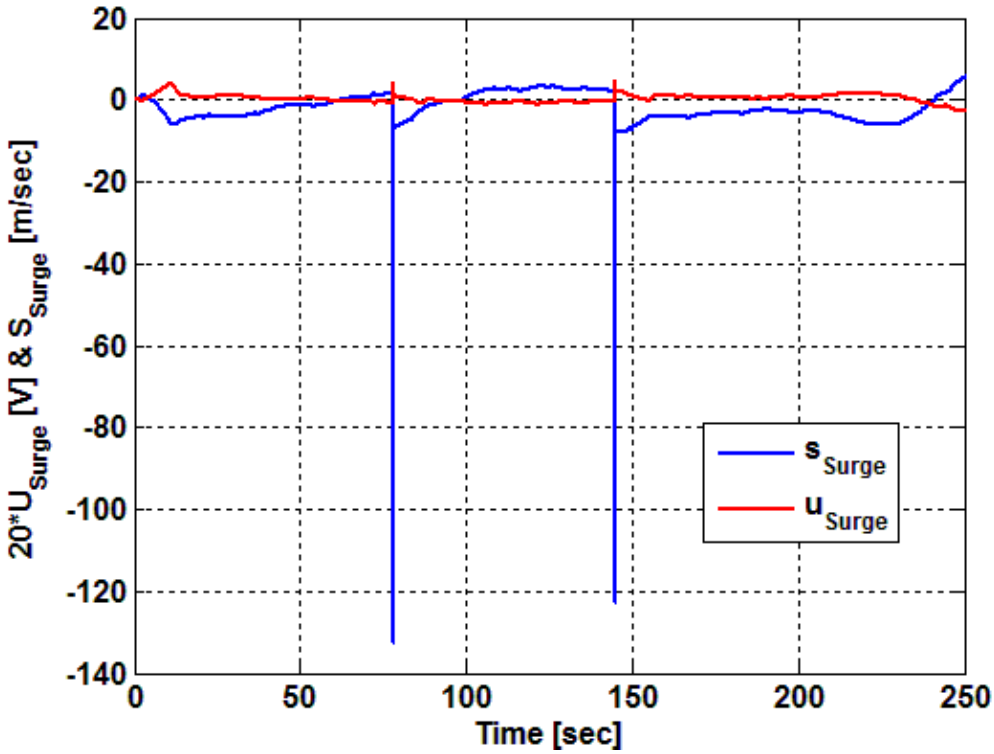

Figure 0-39 Surge sliding surface and a magnified control signal by a factor of 20

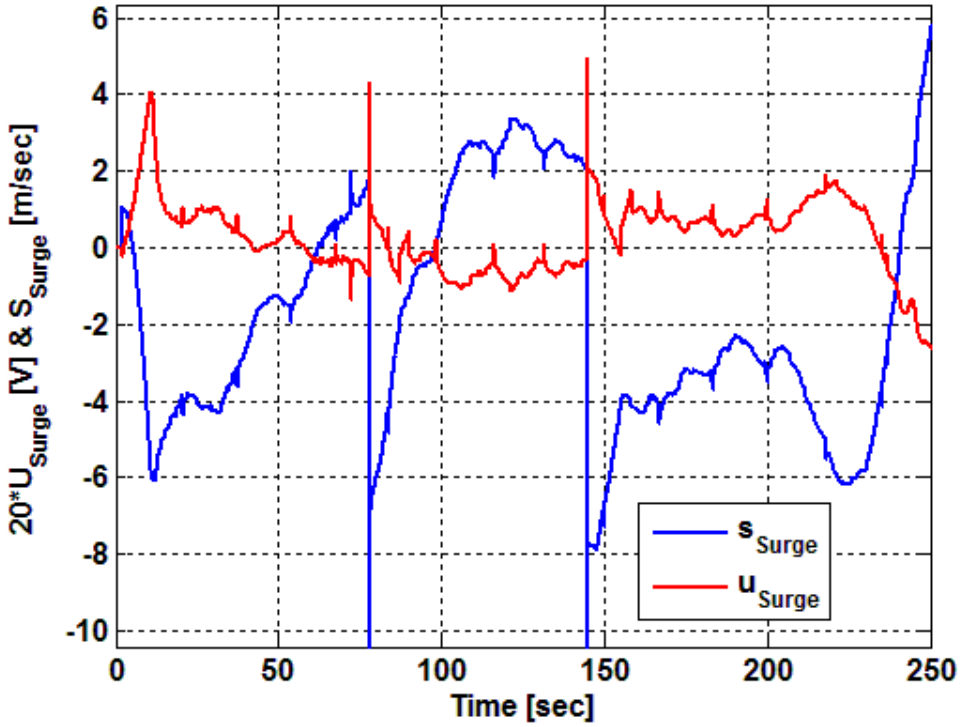

Figure 0-40 A close-up view of the surge sliding surface and the magnified control signal by a factor of 20

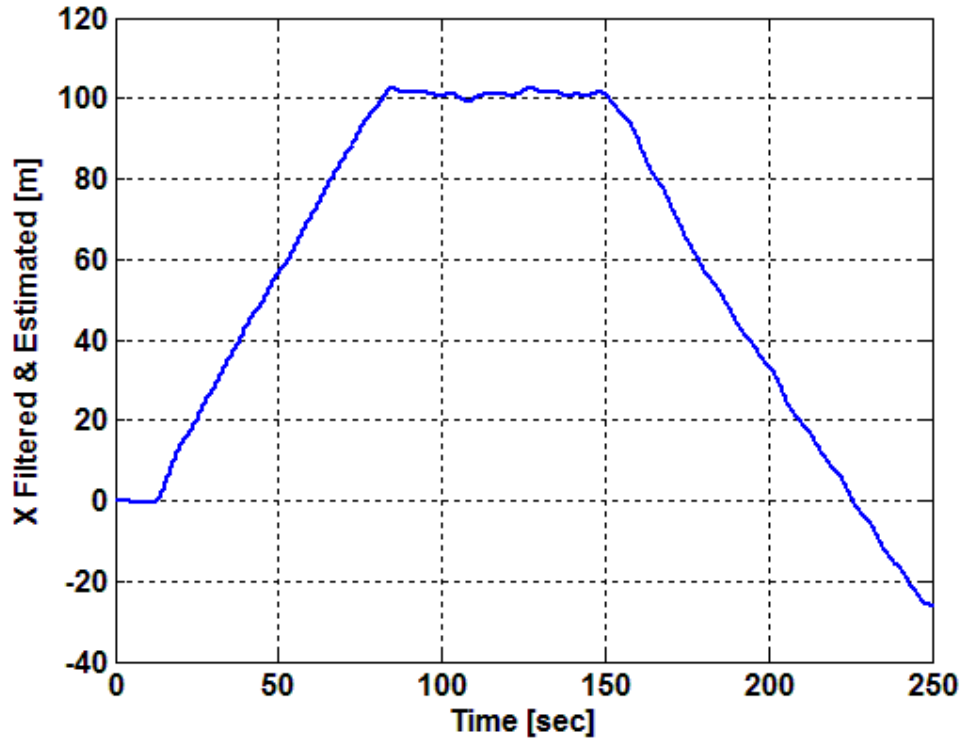

Figure 0-41 Measured and estimated X-coordinate of the boat

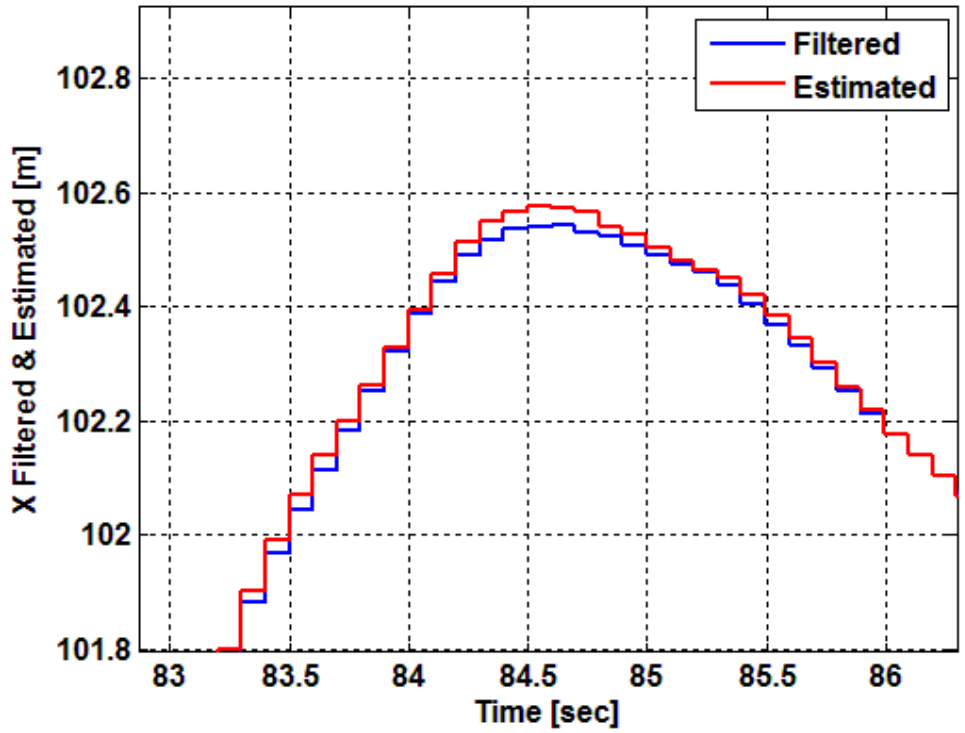

Figure 0-42 A close-up view of the measured and estimated X-coordinate of the boat

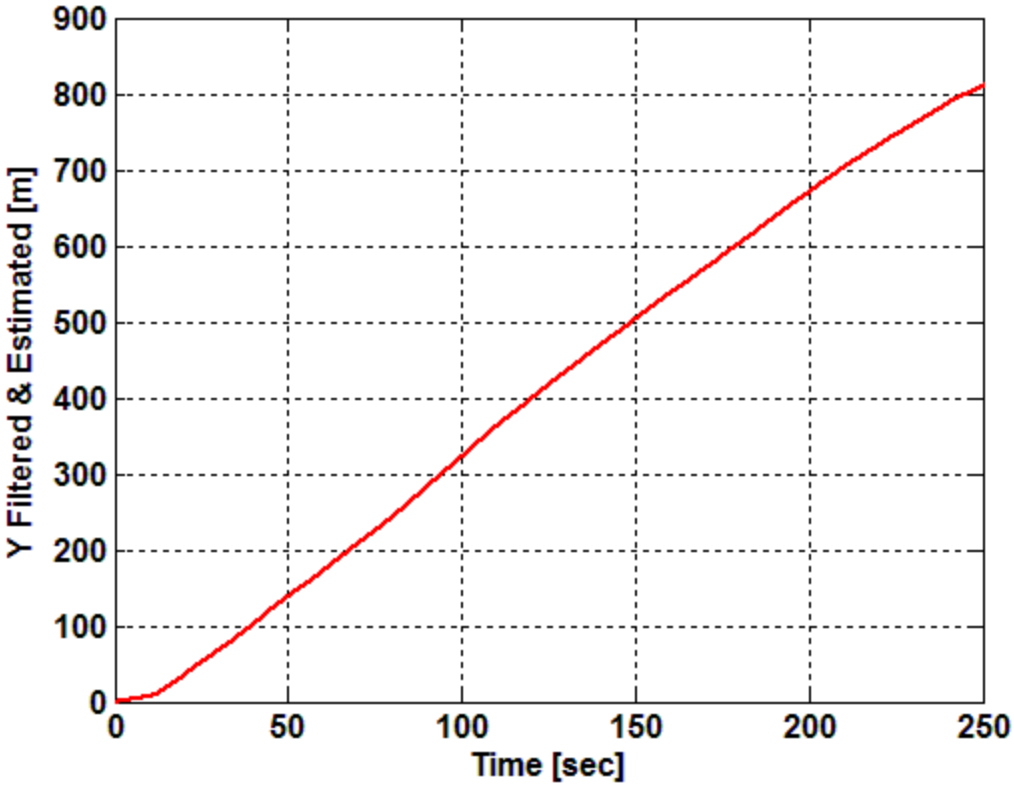

Figure 0-43 Measured and estimated Y-coordinate of the boat

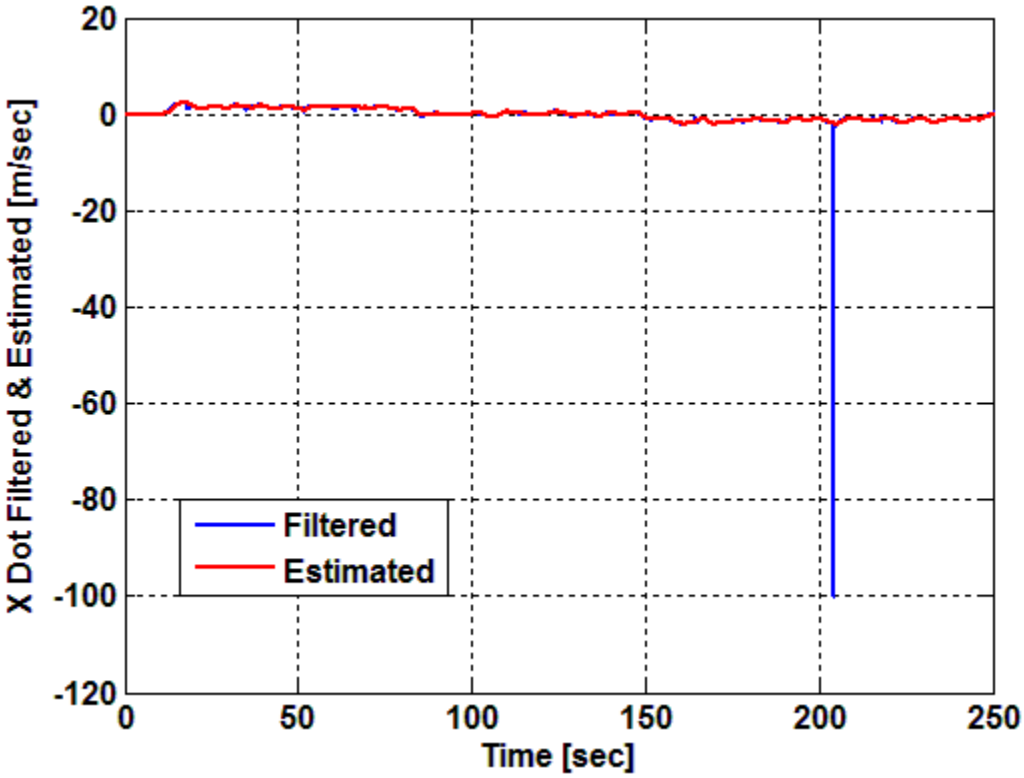

Figure 0-44 Filtered and estimated $\dot{x}$ of the boat

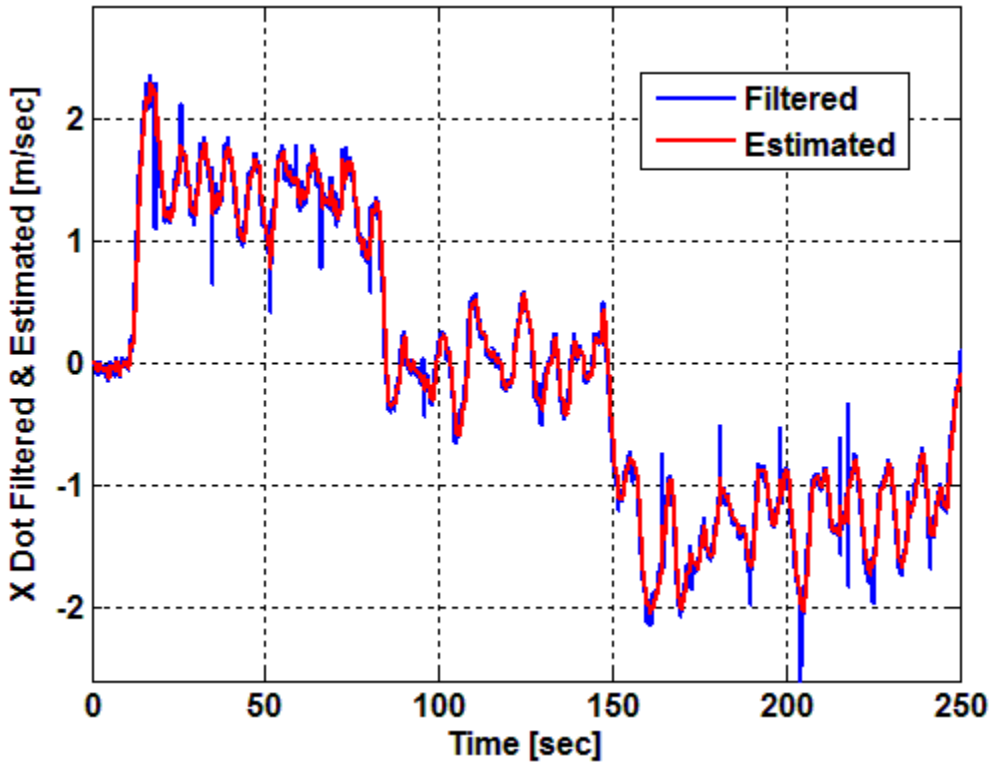

Figure 0-45 A close-up view of the filtered and estimated $\dot{x}$ of the boat

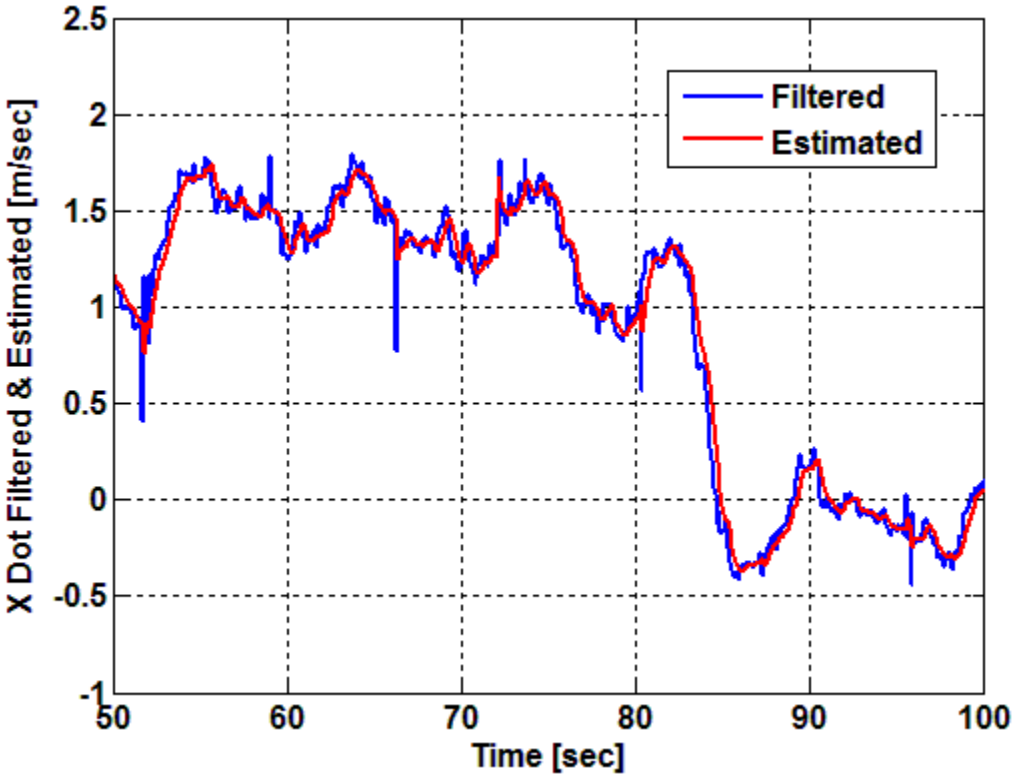

Figure 0-46 Zoomed-in view of the filtered and estimated $\dot{x}$ of the boat

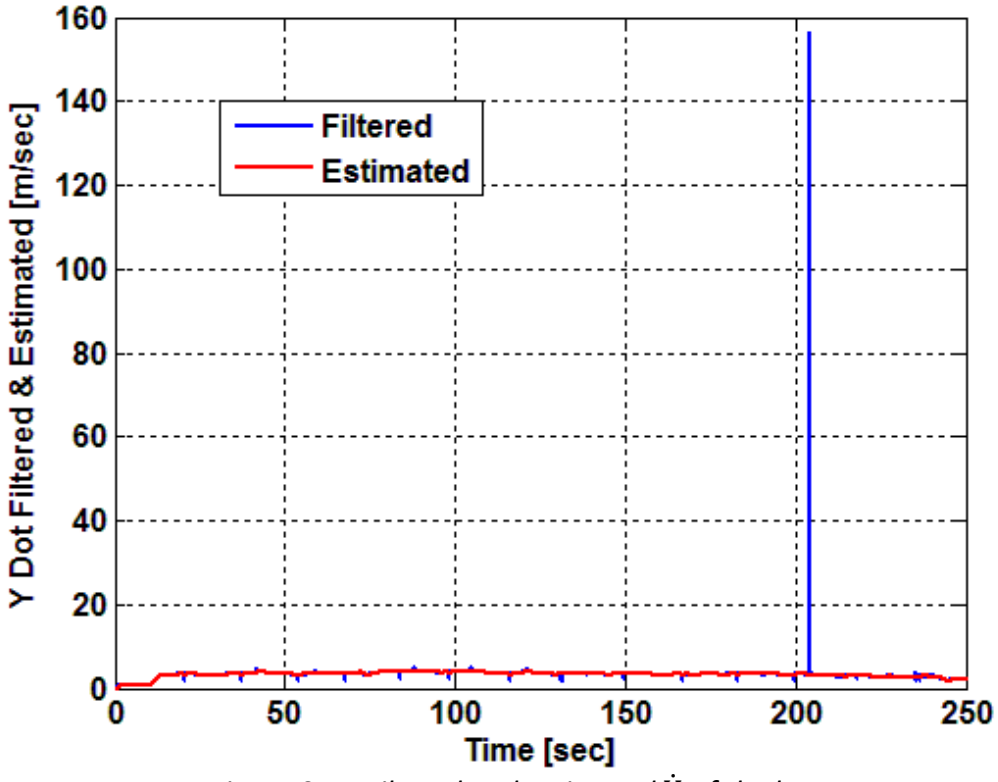

Figure 0-47 Filtered and estimated $\dot{Y}$ of the boat

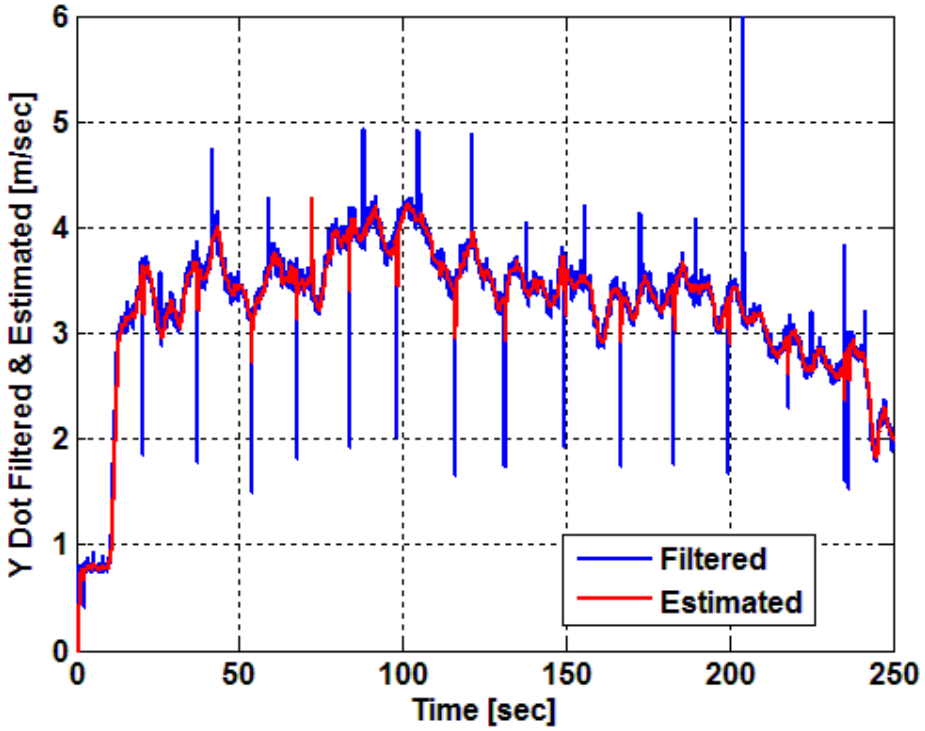

Figure 0-48 A close-up view of the filtered and estimated $\dot{Y}$ of the boat

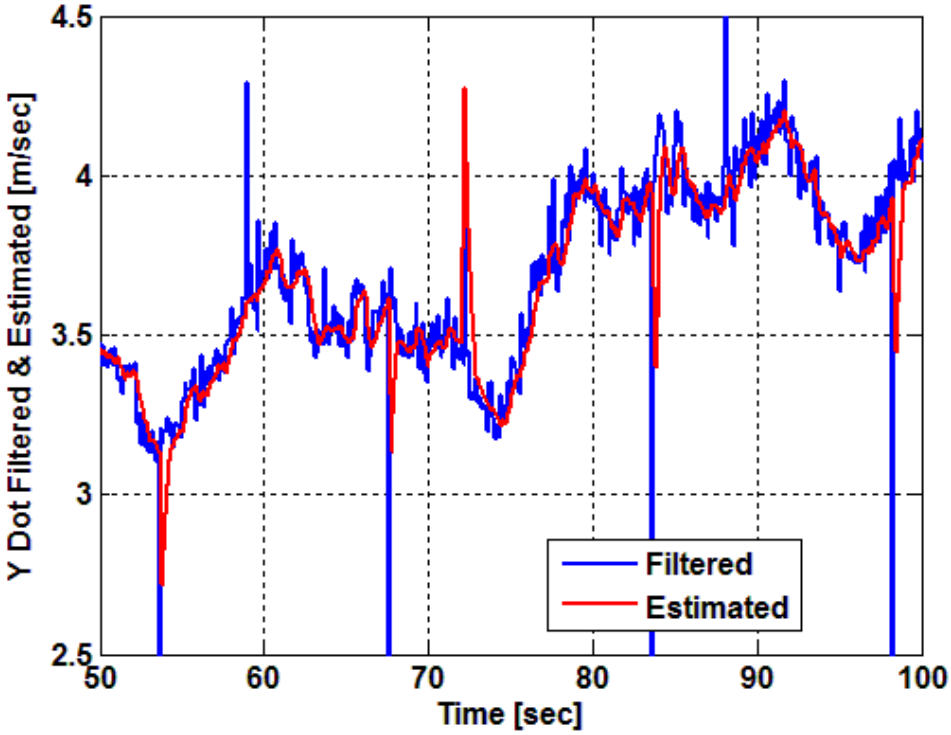

Figure 0-49 Zoomed-in view of the filtered and estimated $\dot{Y}$ of the boat

Summary

The modifications made to the stock configuration of the boat that was used in the experimental work is described in great detail in this chapter. The experimental results were generated in the totally uncontrolled environment of Lake St. Clair, Michigan. They were collected under a variety of weather conditions involving significant variations in lake temperature, wind resistance, wave height, current magnitudes and directions. The results served to experimentally validate the robust performance and tracking characteristics of the fully integrated guidance and controller-observer system in the presence of considerable environmental disturbances and modeling inaccuracies.

The next chapter will focus on the digital simulations that were conducted to validate the collision avoidance scheme.

CHAPTER 5 INTEGRATION AND SIMULATION RESULTS OF THE OBSTACLE AVOIDANCE CODE

The guidance system used in generating the experimental data of the previous chapter did not have any obstacle avoidance features. A second vessel was not available to safely conduct obstacle avoidance experiments involving nonstationary vessels. Therefore, all experiments were aborted by the human operator whenever a nearby vessel gets too close or infringe on the desired path of the autonomous boat. This was accomplished through the RTI GUI running on the laptop computer. Figure 0-1 shows the block diagram of the overall experimental set-up used in conducting the experimental work that was performed on the lake St. Clair.

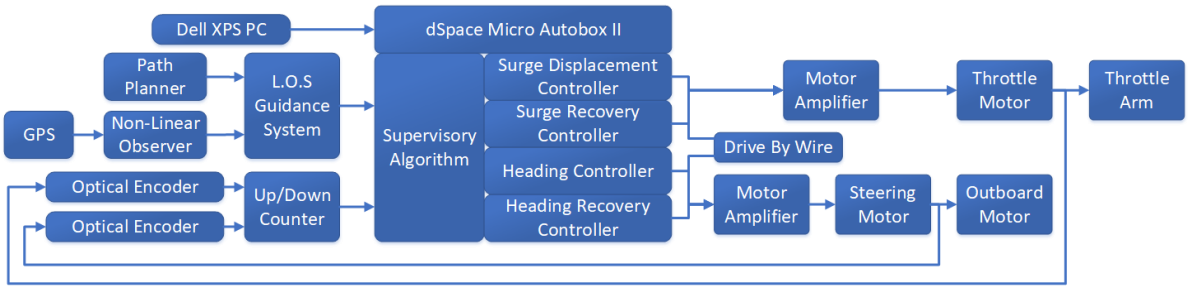

Figure 0-1 Block diagram of the overall experimental apparatus

Therefore, the performance of the proposed collision avoidance scheme with imbedded COLREGs rules has been assessed in the current study through digital simulations.

Integration of the Collision Avoidance Algorithm with the Guidance System

To integrate the collision avoidance scheme with the existing guidance system, the block diagram depicted in Figure 0-1 had to be modified as shown in Figure 0-2. Note that the collision avoidance scheme was designed to override the action of the guidance system in case of an impending danger. Therefore, a "collision avoidance" block is inserted between the LOS guidance system block and the vessel's supervisory control strategy block (see Figure 0-2). Its function is to intercept the desired velocity vector specified by the guidance system and determine if it

would result in an undesirable event. If no collision is predicted then the proposed velocity vector is passed through without any modification. However, if it is found that the proposed velocity vector would lead to an undesirable event then the collision avoidance scheme will compute a new velocity vector in order to avoid the collision with the moving obstacle. Once the threat had passed, the obstacle avoidance scheme would pass through all desired velocity vectors as commanded by the guidance system.

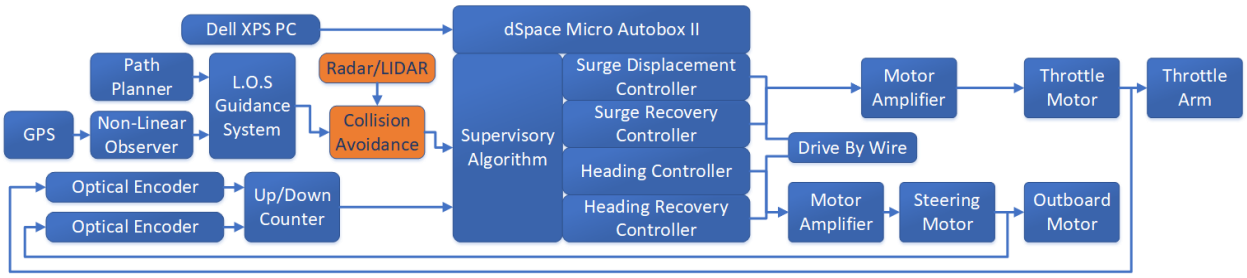

Figure 0-2 Block Diagram of overall system and how collision avoidance was integrated

Since the proposed scheme was only assessed by digital simulations then all measured signals are assumed to be readily available with the understanding that real-world data would require extensive sensor calibration and tuning in order to provide useable measured signals. In spite of recognizing this issue, the current work did not address problems associated with measured signals. Instead, the focus of the current work has been on proving the validity of the proposed collision avoidance scheme with imbedded COLREGs rules.

Corrective Actions by the Collision Avoidance Scheme

The code for the collision avoidance scheme requires the global position vectors and the inertial velocity vectors of both the primary vessel and the moving obstacle/vessel. The program will then use this information to detect any looming collision.

The actions of the proposed collision avoidance scheme with imbedded COLREGs rules under different scenarios are illustrated in Figure 0-3 to Figure 0-5. V_{MO} is the velocity vector of the moving obstacle. V_{PV} is the desired velocity vector prescribed by the guidance system for the primary vessel. (X_{MO}, Y_{MO}) and (X_{PV}, Y_{PV}) are the actual positions of the moving obstacle and the primary vessel, respectively. The blue circle surrounding the obstacle represents the safety zone that should not be encroached by the primary vessel. The solid black lines show the shifted collision cone generated by the velocity obstacles (VO) approach. The V_{PVM} is the desired velocity vector prescribed by the collision avoidance scheme whenever the course of the primary vessel needs to be changed in order to avoid an imminent collision. It should be emphasized that in all scenarios the desired green velocity vector of the primary vessel is passed on to the heading controller of the boat.

The first scenario is shown in Figure 0-3 where no imminent collision is predicted; thus, no deviation from the original course of the primary vessel is required. Consequently, the desired velocity vector specified by the guidance system will be forwarded to the heading controller. Figure 0-4 illustrates the second scenario whereby an undesirable event is predicted and the primary vessel does not have the right-of-way (ROW). In this situation, the course of the primary vessel has to be altered through the action of the collision avoidance scheme. The desired velocity vector commanded by the guidance system and displayed in red in Figure 0-4 will now be overridden by the collision avoidance scheme, which prescribes a new velocity vector that is displayed in green in Figure 0-4. The third scenario is given in Figure 0-5. In this case, an undesirable event is predicted but the primary vessel has the right-of-way. Thus, no corrective

action is needed and the primary vessel will maintain its original course. The other vessel is expected to take corrective measures.

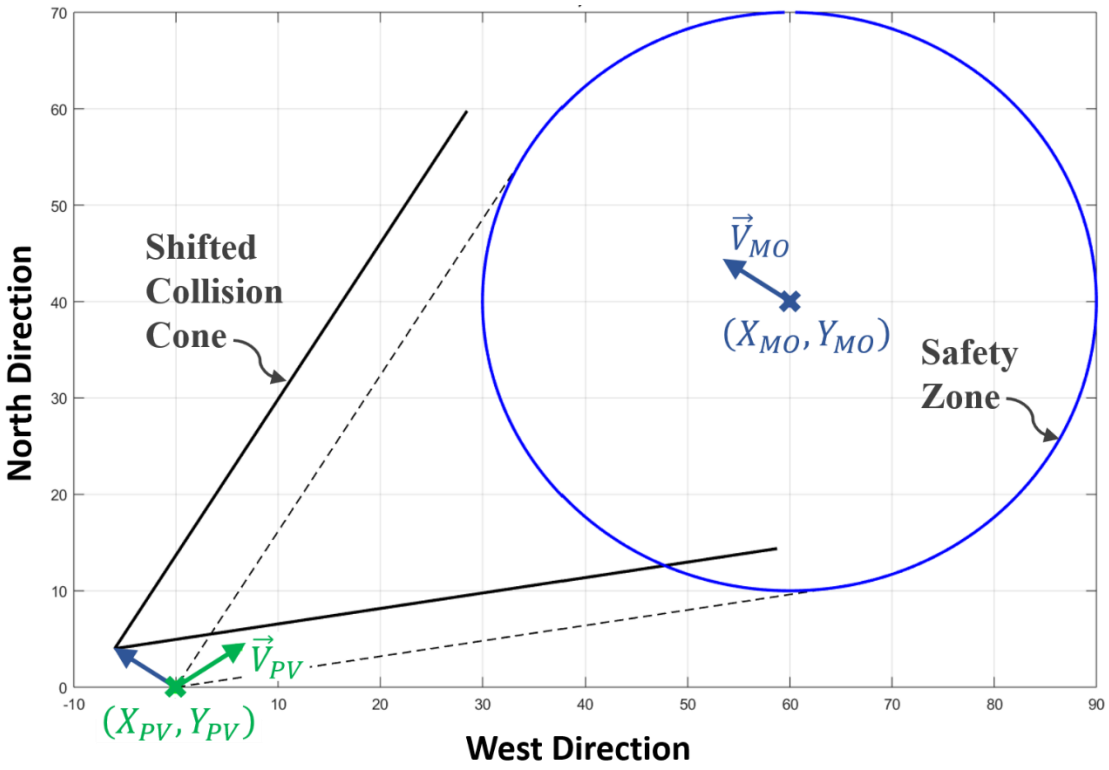

Figure 0-3 Primary vessel remains on course because no undesirable event is detected.

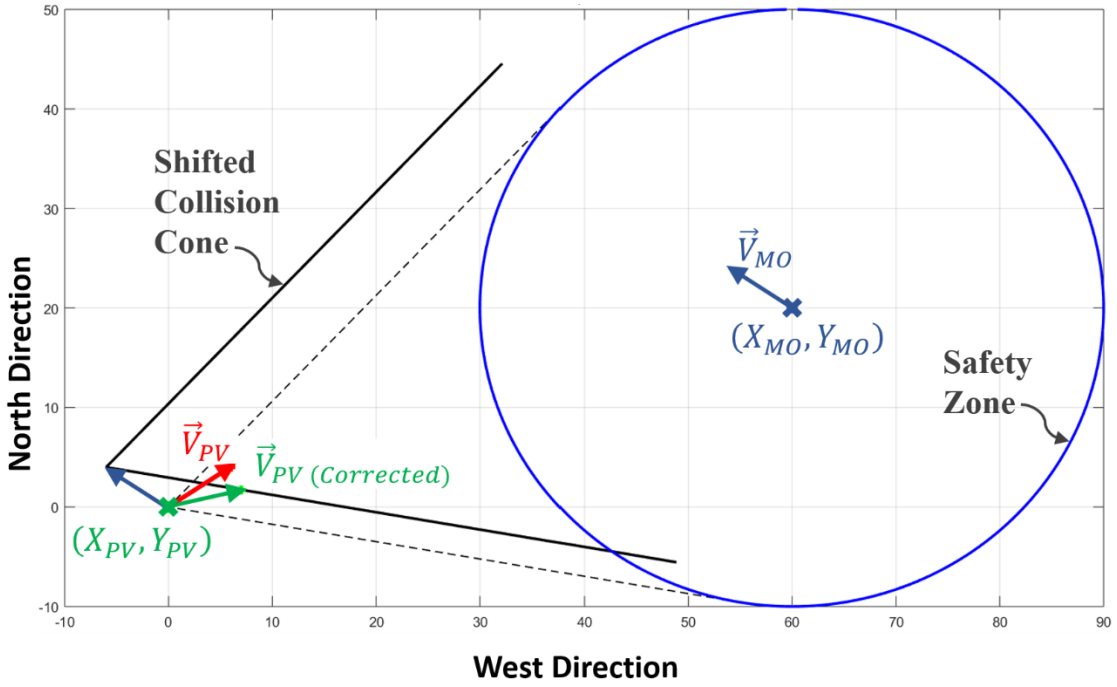

Figure 0-4 Undesirable event is detected and the course of the primary vessel has to be altered.

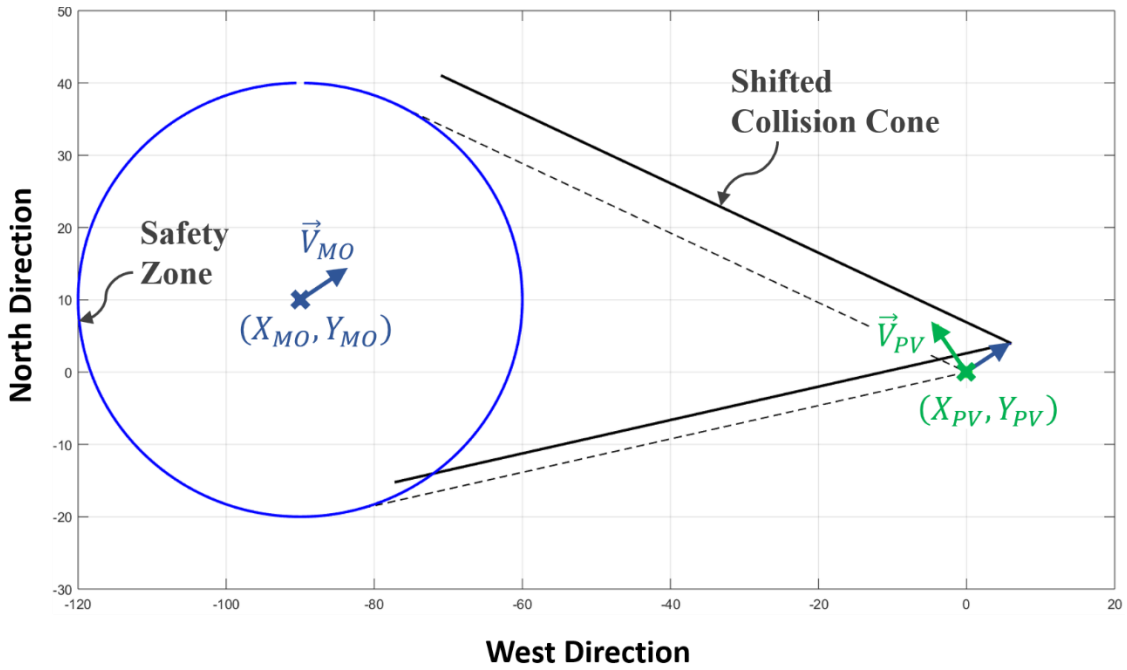

Figure 0-5 Undesirable event is detected and the course of the primary vessel does not have to be altered.

Simulation results

The collision avoidance routine was then integrated in the overall code of the controller/observer/guidance system. As stated earlier, its performance is solely assessed through digital simulations in which the primary vessel was commanded to follow a desired trajectory consisting of three segments passing through four waypoints in the following order $(X_1 = 0, Y_1 = 0), (X_2 = 500, Y_2 = 0), (X_3 = 500, Y_3 = 10000)\ and\ (X_4 = 1500, Y_4 = 1000)$. Two moving obstacles/vessels were introduced and set on courses that would intersect with that of the primary vessel at different stages of the test. The first one moved in a straight line across the test area, while the second one followed a circular path. It is assumed that none of the moving obstacles would obey COLREGs rules. Consequently, they would maintain their trajectories and ignore any potential collisions. Given these assumptions then it became necessary for the primary vessel to take corrective actions whenever undesirable events are detected.

The simulation begins with no undesirable events predicted during the first leg of the test. As seen in Figure 0-6, the primary vessel traverses the first segment without any interference from the collision avoidance scheme. This is depicted in Fig. 5-6 by the green thick line which traces the actual trajectory of the primary vessel in its attempt to accurately track the first segment between the first two waypoints. When the primary vessel encroaches the circle of acceptance surrounding the second waypoint $(X_2 = 500, Y_2 = 0)$, the LOS guidance system switches its pursuit to the second segment of the desired trajectory. Shortly after the boat changes direction to follow the second segment of the desired trajectory, it detects a looming collision with the obstacle 1. At this instance, the thick green line in Figure 0-6 turns red signifying

that the LOS guidance system has been overridden by the collision avoidance system. The latter will now be in command to specify the desired velocity vector that will cause the primary vessel to deviate from its desired trajectory in order to avoid the collision with the moving obstacle. During this phase, one would expect the cross-track error, d, to increase. Since the radius used in the LOS guidance system is defined as $R = R_{Min} + d$ then this system would still be able to guide the boat back to its desired trajectory after the collision threat subsides and the vessel's command is turned over from the collision avoidance scheme back to the LOS guidance system.

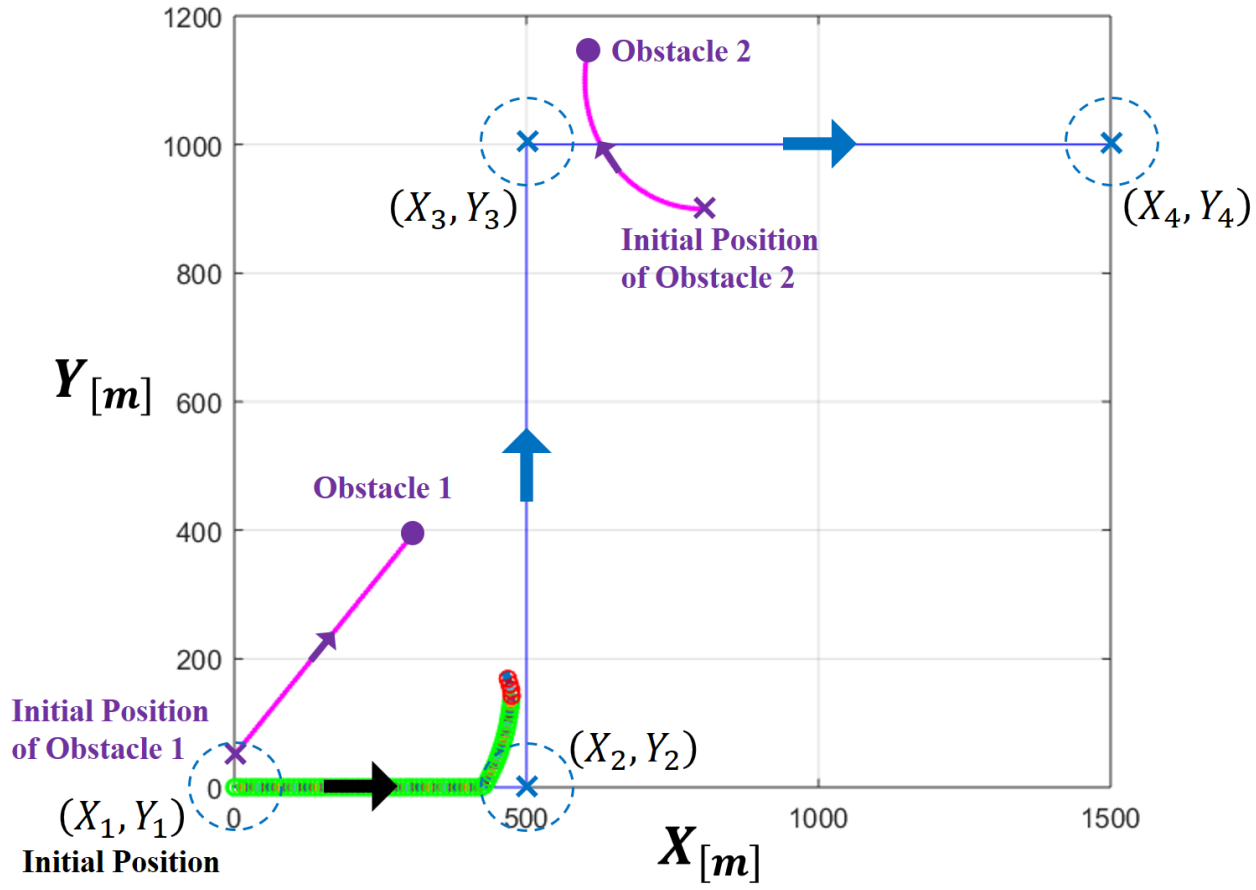

Figure 0-6 When the primary vessel identifies a potential violation the collision avoidance overrides the guidance system to prevent an undesirable situation

During each iteration, the fully-integrated code of the primary vessel examines the desired velocity vector specified by the LOS guidance system to determine if it leads to an undesirable event. Should the assessment detect a looming collision with a moving obstacle then the guidance system will be overridden by the collision avoidance scheme, which will now define a new and suitable velocity vector for the primary vessel. Note that the intent in this work is to minimize the activation period of the collision avoidance scheme. This is due to the fact that deviations from the desired path of the boat will always lead to larger cross track errors. Therefore, the collision avoidance scheme will only be activated whenever the LOS guidance system fails to produce a desired velocity vector that would yield a collision-free passage for the primary vessel.

It should also be emphasized that the integration of the collision avoidance code with the guidance system required a substantial increase in the radius that is used for determining the line-of-sight in the guidance system. This was done to minimize the number of times the command of the boat is switched between the guidance system and the collision avoidance scheme. For instance, if the radius is chosen to be small and the cross-track error is large then the guidance system will provide a desired velocity vector that will not cause any collision with the obstacle (see Figure 0-7a). As a consequence, the boat command will now be turned back to the guidance system. However, as the vessel approaches its desired trajectory (see Figure 0-7b), the guidance system will now produce a desired velocity vector that will lead to a collision; thus, prompting the re-activation of the collision avoidance scheme. Going back-and-forth multiple times in the boat command between the collision avoidance scheme and the guidance system in the handling of a single collision threat is not desirable and has been handled herein by

significantly increasing the radius based on which the line-of-sight has been generated in the guidance system.

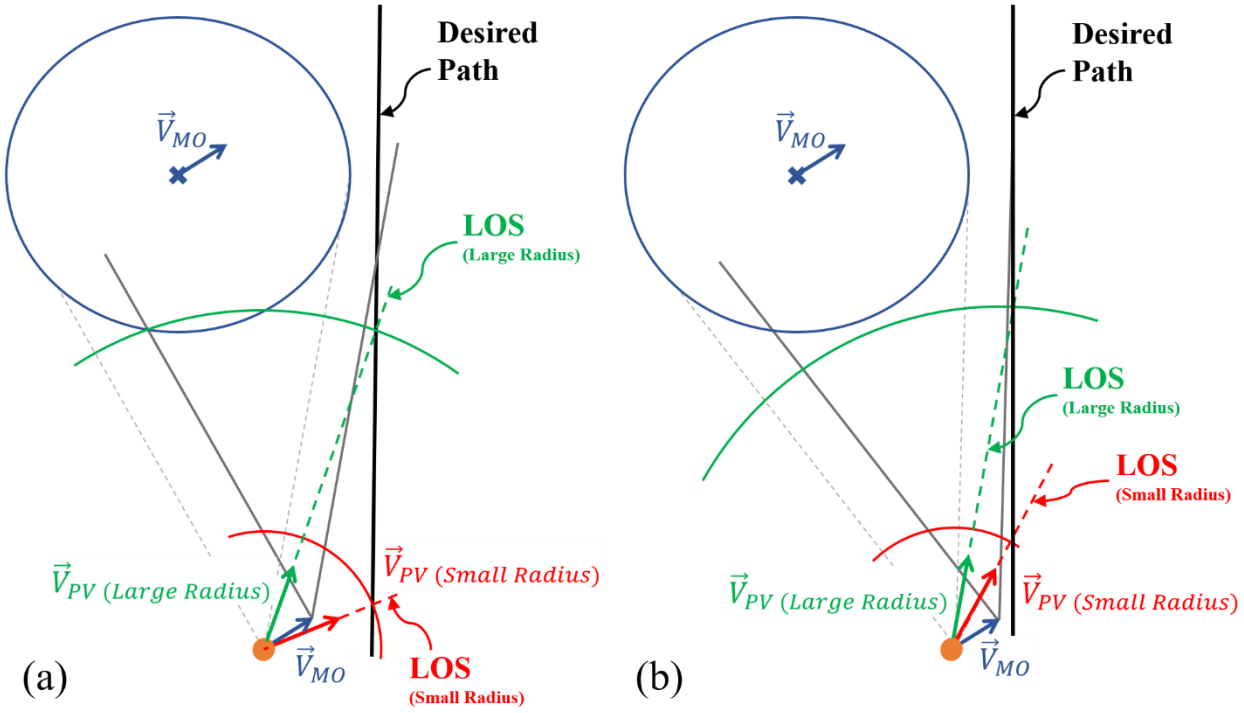

Figure 0-7 Effect of the radius size in the guidance system on the transfer of boat command between collision avoidance scheme and guidance system.

As the simulation continues along the second segment of the desired trajectory, the primary vessel successfully avoids the obstacle that is moving along a straight line by changing its course to pass behind the obstacle according to COLREGs rules. After the threat subsided, the collision avoidance scheme relinquishes the boat command to the guidance system, which will be responsible for converging the primary vessel to its prescribed path. This behavior is illustrated in Figure 0-8 with the vessel's markers returning to green.

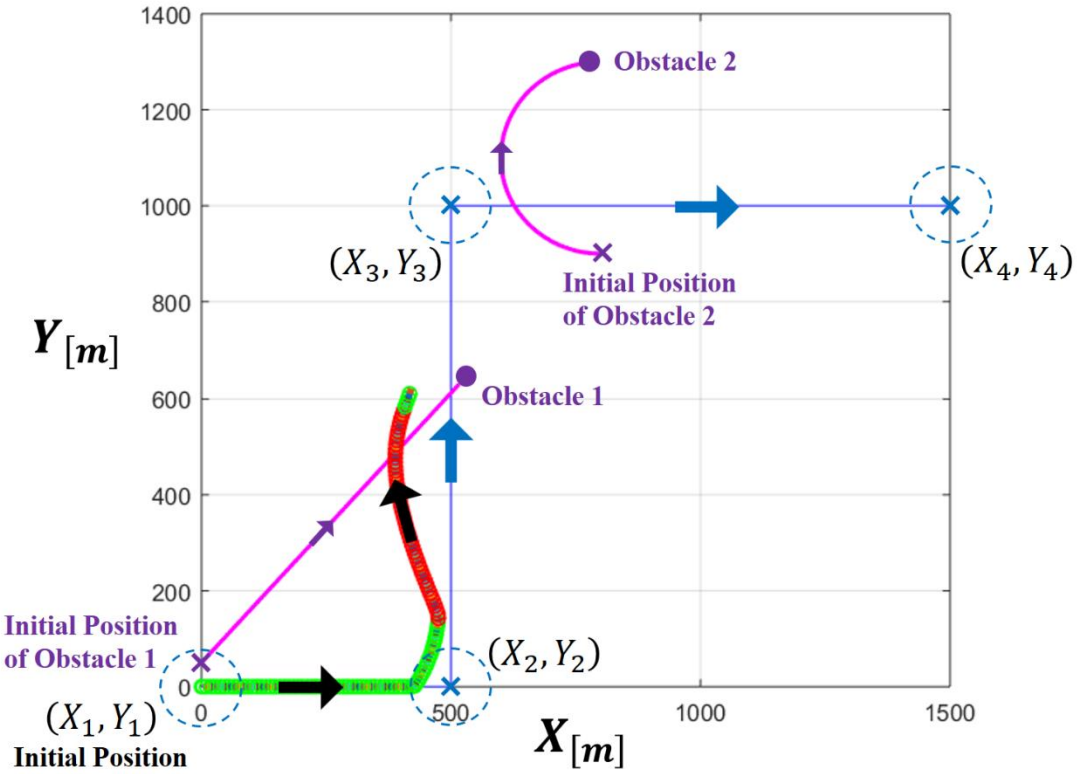

Figure 0-8 After the threat subsided, the collision avoidance scheme relinquished the control back to the guidance system and the vessel converges back onto its desired path

When the primary vessel breaches the circle of acceptance surrounding the third waypoint, the guidance system switches its focus to the third segment of the desired trajectory. At this instant, the system immediately detects an undesirable event with obstacle 1 again. The collision avoidance scheme will once again override the guidance system and direct the vessel around obstacle 1 (Figure 0-9). Once the threat vanished, the collision avoidance scheme relinquishes the boat control back to the guidance system, which guides the vessel toward its desired path (Figure 0-10).

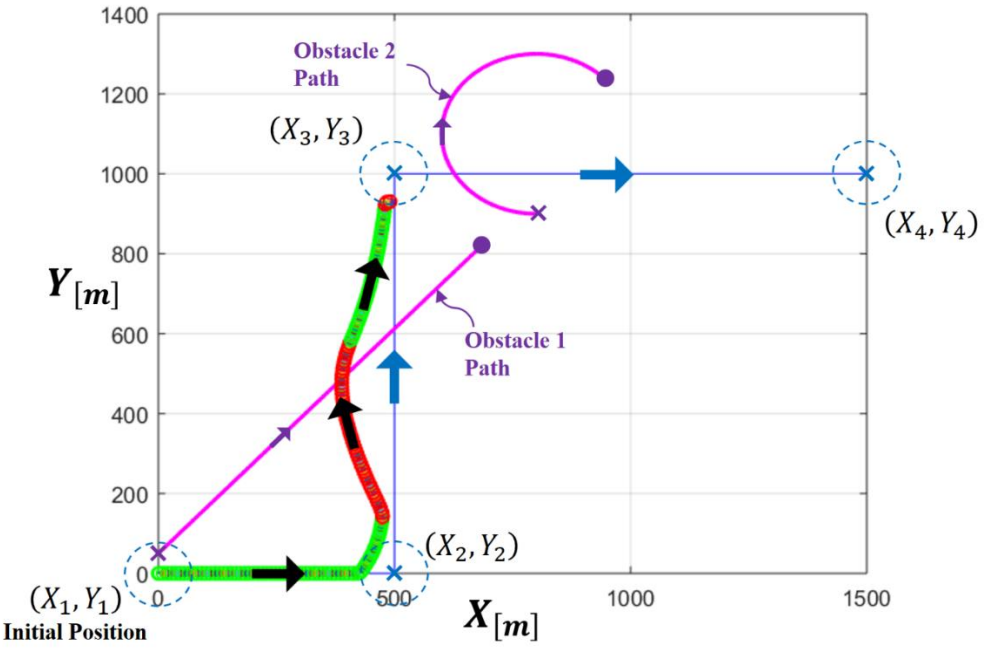

Figure 0-9 As the primary vessel switches to the third segment of the path, it encounters obstacle1 once again and must take corrective actions

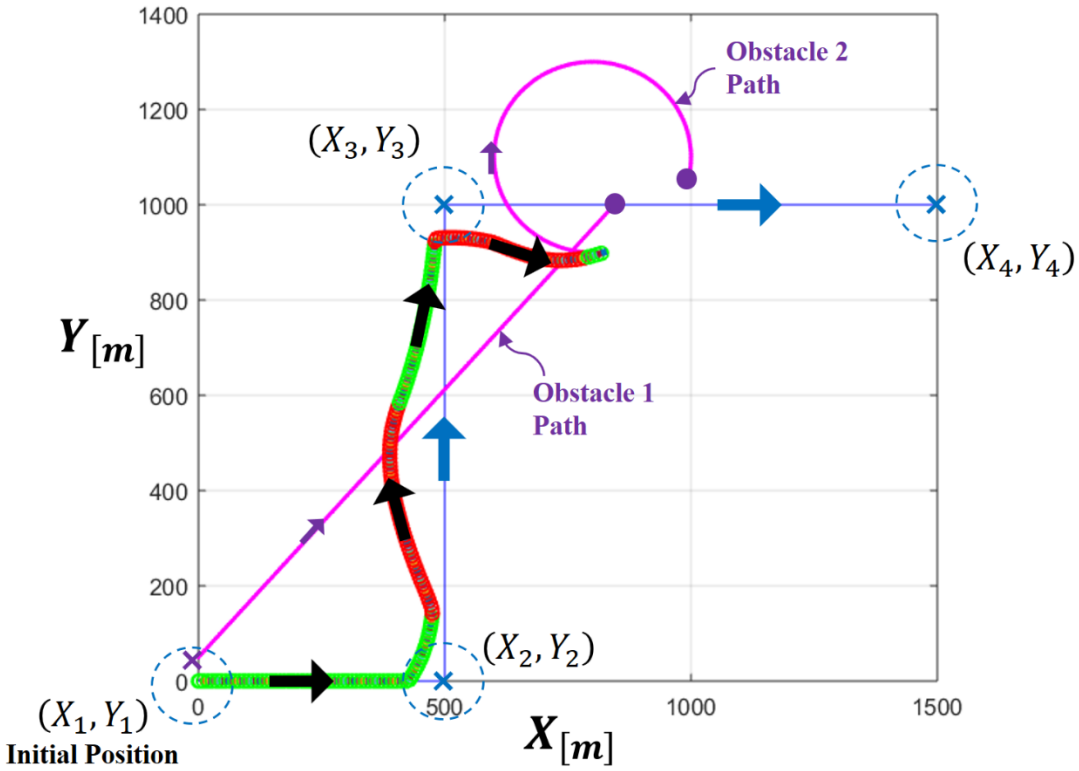

Figure 0-10 The guidance system regains control of the boat once the threat from obstacle 1 is vanished.

As the vessel begins to converge on the third segment of the desired path, obstacle 2 which is moving on a circular path would turn into the vessel's trajectory and becomes a potential threat. Due to the circular path followed by obstacle 2, the collision avoidance scheme would have a very short period to react; thus, requiring the primary vessel to undergo more aggressive maneuvers than usual to avoid the impending collision. This is illustrated in Figure 0-11 Although the primary vessel successfully avoids obstacle 2, this scenario demonstrates a potential shortcoming of this method. The velocity obstacles approach uses the object's instantaneous velocity vector to perform its calculations by assuming that the obstacle moves in a straight line. Since vessels at sea do not necessarily follow straight line paths then such challenges need to be dealt with in future research studies in order to address the shortcomings of the velocity obstacles method. A comment is in order pertaining to the situation represented in this simulation. Such a type of maneuver would only occur with malice intent or extreme neglect. Therefore, it is only marginally relevant to our study. Figure 0-12 shows the primary vessel successfully avoiding obstacle 2 and begin to converge to its desired path. Figure 0-13 shows the vessel finishing the final segment of the prescribed route and converges back to its path as the test is completed.

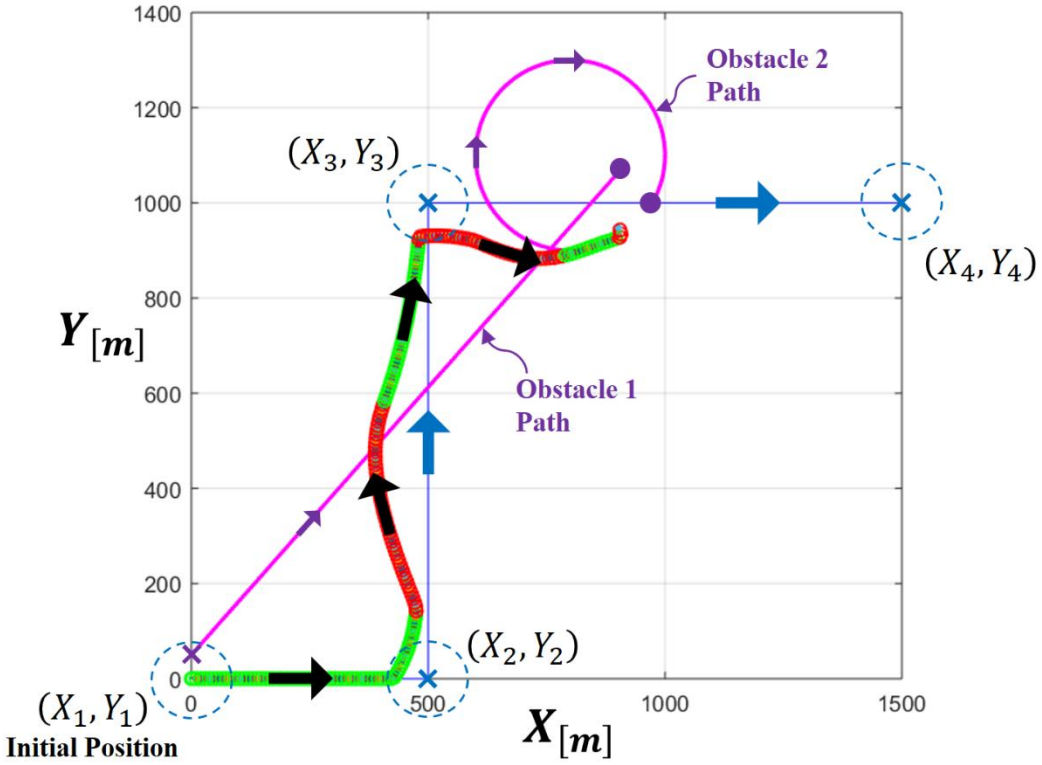

Figure 0-11 The primary vessel now encounters obstacle 2 and must take appropriate actions.

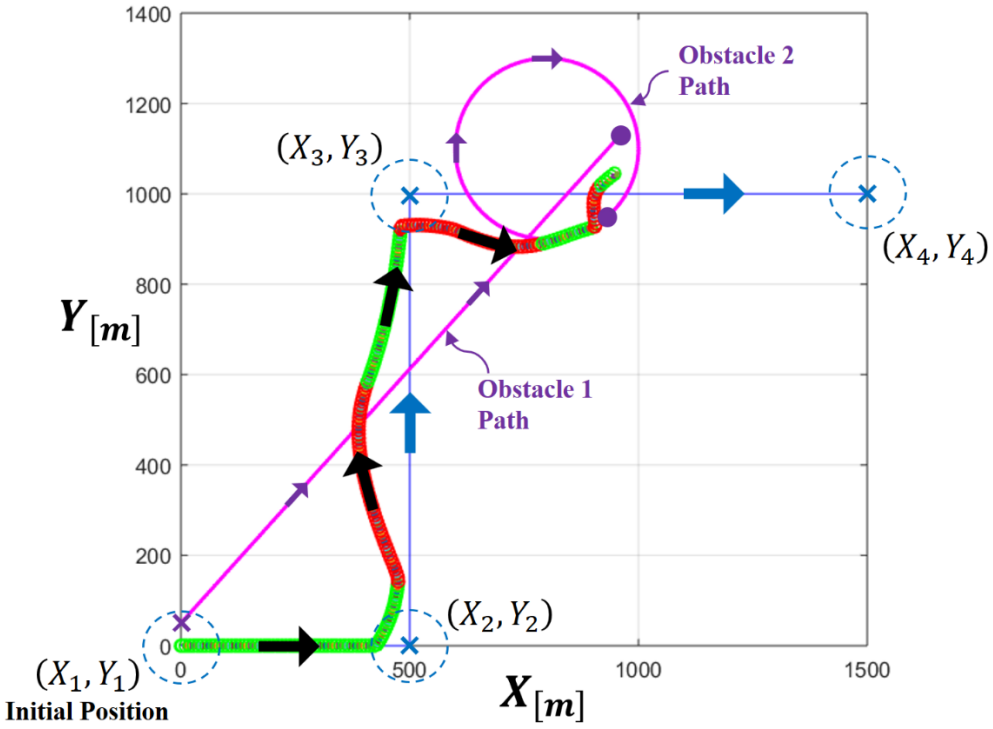

Figure 0-12 Once the threat subsided, the guidance system regains control

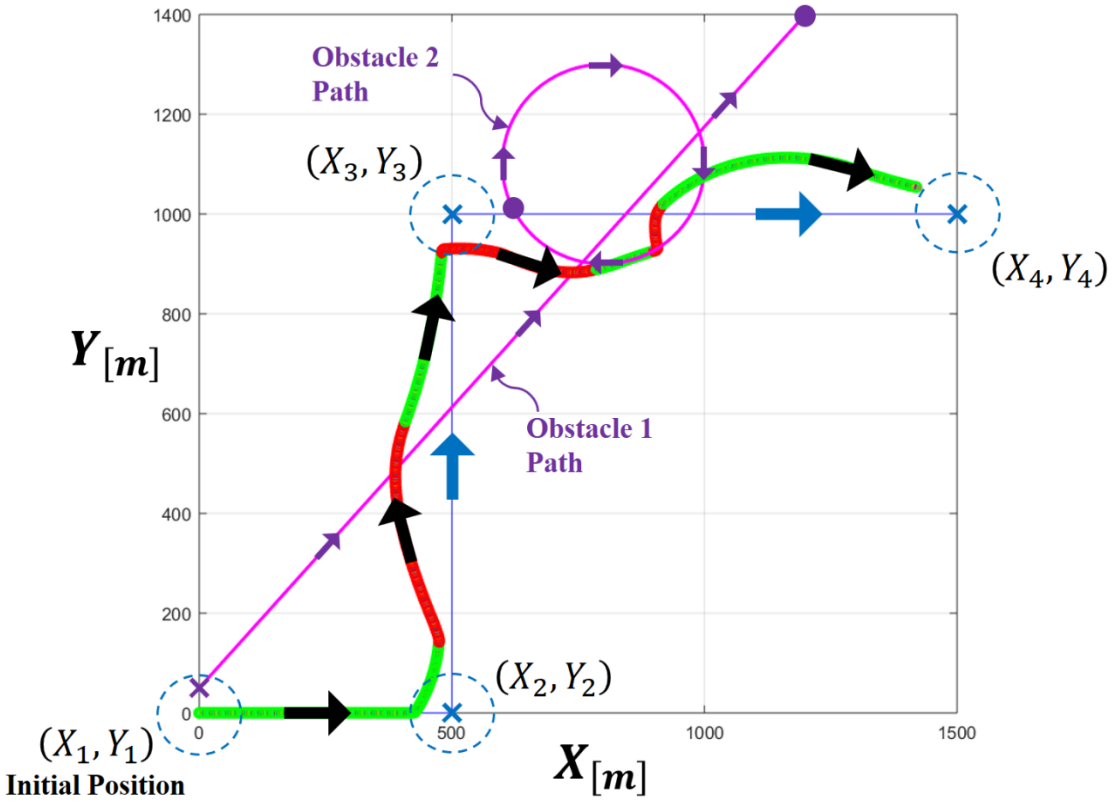

Figure 0-13 No further obstacles are encountered so the guidance system brings the vessel back to the desired path

Figure 0-14 provides the entire result discussed earlier with collision cones overlaid on the actual trajectory of the primary vessel. The rationale is to show which obstacle is being tracked at different stages of the experiment. As mentioned earlier, the current collision avoidance scheme does not track multiple obstacles simultaneously. Whichever obstacle closest to the primary vessel will be considered to pose the highest threat. Such an approach did not have any adverse effect on the simulated scenario whereby the primary vessel encountered two obstacles and dealt with them one at a time. Enhancing the capability of the current collision avoidance scheme to track and avoid multiple obstacles simultaneously would constitute a challenging research project and would be a desirable improvement since it would allow marine vessels to navigate safely through congested areas.

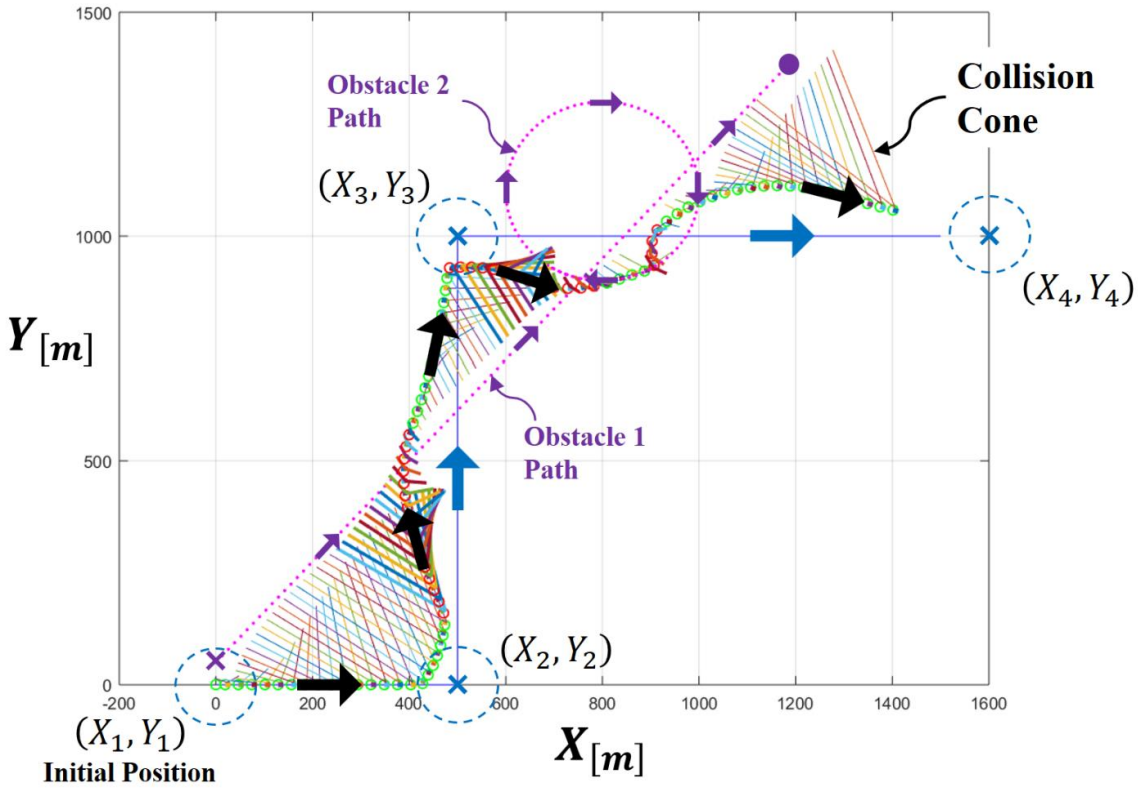

Figure 0-14 The primary vessel tracks whichever obstacle is closest and uses velocity obstacles to calculate a collision cone to determine if action is required

Summary

This chapter explained in detail the procedure used in integrating the collision avoidance scheme with the overall guidance and control code of the primary vessel. The current approach was validated through digital simulations whereby a primary vessel was assigned the task of tracking a desired path that is made up of three straight segments. In doing so, the vessel encountered two obstacles following different trajectories that intercepted the specified trajectory of the primary vessel at different stages of the simulation. The results demonstrated the viability of the proposed scheme in avoiding collision with the moving obstacles while abiding by the COLREGs rules. In the next chapter, a brief summary of the work is provided. The main contributions of the current work are highlighted and prospective research topics are suggested.

CHAPTER 6 SUMMARY AND CONCLUSIONS

In this chapter, the current study is summarized and the main conclusions are deduced. In addition, the contributions of the current work are highlighted and prospective research topics in this field are suggested.

Summary and conclusions of the Work

Experimental Validation of the Fully-Integrated Controller/Observer/Guidance system

Autonomous operation and robust performance of marine surface vessels are essential for minimizing human errors in ship navigation and for yielding efficient operation of ships under different sea states and harsh environmental conditions. This goal presents a challenging task due to inherent nonlinearities of ship dynamics, modeling imprecision stemming from structured and unstructured uncertainties of the system, considerable and unpredictable environmental disturbances induced by wave excitation forces, sea-current and wind resistive loads. This problem is further compounded by the under-actuated configuration of marine surface vessels, which stems from having fewer actuators than degrees of freedom. A plausible approach for enabling under-actuated marine vessels to accurately track their desired trajectories is to pair the ship controller with a navigation system. This will empower the ship steering mechanism to simultaneously control the sway displacement and the heading angle of the ship while the propeller thrust would be mainly devoted for the control of the surge speed and displacement. This approach does not require additional hardware to be installed on the ship and allows for a fully autonomous operation of the ship.

To operate the boat in a fully autonomous manner, the controller had to be able to automatically vary the thrust of the propeller and the rudder angle. Therefore, the Tracker boat

had to be retrofitted with two separate mechanisms that yield the control of the propeller thrust and the rudder angle to the controller. These mechanisms were designed and built in-house. In addition, a Hemisphere V101 Compass Global Positioning System (GPS) receiver was installed to provide the boat global coordinates. An extensive interface code had to be written in-house in MATLAB\Simulink\Stateflow chart and compiled in dSPACE in order to allow the guidance system, controller and observer to interact with the sensors and actuators mounted on the marine surface vessel.

Before any experimental validation of the guidance and control system could be performed in an uncontrolled environment, safety considerations had to be taken by designing a hybrid control strategy in order to ensure synchronized operation of all system components and provide the user with the capability of invoking the "recovery" controller should any unforeseen emergency situation arises. The hybrid control strategy encompasses different versions of surge motion and heading angle controllers along with a recovery controller. It consists of five controllers that are being managed by a main supervisory algorithm. Two of these controllers are devoted for tracking and maneuvering operations of the vessel based on feedback signals representing the actual surge motion and the heading angle of the boat. Another two controllers provide the user with the option of performing either point-to-point (PTP) or prescribed throttle angle and heading angle control tasks. The feedback signals for these controllers are obtained from optical encoders mounted on their respective servomechanisms. The fifth controller, referred to herein as a "recovery" controller, is only activated in the case of unforeseen mishaps. Its main function is to drive back the throttle arm to a neutral position; thus, reducing the propeller thrust to zero in a controlled manner. The supervisory algorithm orchestrates the

functioning of these controllers to successfully track a desired trajectory while ensuring a safe operation of the marine vessel. Its role entails activating the appropriate controllers and triggering the recovery controller when needed. The final safety mechanism that was put in place was a physical switch that disconnected the dSpace unit from the motor actuators and connected a drive by wire system. This allowed the human operator to manually take control if required.

Given the unpredictable nature of open-sea operations of marine vessels and the ensuing external disturbances, both controller and observer must be robust to structured and unstructured uncertainties of the ship along with environmental disturbances. Therefore, the sliding mode methodology has been implemented herein to devise the controllers and observers that were used in tracking and maneuvering operations of the vessel based on feedback signals representing the actual surge motion and the heading angle of the boat. The desired heading angle that will ensure convergence of the under-actuated ship to its specified trajectory is generated by the guidance system. It will lead to a simultaneous compensation of both heading angle and sway motion with a single control action. Consequently, the trajectory tracking problem is now reduced to the control of the surge displacement and the heading angle for which two control variables are readily available, namely, the propeller thrust and the rudder angle.

The focus of the first part of the current work was on the experimental validation of the holistic approach that encompassed a navigation system, a controller and an observer. In this phase, the dynamics of the boat were assumed to be completely unknown and the environmental disturbances are considered to be random in nature. Therefore, both observer and controllers were implemented herein by totally ignoring the boat's dynamics. The sliding mode observer was used to estimate the X, Y and ψ of the boat along with their time derivatives

from the GPS data. The experimental validation has been conducted by relying on the sliding mode observer (SMO) to provide on-line estimates of the state variables that are required by the controller. The experimental results demonstrate the capabilities of the sliding mode controllers in rapidly converging the vessel to its desired trajectory and the sliding mode observer in accurately estimating the state variables of the system in spite of ignoring the system's dynamics and in the presence of unpredictable environmental disturbances.

Integration of Obstacle Avoidance Scheme with the Guidance System

The line-of-sight (LOS) navigation system has been modified in the second phase of this study to expand its capabilities to provide obstacle avoidance with both stationary and moving obstacles. This was done by integrating the LOS guidance scheme with a modified version of the velocity obstacles (VO) technique while incorporating the COLREGS rules of maritime navigation. Note that the LOS navigation system employs waypoints that are chosen by a human operator to avoid known stationary obstacles such as land masses, shallow regions, navigation buoys, etc. Although, the collision avoidance system will have the ability to avoid such obstacles, the current study has focused on dynamic obstacles.

The integration of the collision avoidance scheme with the existing controller/observer/guidance system has been done by adopting an overriding paradigm whereby the desired velocity vector specified by the guidance system will be overridden by the collision avoidance scheme in order to avoid infringement on the collision cones defined by the VO technique. Since the smallest change in the desired velocity vector would lead to the least deviations from the overall desired path of the vessel then the new velocity vector commanded by the VO scheme should be defined such that its tip lies on the edges of the collision cone that

are located within the contour. Any velocity vector having its tip within the contour but further away from the edges of the collision cones would result in unnecessary large deviations from the overall desired course of the vessel.

The function of the collision avoidance scheme is to intercept the desired velocity vector specified by the guidance system and determine if it would result in an undesirable event. If no collision is predicted then the proposed velocity vector is passed through without any modification. However, if it is found that the proposed velocity vector would lead to an undesirable event then the collision avoidance scheme will compute a new velocity vector in order to avoid the collision with the moving obstacle. Once the threat had passed, the obstacle avoidance scheme would pass through all desired velocity vectors as commanded by the guidance system.

In the current study, the performance of the collision avoidance scheme was assessed through digital simulations whereby a primary vessel was assigned the task of tracking a desired path that is made up of three straight segments. In doing so, the vessel encountered two obstacles following different trajectories that intercepted the specified trajectory of the primary vessel at different stages of the simulation. The results demonstrated the viability of the proposed scheme in avoiding collision with the moving obstacles while abiding by the COLREGs rules.

General Contributions of the Work

The main contributions of the current study are as follow

- A successful autonomous operation of a marine surface vessel would require a holistic approach encompassing a navigation system, robust nonlinear controllers and observers.

Nassim and Chalhoub in [3] conducted a theoretical study proposing such a holistic approach. They proved the viability of such an approach through digital simulations. However, it should be emphasized that the theoretical development of advanced control algorithms and nonlinear observers has greatly surpassed the experimental work in this field. Many potential controllers and observers have been developed and never been validated experimentally in an uncontrolled real-world environment. The current study makes a significant stride towards bridging the gap between the experimental validation and theoretical advancements in this field by providing an experimental validation for the robustness and good tracking characteristics of a fully-integrated line-of-sight (LOS) guidance system with a sliding mode controller and observer that were developed for a marine surface vessel. The experimental data were generated by using a 16' boat operating in the uncontrolled open-water environment of Lake St. Clair, Michigan. It should be noted that the experimental work was conducted under a variety of weather conditions involving significant variations in lake temperature, wind resistance, wave height, current magnitudes and directions.

- A collision avoidance scheme was developed by modifying the velocity obstacles (VO) approach while incorporating the COLREGS rules of maritime navigation. All studies reported in the literature regarding the velocity obstacles scheme have been validated through digital simulations by considering simple scenarios or situations. In the current work, the performance of the proposed collision avoidance scheme combined with the existing LOS guidance system was assessed through digital simulations by using complex interactions between two vessels as well as between vessels that do not follow the COLREGs rules; thus, requiring the primary vessel to react to all real-life situations that may occur. The current

results prove the robust performance of the proposed obstacle avoidance scheme while providing a high level of confidence that it is suitable for real-world applications.

Future Research Topics

As with all studies, while the work progresses, ideas present themselves for potential improvements or alternate methods for solving challenges. Although the work performed in this study was successful, there have been many ideas to improve the methods used in these tests. Therefore, the following prospective research topics are suggested:

- New features should be added to the current robust nonlinear controller to self-tune its parameters based on varying environmental conditions.
- The current collision obstacle has the capability of searching for a solution to avoid multiple obstacles concurrently. However, this would require a sophisticated algorithm to search for an optimal solution. In the current implementation, a solution is found by rotating the current velocity vector until it is outside of the collision cone. In the presence of multiple obstacles, changing the magnitude and direction of the velocity vector would need to be searched in order to obtain an optimal solution. Such tasks require an exhaustive search that would be computationally intensive. Further studies are needed to refine and empower the collision obstacle scheme to make it suitable for navigation of marine vessels in closed quarters such as in a harbor.
- COLREGs was written for human interpretation. This tend to make the coding of these rules very difficult since the limits for applying the rules need to be defined. In the current simulation work, these limits were defined based on personal experience on the lake. Real-life data should be gathered to refine these limits based on real-life applications.

REFERENCES

1. Ueng, S.-K., D. Lin, and C.-H. Liu, *A ship motion simulation system.* Virtual reality, 2008. **12**(1): p. 65-76.

2. Newman, J.N., *Marine hydrodynamics*. 1977: MIT press.

3. Ogilvie, T.F. *Recent progress toward the understanding and prediction of ship motions*. in *5th Symposium on naval hydrodynamics*. 1964. Bergen, Norway.

4. Lewis, E.V., *Principles of Naval Architecture: Motions in waves and controllability*. Vol. 3. 1988: Society of Naval Architects &.

5. Khaled, N. and N.G. Chalhoub, *A dynamic model and a robust controller for a fully-actuated marine surface vessel.* Journal of Vibration and Control, 2011. **17**(6): p. 801-812.

6. Journèe, J.M. and W. Massie, *Offshore hydrodynamics.* Delft University of Technology, 2001. **4**: p. 38.

7. Journée, J. and J. Pinkster, *Introduction In Ship Hydromechanics, Lecture MT519; Draft Edition.* Delft University of Technology, Nederland, 2002.

8. Jiang, Z.P. and H. Nijmeijer, *A recursive technique for tracking control of nonholonomic systems in chained form.* Ieee Transactions on Automatic Control, 1999. **44**(2): p. 265-279.

9. Velasco, J., et al., *Simulations of an autonomous in-scale fast-ferry model.* International Journal of of systems applications, engineering a development, 2008(3).

10. Fossen, T.I., *Guidance and control of ocean vehicles*. 1994: John Wiley & Sons Inc.

11. Faltinsen, O., *Sea loads on ships and offshore structures*. Vol. 1. 1993: Cambridge university press.

12. Barrass, B. and C.D. Derrett, *Ship stability for masters and mates*. 2011: Butterworth-Heinemann.

13. Perez, T., *Ship Motion Control. Advances in Industrial Control*. 2005, Springer-Verlag, London.

14. Falzarano, J.M. and C. Lakhotia, *Effect of Icing on Ship Maneuvering Characteristics.* Proceedings of the 27th International Conference on Offshore Mechanics and Arctic Engineering - 2008, Vol 3, 2008: p. 997-1001.

15. Ibrahim, R.A., N.G. Chalhoub, and J. Falzarano, *Interaction of ships and ocean structures with ice loads and stochastic ocean waves.* Applied Mechanics Reviews, 2007. **60**(1-6): p. 246-289.

16. Cammaert, A.B. and D.B. Muggeridge, *Ice interaction with offshore structures*. 1988, New York: Van Nostrand Reinhold. xvi, 432 p.

17. Grace, I.F. and R.A. Ibrahim, *Modelling and analysis of ship roll oscillations interacting with stationary icebergs.* Proceedings of the Institution of Mechanical Engineers Part C-Journal of Mechanical Engineering Science, 2008. **222**(10): p. 1873-1884.

18. Pettersen, K.Y. and H. Nijmeijer, *Underactuated ship tracking control: theory and experiments.* International Journal of Control, 2001. **74**(14): p. 1435-1446.

19. Moreira, L., T.I. Fossen, and C.G. Soares, *Path following control system for a tanker ship model.* Ocean Engineering, 2007. **34**(14-15): p. 2074-2085.

20. Khaled, N. and N.G. Chalhoub, *A self-tuning guidance and control system for marine surface vessels.* Nonlinear Dynamics, 2013. **73**(1-2): p. 897-906.

21. Healey, A.J. and D. Marco. *Slow speed flight control of autonomous underwater vehicles: Experimental results with NPS AUV II*. in *The Second International Offshore and Polar Engineering Conference*. 1992. International Society of Offshore and Polar Engineers.

22. Pettersen, K.Y. and E. Lefeber, *Way-point tracking control of ships.* Proceedings of the 40th Ieee Conference on Decision and Control, Vols 1-5, 2001: p. 940-945.

23. Jiang, Z.P., *Global tracking control of underactuated ships by Lyapunov's direct method.* Automatica, 2002. **38**(2): p. 301-309.

24. Fossen, T.I., *Marine control systems: guidance, navigation and control of ships, rigs and underwater vehicles*. 2002.

25. Fossen, T.I., M. Breivik, and R. Skjetne, *Line-of-sight path following of underactuated marine craft.* Proceedings of the 6th IFAC MCMC, Girona, Spain, 2003: p. 244-249.

26. Do, K.D., J. Pan, and Z.P. Jiang, *Robust adaptive control of underactuated ships on a linear course with comfort.* Ocean Engineering, 2003. **30**(17): p. 2201-2225.

27. Do, K., Z.-P. Jiang, and J. Pan, *Global partial-state feedback and output-feedback tracking controllers for underactuated ships.* Systems & control letters, 2005. **54**(10): p. 1015-1036.

28. Lefeber, E., K.Y. Pettersen, and H. Nijmeijer, *Tracking control of an underactuated ship.* Ieee Transactions on Control Systems Technology, 2003. **11**(1): p. 52-61.

29. Breivik, M., *Nonlinear maneuvering control of underactuated ships*. 2003.

30. Khaled, N. and N.G. Chalhoub, *Guidance and Control Scheme for Under-actuated Marine Surface Vessels.* 2010 American Control Conference, 2010: p. 5230-5235.

31. Ferries, B., *06-014queenofthe north2*, in *Press Release*. 2006.

32. Fossen, T.I. *High performance ship autopilot with wave filter*. in *Proc. Ship Control System Symp*. 1993.

33. Kim, M.H., *Nonlinear control and robust observer design for marine vehicles*. 2000, Virginia Polytechnic Institute and State University.

34. Cheng, J., J. Yi, and D. Zhao, *Design of a sliding mode controller for trajectory tracking problem of marine vessels.* Iet Control Theory and Applications, 2007. **1**(1): p. 233-237.

35. Chalhoub, N.G. and N. Khaled. *Robust controller and observer for marine surface vessels*. in *Proceedings of the 2009 Grand Challenges in Modeling & Simulation Conference*. 2009. Society for Modeling & Simulation International.

36. Li, Z., J. Sun, and S. Oh, *Design, analysis and experimental validation of a robust nonlinear path following controller for marine surface vessels.* Automatica, 2009. **45**(7): p. 1649-1658.

37. Perera, L.P. and C.G. Soares, *Pre-filtered sliding mode control for nonlinear ship steering associated with disturbances.* Ocean Engineering, 2012. **51**: p. 49-62.

38. Wang, H., et al., *Adaptive dynamic surface control for cooperative path following of underactuated marine surface vehicles via fast learning.* Iet Control Theory and Applications, 2013. **7**(15): p. 1888-1898.

39. Fahimi, F. and C. Van Kleeck, *Alternative trajectory-tracking control approach for marine surface vessels with experimental verification.* Robotica, 2013. **31**: p. 25-33.

40. Nayfeh, A.H., D.T. Mook, and L.R. Marshall, *Nonlinear coupling of pitch and roll modes in ship motions.* Journal of Hydronautics, 1973. **7**(4): p. 145-152.

41. Nayfeh, A.H., D.T. Mook, and L.R. Marshall, *Perturbation-energy approach for the development of the nonlinear equations of ship motion.* Journal of Hydronautics, 1974. **8**(4): p. 130-136.

42. Mook, D. and A. Nayfeh, *Nonlinear oscillations*. 1979, John Wiley & sons, New York.

43. Barr, R.A., et al., *Technical Basis for Maneuvering Performance Standards*. 1981, DTIC Document.

44. Bernitsas, M.M. and F.A. Papoulias, *Stability of single point mooring systems.* Applied ocean research, 1986. **8**(1): p. 49-58.

45. Bernitsas, M. and F. Papoulias. *'Nonlinear Stability and Maneuvering Simulation of Single Point Mooring Systems*. in *Proceedings of Offshore Station Keeping Symposium*. 1990.

46. Sagatun, S.I. and T.I. Fossen. *Lagrangian formulation of underwater vehicles' dynamics*. in *Systems, Man, and Cybernetics, 1991.'Decision Aiding for Complex Systems, Conference Proceedings., 1991 IEEE International Conference on*. 1991. IEEE.

47. Sagatun, S., *Modeling and control of underwater vehicles: A lagrangian approach*. 1992, Norwegian Institute of Technology, Division of Engineering Cybernetics Trondheim,, Norway.

48. Vassalos, D., *Contemporary ideas on ship stability*. 1st ed. 2000, Amsterdam ; New York: Elsevier. x, 597 p.

49. Suleiman, B.M., *Identification of finite-degree-of-freedom models for ship motions*. 2000, Citeseer.

50. El-Hawary, F., *The ocean engineering handbook*. 2000: Crc Press.

51. Lewandowski, E.M., *The dynamics of marine craft: maneuvering and seakeeping*. Vol. 22. 2004: World scientific.

52. Bulian, G., *Nonlinear parametric rolling in regular waves - a general procedure for the analytical approximation of the GZ curve and its use in time domain simulations.* Ocean Engineering, 2005. **32**(3-4): p. 309-330.

53. Ogilvie, T.F. and R.F. Beck, *Workshop on Slender-Body Theory*. 1974: Department of Naval Architecture and Marine Engineering, College of Engineering, University of Michigan.

54. Ogilvie, T.F. *Second-order hydrodynamic effects on ocean platforms*. in *International Workshop on Ship and Platform Motions, University of California, Berkeley*. 1983.

55. Wang, S., *Dynamical theory of potential flows with a free surface: A classical approach to strip theory of ship motions.* Journal of Ship Research, 1976. **20**(3).

56. Lee, C. and J. Newman, *First-and second-order wave effects on a submerged spheroid.* 1991.

57. Clamond, D., et al., *An efficient model for three-dimensional surface wave simulations. Part II: Generation and absorption.* Journal of Computational Physics, 2005. **205**(2): p. 686-705.

58. Morel, Y., *Applied nonlinear control of unmanned vehicles with uncertain dynamics.* 2009.

59. Minsk, L.D., *Ice accumulation on ocean structures*. 1977, DTIC Document.

60. Laranjinha, M., J.M. Falzarano, and C.G. Soares. *Analysis of the dynamical behaviour of an offshore supply vessel with water on deck*. in *ASME 2002 21st International Conference on Offshore Mechanics and Arctic Engineering*. 2002. American Society of Mechanical Engineers.

61. (IMO), I.M.O. *Revised IMO Intact Stability Code*. 2007; Available from: www.imo.org.

62. Minorsky, N., *Directional stability of automatically steered bodies.* Journal of ASNE, 1922. **42**(2): p. 280-309.

63. Kallstrom, C.G., et al., *Adaptive Autopilots for Tankers.* Automatica, 1979. **15**(3): p. 241-254.

64. Vahedipour, A. and J.P. Bobis, *Smart Autopilots.* Proceedings of the 1992 International Conference on Industrial Electronics, Control, Instrumentation, and Automation, Vols 1-3, 1992: p. 1437-1442.

65. Vukic, Z., L. Kuljaca, and D. Milinovic, *Predictive gain scheduling autopilot for ships.* Melecon '96 - 8th Mediterranean Electrotechnical Conference, Proceedings, Vols I-Iii, 1996: p. 1133-1136.

66. Wang, M.H., et al., *Optimization of Fuzzy Control System Based on Extension Method for Ship Course-Changing/Keeping.* 2008 Ieee International Conference on Fuzzy Systems, Vols 1-5, 2008: p. 434-438.

67. Bennett, S., *Nicolas Minorsky and the Automatic Steering of Ships.* 1984.

68. Moradi, M., M. Katebi, and M. Johnson, *The MIMO predictive PID controller design.* Asian Journal of Control, 2002. **4**(4): p. 452-463.

69. Ogata, K., *Modern Control Engineering.* 1997.

70. Fossen, T.I., *Recent developments in ship control systems design.* World Superyacht Review, Sterling Publications Limited, London, 2000: p. 115-116.

71. Caccia, M., et al., *Basic navigation, guidance and control of an Unmanned Surface Vehicle.* Autonomous Robots, 2008. **25**(4): p. 349-365.

72. Vanamerongen, J. and A.J. Udinktencate, *Model Reference Adaptive Autopilots for Ships.* Automatica, 1975. **11**(5): p. 441-449.

73. Vanamerongen, J., *Adaptive Steering of Ships - a Model-Reference Approach.* Automatica, 1984. **20**(1): p. 3-14.

74. Godhavn, J.M., *Nonlinear tracking of underactuated surface vessels.* Proceedings of the 35th Ieee Conference on Decision and Control, Vols 1-4, 1996: p. 975-980.

75. Fossen, T.I. and A. Grovlen, *Nonlinear output feedback control of dynamically positioned ships using vectorial observer backstepping.* Ieee Transactions on Control Systems Technology, 1998. **6**(1): p. 121-128.

76. Strand, J.P., et al., *Nonlinear control of ships: A locally optimal design.* Nonlinear Control Systems Design 1998, Vols 1& 2, 1998: p. 705-710.

77. Berge, S.P., K. Ohtsu, and T.I. Fossen, *Nonlinear control of ships minimizing the position tracking errors.* Modeling Identification and Control, 1999. **20**(3): p. 177-187.

78. Fossen, T.I. and J.P. Strand, *Tutorial on nonlinear backstepping: Applications to ship control.* Modeling, identification and control, 1999. **20**(2): p. 83.

79. Pivano, L., et al., *Nonlinear thrust controller for marine propellers in four-quadrant operations.* 2007 American Control Conference, Vols 1-13, 2007: p. 2259-2264.

80. Lopez, M.J. and F.R. Rubio, *Lqg/Ltr Control of Ship Steering Autopilots.* Proceedings of the 1992 Ieee International Symposium on Intelligent Control, 1992: p. 447-450.

81. Roman, A.W., *Nonlinear Backstepping Ship Course Controller.* International Journal, 2009. **3**: p. 010.

82. Layne, J.R. and K.M. Passino, *Fuzzy Model-Reference Learning Control for Cargo Ship Steering.* Proceedings of the 1993 Ieee International Symposium on Intelligent Control, 1993: p. 457-462.

83. Polkinghorne, M.N., et al., *The Implementation of Fixed Rulebase Fuzzy-Logic to the Control of Small Surface Ships.* Control Engineering Practice, 1995. **3**(3): p. 321-328.

84. Polkinghorne, M.N., G.N. Roberts, and B.S. Burns, *Intelligent ship control with online learning ability.* Computing & Control Engineering Journal, 1997. **8**(5): p. 196-200.

85. Yang, Y., C. Zhou, and J. Ren, *Model reference adaptive robust fuzzy control for ship steering autopilot with uncertain nonlinear systems.* Applied Soft Computing, 2003. **3**(4): p. 305-316.

86. Yang, Y. and B. Jiang. *Robust adaptive fuzzy control (rafc) for ship steering with uncertain nonlinear systems*. in *Intelligent Control and Automation, 2004. WCICA 2004. Fifth World Congress on*. 2004. IEEE.

87. Yeh, Z.M., *A Performance Approach to Fuzzy Control Design for Nonlinear-Systems.* Fuzzy Sets and Systems, 1994. **64**(3): p. 339-352.

88. Procyk, T.J. and E.H. Mamdani, *A linguistic self-organizing process controller.* Automatica, 1979. **15**(1): p. 15-30.

89. Sutton, R. and D.R. Towill, *A Fuzzy Model of the Helmsman Performing a Course-Keeping Task.* Applied Ergonomics, 1987. **18**(2): p. 137-145.

90. Sutton, R. and I.M. Jess, *Real-Time Application of a Self-Organizing Autopilot to Warship Yaw Control.* International Conference on Control 91, Vols 1 and 2, 1991. **332**: p. 827-832.

91. Maeda, M. and S. Murakami, *A Self-Tuning Fuzzy Controller.* Fuzzy Sets and Systems, 1992. **51**(1): p. 29-40.

92. Chou, C.H. and H.C. Lu, *A Heuristic Self-Tuning Fuzzy Controller.* Fuzzy Sets and Systems, 1994. **61**(3): p. 249-264.

93. de Abreu, G.L.C. and J.F. Ribeiro, *A self-organizing fuzzy logic controller for the active control of flexible structures using piezoelectric actuators.* Applied soft computing, 2002. **1**(4): p. 271-283.

94. Ji, J., Y.O. Li, and L. Zheng, *Self-adjusting fuzzy logic control for vehicle lateral control.* Fourth International Conference on Fuzzy Systems and Knowledge Discovery, Vol 2, Proceedings, 2007: p. 614-618.

95. Tonshoff, H.K. and A. Walter, *Self-Tuning Fuzzy-Controller for Process-Control in Internal Grinding.* Fuzzy Sets and Systems, 1994. **63**(3): p. 359-373.

96. Velagic, J., Z. Vukic, and E. Omerdic, *Adaptive fuzzy ship autopilot for track-keeping.* Control Engineering Practice, 2003. **11**(4): p. 433-443.

97. Wai, R.J., C.M. Lin, and C.F. Hsu, *Self-organizing fuzzy control for motor-toggle servomechanism via sliding-mode technique.* Fuzzy Sets and Systems, 2002. **131**(2): p. 235-249.

98. Yu, F.M., *A self-tuning fuzzy logic design for perturbed time-delay systems with nonlinear input.* Expert Systems with Applications, 2009. **36**(3): p. 5304-5309.

99. Utkin, V.I., *Variable Structure Systems with Sliding Modes.* Ieee Transactions on Automatic Control, 1977. **22**(2): p. 212-222.

100. Utkin, V. *Principles of identification using sliding regimes*. in *Soviet Physics Doklady*. 1981.

101. Drakunov, S.V., *An Adaptive Quasioptimal Filter with Discontinuous Parameters.* Automation and Remote Control, 1983. **44**(9): p. 1167-1175.

102. Khalil, H.K. and J. Grizzle, *Nonlinear systems*. Vol. 3. 1996: Prentice hall New Jersey.

103. Slotine, J.-J.E. and W. Li, *Applied nonlinear control*. Vol. 199. 1991: Prentice-Hall Englewood Cliffs, NJ.

104. Rundell, A.E., S.V. Drakunov, and R.A. DeCarlo, *A sliding mode observer and controller for stabilization of rotational motion of a vertical shaft magnetic bearing.* Ieee Transactions on Control Systems Technology, 1996. **4**(5): p. 598-608.

105. Kim, M.H. and D.J. Inman, *Development of a robust non-linear observer for dynamic positioning of ships.* Proceedings of the Institution of Mechanical Engineers Part I-Journal of Systems and Control Engineering, 2004. **218**(I1): p. 1-11.

106. Le, M.D., et al., *Control of large ship motions in harbor maneuvers by applying sliding mode control.* 8th Ieee International Workshop on Advanced Motion Control, Proceedings, 2004: p. 695-700.

107. Chalhoub, N.G., G.A. Kfoury, and B.A. Bazzi, *Design of robust controllers and a nonlinear observer for the control of a single-link flexible robotic manipulator.* Journal of Sound and Vibration, 2006. **291**(1-2): p. 437-461.

108. Decarlo, R.A., S.H. Zak, and G.P. Matthews, *Variable Structure Control of Nonlinear Multivariable Systems - a Tutorial.* Proceedings of the Ieee, 1988. **76**(3): p. 212-232.

109. Choi, S.-B. and D.-W. Park, *Moving sliding surfaces for fast tracking control of second-order dynamical systems.* Journal of dynamic systems, measurement, and control, 1994. **116**(1): p. 154-158.

110. Slotine, J.J. and S.S. Sastry, *Tracking Control of Non-Linear Systems Using Sliding Surfaces, with Application to Robot Manipulators.* International Journal of Control, 1983. **38**(2): p. 465-492.

111. Choi, S.B. and J.S. Kim, *A fuzzy-sliding mode controller for robust tracking of robotic manipulators.* Mechatronics, 1997. **7**(2): p. 199-216.

112. Ha, Q.P., D.C. Rye, and H.F. Durrant-Whyte, *Fuzzy moving sliding mode control with application to robotic manipulators.* Automatica, 1999. **35**(4): p. 607-616.

113. Bartoszewicz, A., *A time-varying sliding surface for fast and robust tracking control of second-order uncertain systems - A comment.* Automatica, 1995. **31**(12): p. 1893-1895.

114. Lee, H., et al., *A new sliding-mode control with fuzzy boundary layer.* Fuzzy Sets and Systems, 2001. **120**(1): p. 135-143.

115. Tong, S.C., C.Y. Li, and Y.M. Li, *Fuzzy adaptive observer backstepping control for MIMO nonlinear systems.* Fuzzy Sets and Systems, 2009. **160**(19): p. 2755-2775.

116. Tong, S.C. and Y.M. Li, *Observer-based fuzzy adaptive control for strict-feedback nonlinear systems.* Fuzzy Sets and Systems, 2009. **160**(12): p. 1749-1764.

117. Breivik, M., V.E. Hovstein, and T.I. Fossen, *Straight-Line Target Tracking for Unmanned Surface Vehicles.* Modeling Identification and Control, 2008. **29**(4): p. 131-149.

118. Ashrafiuon, H., et al., *Sliding-mode tracking control of surface vessels.* IEEE Transactions on Industrial Electronics, 2008. **55**(11): p. 4004-4012.

119. Schoerling, D., et al., *Experimental test of a robust formation controller for marine unmanned surface vessels.* Autonomous Robots, 2010. **28**(2): p. 213-230.

120. Kim, M.H. and D.J. Inman, *Reduction of observation spillover in vibration suppression using a sliding mode observer.* Journal of Vibration and Control, 2001. **7**(7): p. 1087-1105.

121. Parkinson, B.W., *Progress in Astronautics and Aeronautics: Global Positioning System: Theory and Applications*. Vol. 2. 1996: Aiaa.

122. Corporation, K.M. 2010; Available from: http://www.km.kongsberg.com/.

123. Vik, B., A. Shiriaev, and T.I. Fossen, *Nonlinear observer design for integration of DGPS and INS.* New Directions in Nonlinear and Observer Design, 1999. **244**: p. 135-159.

124. Vik, B., *Nonlinear design and analysis of integrated GPS and inertial navigation systems*. 2000: NTNU.

125. Vik, B. and T.I. Fossen, *A nonlinear observer for integration of GPS and Inertial Navigation Systems.* Modeling Identification and Control, 2000. **21**(4): p. 193-208.

126. Lindegaard, K.P. and T.I. Fossen, *On global model based observer designs for surface vessels.* Control Applications in Marine Systems 2001 (Cams 2001), 2002: p. 389-394.

127. Chalhoub, N.G. and G.A. Kfoury, *Development of a robust nonlinear observer for a single-link flexible manipulator.* Nonlinear Dynamics, 2005. **39**(3): p. 217-233.

128. Luenberger, D.G., *Observing the state of a linear system.* Military Electronics, IEEE Transactions on, 1964. **8**(2): p. 74-80.

129. Luenberger, D.G., *Observers for multivariable systems.* Automatic Control, IEEE Transactions on, 1966. **11**(2): p. 190-197.

130. Luenberger, D., *Introduction to dynamic systems: theory, models, and applications.* 1979.

131. Kailath, T., *Linear systems*. Vol. 156. 1980: Prentice-Hall Englewood Cliffs, NJ.

132. Chen, C.-T., *Introduction to linear system theory*. 1970: Holt, Rinehart and Winston.

133. Friedland, B., *Control system design: an introduction to state-space methods*. 2012: Courier Corporation.

134. Ogata, K., *Modern control engineering*. 2001: Prentice Hall PTR.

135. Zeitz, M., *The Extended Luenberger Observer for Nonlinear-Systems.* Systems & Control Letters, 1987. **9**(2): p. 149-156.

136. Yanada, H. and M. Shimahara, *Sliding mode control of an electrohydraulic servo motor using a gain scheduling type observer and controller.* Proceedings of the Institution of Mechanical Engineers Part I-Journal of Systems and Control Engineering, 1997. **211**(6): p. 407-416.

137. Nandam, P.K. and P.C. Sen, *A Comparative-Study of a Luenberger Observer and Adaptive Observer-Based Variable Structure Speed Control-System Using a Self-Controlled Synchronous Motor.* Ieee Transactions on Industrial Electronics, 1990. **37**(2): p. 127-132.

138. Sorenson, H.W., *Kalman filtering: theory and application*. 1985: IEEE.

139. Lewis, F.L. and F. Lewis, *Optimal estimation: with an introduction to stochastic control theory*. 1986: Wiley New York et al.

140. Anderson, B.D. and J.B. Moore, *Optimal control: linear quadratic methods*. 2007: Courier Corporation.

141. Sorensen, A.J., S.I. Sagatun, and T.I. Fossen, *Design of a dynamic positioning system using model-based control.* Control Engineering Practice, 1996. **4**(3): p. 359-368.

142. Sandler, M., et al., *Autonomous guidance of ships on waterways.* Robotics and Autonomous Systems, 1996. **18**(3): p. 327-335.

143. Jwo, D.J. and T.S. Cho, *A practical note on evaluating Kalman filter performance optimality and degradation.* Applied Mathematics and Computation, 2007. **193**(2): p. 482-505.

144. Rajamani, R. and J.K. Hedrick, *Adaptive-Observer for Active Automotive Suspensions.* Proceedings of the 1993 American Control Conference, Vols 1-3, 1993: p. 706-710.

145. Cho, Y.M. and R. Rajamani, *A systematic approach to adaptive observer synthesis for nonlinear systems.* Ieee Transactions on Automatic Control, 1997. **42**(4): p. 534-537.

146. Banks, S.P., *A Note on Non-Linear Observers.* International Journal of Control, 1981. **34**(1): p. 185-190.

147. Besançon, G., *On output transformations for state linearization up to output injection.* Automatic Control, IEEE Transactions on, 1999. **44**(10): p. 1975-1981.

148. Boyd, S.P., et al., *Linear matrix inequalities in system and control theory*. Vol. 15. 1994: SIAM.

149. Kou, S.R., D.L. Elliott, and T.J. Tarn, *Exponential Observers for Nonlinear Dynamic-Systems.* Information and Control, 1975. **29**(3): p. 204-216.

150. Krener, A.J. and A. Isidori, *Linearization by output injection and nonlinear observers.* Systems & Control Letters, 1983. **3**(1): p. 47-52.

151. Raghavan, S. and J.K. Hedrick, *Observer design for a class of nonlinear systems.* International Journal of Control, 1994. **59**(2): p. 515-528.

152. Rajamani, R., *Observers for Lipschitz nonlinear systems.* Automatic Control, IEEE Transactions on, 1998. **43**(3): p. 397-401.

153. Thau, F., *Observing the state of non-linear dynamic systems†.* International journal of control, 1973. **17**(3): p. 471-479.

154. Tsinias, J., *Observer design for nonlinear systems.* Systems & Control Letters, 1989. **13**(2): p. 135-142.

155. Bestle, D. and M. Zeitz, *Canonical form observer design for non-linear time-variable systems.* International Journal of control, 1983. **38**(2): p. 419-431.

156. Walcott, B. and S. Zak. *Observation of dynamical systems in the presence of bounded nonlinearities/uncertainties*. in *1986 25th IEEE Conference on Decision and Control*. 1986.

157. Slotine, J.J.E., J.K. Hedrick, and E.A. Misawa, *On Sliding Observers for Nonlinear-Systems.* Journal of Dynamic Systems Measurement and Control-Transactions of the Asme, 1987. **109**(3): p. 245-252.

158. Misawa, E.A. and J.K. Hedrick, *Nonlinear Observers-A State-of-the-Art Survey.* Journal of Dynamic Systems Measurement and Control-Transactions of the Asme, 1989. **111**(3): p. 344-352.

159. Kfoury, G.A., *Computation of the Instantaneous Frictional Losses in Internal Combustion Engines Using Estimated Variables*. 2008: ProQuest.

160. Kfoury, G.A. and N.G. Chalhoub, *Development of a robust observer for constrained nonlinear systems.* Proceedings of the Asme International Mechanical Enginering Congress and Exposition 2007, Vol 9, Pts a-C, 2008: p. 233-241.

161. Chalhoub, N.G. and N. Khaled, *Integrated controller-observer system for marine surface vessels.* Journal of Vibration and Control, 2014. **20**(3): p. 381-394.

162. Mastory, C., *Non-Linear Robust Observers For Systems With Non-Collocated Sensors And Actuators.* 2014.

163. Khaled, N. and N.G. Chalhoub, *A self-tuning robust observer for marine surface vessels.* Nonlinear Dynamics, 2015. **79**(2): p. 937-951.

164. Chalhoub, N. and N. Khaled, *Guidance and control system for under-actuated marine surface ships and other autonomous-platforms*. 2015, Google Patents.

165. Naeem, W., et al., *A review of guidance laws applicable to unmanned underwater vehicles.* Journal of Navigation, 2003. **56**(1): p. 15-29.

166. Bibuli, M., et al. *ILOS guidance-experiments and tuning*. in *Proc. of the 19th IF AC World Congress*. 2014.

167. Khatib, O., *Real-Time Obstacle Avoidance for Manipulators and Mobile Robots.* International Journal of Robotics Research, 1986. **5**(1): p. 90-98.

168. Tilove, R.B. *Local obstacle avoidance for mobile robots based on the method of artificial potentials*. in *Robotics and Automation, 1990. Proceedings., 1990 IEEE International Conference on*. 1990. IEEE.

169. Koren, Y. and J. Borenstein, *Potential-Field Methods and Their Inherent Limitations for Mobile Robot Navigation.* 1991 Ieee International Conference on Robotics and Automation, Vols 1-3, 1991: p. 1398-1404.

170. Fox, D., W. Burgard, and S. Thrun, *The dynamic window approach to collision avoidance.* Ieee Robotics & Automation Magazine, 1997. **4**(1): p. 23-33.

171. Berti, H., A.D. Sappa, and O.E. Agamennoni, *Improved Dynamic Window Approach by Using Lyapunov Stability Criteria.* Latin American Applied Research, 2008. **38**(4): p. 289-298.

172. Brock, O. and O. Khatib, *High-speed navigation using the global dynamic window approach.* Icra '99: Ieee International Conference on Robotics and Automation, Vols 1-4, Proceedings, 1999: p. 341-346.

173. Stachniss, C. and W. Burgard, *An integrated approach to goal-directed obstacle avoidance under dynamic constraints for dynamic environments.* 2002 Ieee/Rsj International Conference on Intelligent Robots and Systems, Vols 1-3, Proceedings, 2002: p. 508-513.

174. Wilkie, D., J. van den Berg, and D. Manocha, *Generalized Velocity Obstacles.* 2009 Ieee-Rsj International Conference on Intelligent Robots and Systems, 2009: p. 5573-5578.

175. Fiorini, P. and Z. Shiller, *Motion planning in dynamic environments using velocity obstacles.* International Journal of Robotics Research, 1998. **17**(7): p. 760-772.

176. Kuwata, Y., et al., *Safe Maritime Autonomous Navigation With COLREGS, Using Velocity Obstacles.* Ieee Journal of Oceanic Engineering, 2014. **39**(1): p. 110-119.

177. Kuwata, Y., et al., *Safe Maritime Navigation with COLREGS Using Velocity Obstacles.* 2011 Ieee/Rsj International Conference on Intelligent Robots and Systems, 2011.

ABSTRACT

EXPERIMENTAL VALIDATION OF AN INTEGRATED GUIDANCE AND CONTROL SYSTEM FOR MARINE SURFACE VESSELS

by

ANTHONY COMPOSTO

December 2018

Advisor: Dr. Nabil Chalhoub

Major: Mechanical Engineering

Degree: Doctor of Philosophy

Autonomous operation of marine surface vessels is vital for minimizing human errors and providing efficient operations of ships under varying sea states and environmental conditions which is complicated by the highly nonlinear dynamics of marine surface vessels. To deal with modelling imprecision and unpredictable disturbances, the sliding mode methodology has been employed to devise a heading and a surge displacement controller. The implementation of such a controller necessitates the availability of all state variables of the vessel. However, the measured signals in the current study are limited to the global X and Y positioning coordinates of the boat that are generated by a GPS system. Thus, a nonlinear observer, based on the sliding mode methodology, has been implemented to yield accurate estimates of the state variables in the presence of both structured and unstructured uncertainties. Successful autonomous operation of a marine surface vessel requires a holistic approach encompassing a navigation system, robust nonlinear controllers and observers. Since the overwhelming majority of the experimental work on autonomous marine surface vessels was not conducted in truly

uncontrolled real-world environments. The first goal of this work was to experimentally validate a fully-integrated LOS guidance system with a sliding mode controller and observer using a 16' Tracker Pro Guide V-16 aluminium boat with a 60 hp. Mercury outboard motor operating in the uncontrolled open-water environment of Lake St. Clair, Michigan. The fully integrated guidance and controller-observer system was tested in a model-less configuration, whereby all information provided from the vessel's nominal model have been ignored. The experimental data serves to demonstrate the robustness and good tracking characteristics of the fully-integrated guidance and controller/observer system by overcoming the large errors induced at the beginning of each segment and converging the boat to the desired trajectory in spite of the presence of environmental disturbances. The second focus of this work was to combine a collision avoidance method with the guidance system that accounted for "International Regulations for Prevention of Collisions at Sea" abbreviated as COLREGS. This new system then needed to be added into the existing architecture. The velocity obstacles method was selected as the base to build upon and additional restrictions were incorporated to account for these additional rules. This completed system was then validated with a software in the loop simulation.

AUTOBIOGRAPHICAL STATEMENT

ANTHONY COMPOSTO

Ever since I was a child I've always wanted to understand how things worked. When I received a new toy, I usually took it apart to figure out how it worked before I even played with it. Although I was always able to disassemble them, I had varied success in correctly putting them back together. As a result, Legos, Erector Sets, and Robotix were the toys that my parents mostly favored. Their thinking was that if they weren't assembled in the first place, then I couldn't take them apart. This passion for understanding how things work has remained consistent throughout my life, which is why I chose to go into engineering as a career. After finishing a BS in Mechanical Engineering, I decided to broaden my education and pursue a MS in Biomedical Engineering. I enjoyed this area of study since I was able to focus on areas such as prosthetics and other enabling technologies for people with special needs. Although the idea of using my passion to help people with disabilities was appealing, my true passion was still in mechanical systems. Therefore, I decided to switch back to Mechanical Engineering to pursue my PhD. I always had an interest in mechanical systems and using computers to control them. Robots especially fascinated me, everything from robotic arms to robotic ground vehicles. I knew I wanted my PhD research to focus around this area. As luck would have it, I was accepted as a PhD student by a professor that had a robotic marine surface vessel research project for ONR (The Office of Naval Research). The focus of my research was the control, guidance and collision avoidance for a marine surface vessel. Because of what I learned during my graduate studies, I am now working for TARDEC on the Ground Vehicle Robotics team developing future combat vehicles for the Army.